

STUDIES ON IMPROVEMENT OF INTAKE MANIFOLD FOR COMPRESSED NATURAL GAS ENGINE

A THESIS

Submitted in partial fulfilment of the requirements for the award of degree of

Masters of Engineering

In

Thermal Engineering

Submitted By

DEVENDER KUMAR

Regd. No. 801083008

UNDER THE GUIDANCE OF

Mr. SUMEET SHARMA

Associate Professor

Department of Mechanical Engineering

Dr. D. GANGACHARYULU

Professor

Department of Chemical Engineering



DEPARTMENT OF MECHANICAL ENGINEERING

THAPAR UNIVERSITY

(Established under section 3 of UGC Act, 1956)

PATIALA -147001, INDIA

JULY, 2012.

DECLARATION

I hereby certify that the work which is being presented in the thesis entitled “**Studies on Improvement of Intake Manifold for Compressed Natural Gas Engine**” by me in partial fulfilment of the requirements for the award of degree of Masters of Engineering in Thermal Engineering, from Department of Mechanical Engineering, Thapar University, Patiala is an authentic record of my own work carried under the supervision of Mr. Sumeet Sharma, Assistant Professor, Department of Mechanical Engineering and Dr. D. Gangacharyulu, Professor, Department of Chemical Engineering. The matter presented in this report has not been submitted in any other University/Institute for the award of Masters of Engineering or any other degree.

Date:16-july-2012



(Devender Kumar)

Regd. No. 801083008

CERTIFICATE

This is to certify that the thesis entitled “**Studies on Improvement of Intake Manifold for Compressed Natural Gas Engine**” being submitted by **Mr. Devender Kumar** (Regd. No: 801083008), in partial fulfilment of the requirements for the award of degree of Master of Engineering in Thermal Engineering of Mechanical Engineering Department, Thapar University, Patiala, is a record of candidate’s own work carried out by him under my supervision. To the best of our knowledge, that no part of this thesis has been submitted for the award of any other degree.

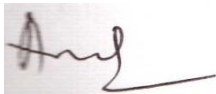


(SUMEET SHARMA)
Associate Professor
Department of Mechanical Engineering
Thapar University, Patiala



(D. GANGACHARYULU)
Professor
Department of Chemical Engineering
Thapar University, Patiala

Countersigned by:



(AJAY BATISH)
Professor and Head
Mechanical Engineering Department
Thapar University
Patiala - 147004



(S.K. MOHAPATRA)
Senior Professor
Dean of Academic Affairs
Thapar University
Patiala – 147004

ACKNOWLEDGEMENT

I would like to express my deep sense of gratitude to **Mr. Sumeet Sharma**, Associate Professor, Department of Mechanical Engineering And **Dr. D. Gangacharyulu**, Professor, Department of Chemical Engineering, Thapar University, Patiala for their invaluable suggestions, excellent supervision, constant encouragement and critical discussion throughout the research work.

I am also thankful to **Dr. Ajay Batish**, Professor and Head, Mechanical Engineering Department, Thapar University and **Mr. Sandeep Sharma**, PG Coordinator, Mechanical Engineering Department, Thapar University for providing me an opportunity to do my project work on the topic of my interest

I would also like to thanks my friends specially Mr. Parshant Sharma who have assisted me at all moments of need.

The greatest thanks go to my family for their infinite support. Besides, I would like to acknowledge my institute i.e. Thapar University.

Above all, I express my indebtedness to the “ALMIGHT” for all His blessing and kindness.



(Devender Kumar)

ABSTRACT

Geometrical design of intake manifold is very important for the good performance of an I.C. Engine. Unequal velocity distribution of intake air at runner's outlets of intake manifold makes it less efficient. The reported work aims to make this unequal distribution of velocity in nearly equal manner with increase of velocity at outlets without any major modification in design of intake manifold. Maruti Wagnor (petrol version) engine intake manifold is used for experimental testing, to examine the variation of velocity of air flow at outlet of four runners. To modify the intake manifold first a 3-D model of actual manifold is made in design software (PRO-E) and then validation of design model is done by using commercial CFD software FLUENT. To achieve the desired improve results two other models of same intake manifold with different design configuration are made in software then examine the result of these two models with original one to find out pressure and velocity losses. After analysis of models it noticed that the hidden projections of nut, projected stiffeners and depth cuts at extreme of plenum causes pressure losses due to which uneven distribution take place at runner's outlets. The nearly equal velocities in all four runners are achieved in the inlet manifold by redesigning the plenum of intake manifold and free it from unwanted hidden projection inside the plenum. The results show nearly equal distribution in all four runners with an increase in velocity of air flow by 14% in outlet-1 and 5% to 7% approx. in other three runners of inlet manifold.

CONTENTS

DECLARATION	ii
CERTIFICATE	iii
ACKNOWLEDGEMENT	iv
ABSTRACT	v
LIST OF FIGURES	ix
LIST OF TABLES	xiii
NOMENCLATURE	xiv

Chapter No.	Description	Page No.
1.0	Introduction	1
1.1	Internal Combustion Engine	1
1.2	Alternative Fuels	2
1.2.1	Liquefied Petroleum Gas	2
1.2.2	Compress Natural Gas	2
1.3	Compress Natural Gas(CNG) Engines	3
1.4	Intake Manifold	3
1.4.1	Static Length Intake Manifold	4
1.4.2	Variable length Intake Manifold	4
1.5	Modification scope of Intake Manifold	4
1.6	CFD (Computational Flow Dynamics)	5
1.7	Conclusion	5
	References	6
 2.0	 Literature Review	 7
2.1	Categorization	7
2.1.1	Computational fluid dynamics (CFD) analysis	7-12
2.1.2	Experimental analysis	12-18
2.1.3	Numerical approach analysis	18-21
2.2	Formulae Work	21

2.3	Gap analysis	21
	References	22-24
3.0	Objective	25
4.0	Methodology	26
4.1	Experimental analysis of intake manifold	26
4.1.1	Tools and Instruments	26
4.1.2	Experimental setup	27
4.1.3	U-tube Manometer	
4.2	Modelling of Intake manifold system	30
4.2.1	Destructive testing	30-31
4.2.2	Dimensioning of manifold	31
4.2.3	Prelim design drawing	32
4.2.4	Final model drawing	33
4.2.5	3-D view of final model of intake manifold	33
4.2.6	Stress analysis of model	34
4.2.6.1	Mathematical stress analysis	34-35
4.2.6.2	Computational Stress analysis of intake manifold	35-36
	Result of stress analysis	36
	Conclusion	36
	References	37
4.3	CFD analysis of intake manifold	38
4.3.1	Strategy for study of intake model	38
4.3.1.1	Model 1- Flow model of original geometry	39-44
4.3.1.2	Model 2- Model without internal projection at plenum	45-50
4.3.1.2	Model 3-Model without projection at plenum and without curve at end of runners	51-55
5.0	Results and Discussion	56
5.1	Experimental result of Intake manifold	56
5.1.1	Experimental data of Anemometer	56

5.1.2	Experimental Data of Intake manifold by U-tube manometer	57-58
5.2	Density variation analysis for compressible air flow at outlets	58
5.2.1	At NTP condition	58
5.2.2	At Experimental data of intake velocity 14 m/s	59
5.3	CFD Simulation result	60
5.3.1	Model-1 results	60
5.3.2	Model-2 results	61
5.3.3	Model-3 results	62
5.4	Validation	63
5.4.1	Experimental model validation	63-64
5.4.2	CFD model validation with experimental model	64
5.5	Examine the three models at different outlets	65-67
5.6	Examine the three models at different inlet velocities	67-69
5.7	Purposed Geometry	69
5.8	Comparison of result of purposed and actual intake manifold	70
6.0	CONCLUSIONS	71
	FUTURE SCOPE	72

List of Figures

Figure No.	Description	Page No.
1.1	Internal combustion engine	1
1.2	Intake Manifold	3
1.3	Variable length intake manifold	4
1.4	CFD Simulated intake manifold	5
2.1	Inlet Manifold without and with optimization	7
2.2	Modelled Spiral, Helical, Helical spiral manifolds	8
2.3	Mixer flow in without and without manifold	9
2.4	Computational modelled of six cylinder engine and schematic diagram of experimental apparatus	10
2.5	Mesh of throttle body injection mixer	11
2.6	Histogram of M_{ch_4} used to determine M_{hf}	11
2.7	Constructed Grid and single cylinder schematic for CAI (control auto ignition) research	12
2.8	Volumetric efficiency at various speed w.r.t pipe length or plenum volume chamber	13
2.9	Mixer	15
2.10	Variation of specific fuel consumption and thermal efficiency with engine speed for three different intake plenum volumes	16
2.11	Engine manifold and modelled vs. measured air mass flow through engine manifold	17
2.12	Cylinder volumetric efficiency and total fuel consumption per cycle for CNG(compress natural gas) and diesel engine	18
3.1	Losses comprising figure of intake manifold	25
4.1	Intake Manifold	26
4.2	Anemometer	27
4.3	Blower	27
4.4	U tube manometer	27

4.5	Pressure taps, pipe attachments	27
4.6	Air flow Regulator	27
4.7	Thermometer	27
4.8	Experimental Setup	27
4.9	Intake manifold block diagram	28
4.10	Measurement in U-Tube Manometer	28
4.11	Physical appearance of Intake manifold	30
4.12	Destructive test of intake manifold	30
4.13	Hidden inside projection	31
4.14	Prelim design drawing of original intake manifold	32
4.15	Complete drawing of intake manifold	33
4.16	3-D Front view intake manifold	33
4.17	3-D Back view intake manifold	33
4.18	3-D Left side view intake manifold	33
4.19	3-D Right side view of intake manifold	33
4.20	Material detail of manifold for stress analysis	35
4.21	Static case of one runner of intake manifold	36
4.22	Deformed mesh	36
4.23	Von miss stress analysis	36
4.24	Model-1	38
4.25	Model-2	38
4.26	Model-3	38
4.27	Meshing of flow domain (Model-1)	39
4.28	Name selection (Model-1)	39
4.29(a)	Residual plot (Model-1,18m/s)	40
4.29(b)	Convergence of Residual Plot (Model-1,18m/s)	40
4.30	Velocity streamlines Front view and Back view (Model-1,18m/s)	41
4.31	Velocity vector (Model-1,18m/s)	41
4.32(a)	Velocity profile at different outlets (Model-1,18m/s)	42
4.32(b)	Velocities values at different outlets (Model-1,18m/s)	42
4.33	Residual Plot (Model-1,15m/s)	43

4.34	Velocity contour (Model-1,15m/s)	43
4.35	Velocities profile at different outlets (Model-1,15m/s)	44
4.36	Meshing (Model-2)	45
4.37	Name selections (Model-2)	45
4.38(a)	Residual Plot (Model-2,18m/s)	46
4.38(b)	Convergence of Residual plot (Model-2,18m/s)	46
4.39	Velocity streamline (Model-2,18m/s)	47
4.40	Velocity vector in different plane (Model-2, 18 m/s)	47
4.41(a)	Velocities profile at different outlets(Model-2,18m/s)	48
4.41(b)	Velocities values at different outlets(Model-2,18m/s)	48
4.42	Converge point of residual plot(Model-2,15m/s)	49
4.43	Velocity streamline (Model-2,15m/s)	49
4.44	Velocity contour (Model-2,15m/s)	49
4.45	Velocities profile at different outlets (Model-2,15m/s)	50
4.46	Meshing (Model-3)	51
4.47	Named selection(Model-3)	51
4.48(a)	Residual Plot (Model-3,18m/s)	52
4.48(b)	Convergence of Residual plot (Model-3,18m/s)	52
4.49	Velocity vector in different plane (Model-3,18m/s)	53
4.50(a)	Velocities Profile at different outlets(Model-3,18m/s)	53
4.50(b)	Velocities values at different outlets (Model-3,18m/s)	54
4.51	Residual plot(Model-3,15m/s)	54
4.52(a)	Velocities profile at different outlets(Model-3,15m/s)	55
4.52(b)	Velocity at different outlets (Model-3,15m/s)	55
5.1	Velocities at outlets with variable inlet velocities (Anemometer readings)	56
5.2	Pressure at outlets on variable inlet velocities	58
5.3	Velocities at outlets with variable inlet velocities (CFD Simulation of Model-1)	60
5.4	Velocities at outlets with variable inlet velocities(CFD Simulation of Model-2)	61

5.5	Velocities at outlets with variable inlet velocities (CFD Simulation of Model-3)	62
5.6	Outlet vs. inlet velocities at outlet-1 of 3 Models	65
5.7	Outlet vs. inlet velocities at outlet-2 of 3 Models	65
5.8	Outlet vs. inlet velocities at outlet-3 of 3 Models	66
5.9	Outlet vs. inlet velocities at outlet-4 of 3 Models	66
5.10	Velocity at outlets vs. outlets of 3 model at Inlet velocity 18m/s	67
5.11	Velocity at outlets vs. outlets of 3 model at Inlet velocity 15m/s	68
5.12	Velocity at outlets vs. outlets of 3 model at Inlet velocity 13m/s	68
5.13	3-D model of Purposed Geometry	69
5.14	Velocity at outlets (Purposed Geometry ,18 m/s)	70
5.15	Comparison of velocity of Actual and Purposed model	70

List of Tables

Table No.	Description	Page No.
2.1	Comparison current and optimum design valve using SVR	19
4.1	Basic dimension of intake manifold	31
4.2	Meshing properties of model -1	39
4.3	Meshing properties of model -2	45
4.4	Meshing properties of model -3	51
5.1	Experimental data of Anemometer	56
5.2	U-tube manometer data at inlet velocity 14 m/s	57
5.3	U-tube manometer data at inlet velocity 12.5 m/s	57
5.4	U-tube manometer data at inlet velocity 11.2 m/s	57
5.5	U-tube manometer data at inlet velocity 8.5 m/s	58
5.6	CFD simulation result data for Model-1	60
5.7	CFD simulation result data for Model-2	61
5.8	CFD simulation result data for Model-3	62
5.9	Comparison of result of purposed and actual intake manifold	70

Nomenclature

Symbol	Description	Dimensions
ρ	Density	kg/m^3
t	Time	Sec
p	Pressure	Pa
E	Energy	W
m_a	Mass of air	kg
V_{disp}	Volume displaced	m^3
η_v	Volumetric efficiency	Dimensionless
N	No of stroke	---
A	Area	m^2
r	Radius	m
Q	Mass flow rate	m^3/s
R	Gas constant	$\text{J}/(\text{Kg K})$
T	Temperature	K
z	Datum height	m
v	Velocity	m/s
g	Gravity	m/s^2
s	Material strength	N/m^2

Chapter – 1

Introduction

1.0 Introduction

Engines are being developed to achieve high performance and gaining the potential to fulfill the need of next generation. The main objective of this introductory chapter is to sketch out a brief review of Automobile Sector such as concept of Natural gas vehicle, alternate fuel technology, better performance methods in developing engines and there benefits to the Automobile world.

1.1 Internal Combustion Engine

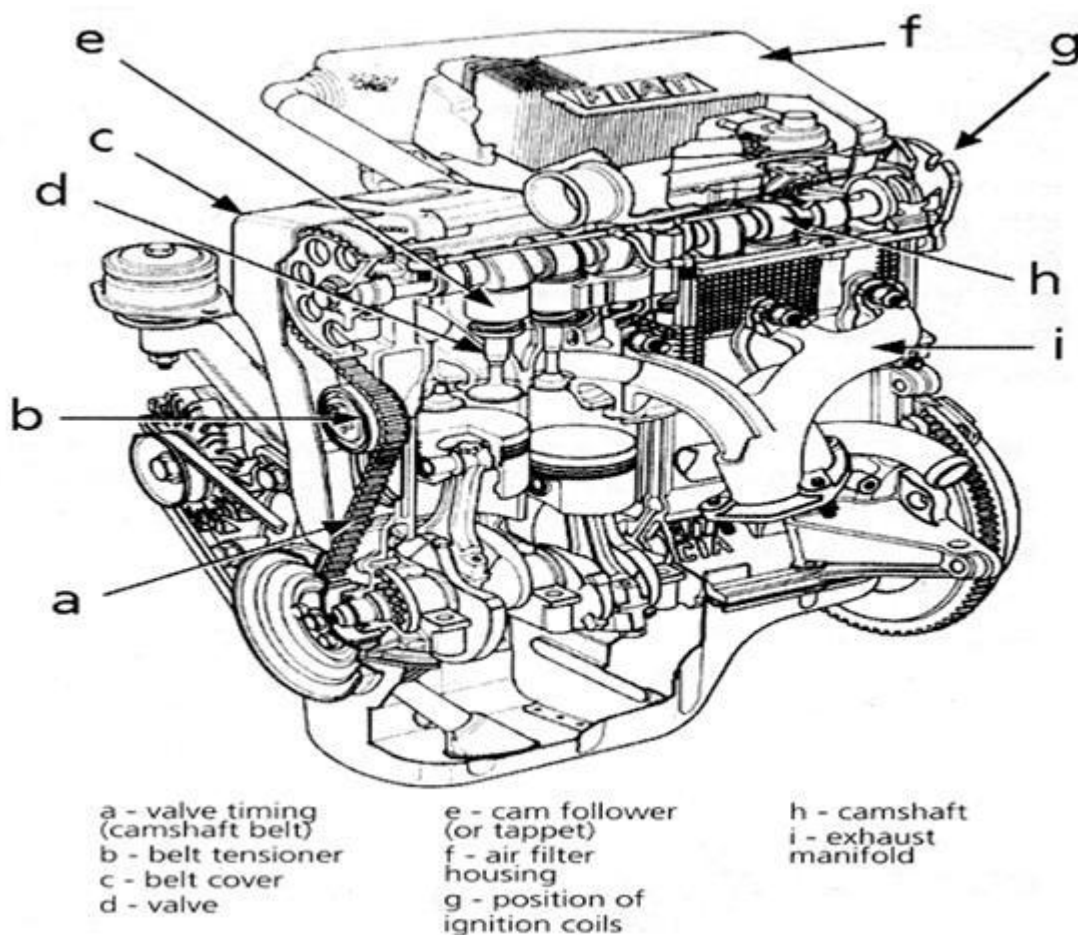


Fig.1.1: Internal combustion engine

The engine plays a very crucial role in the whole vehicle operation. What this auto part does is it produces and supplies the energy needed by other car components to function. They are the devices which transform the chemical energy of fuel into thermal energy and utilize this thermal energy to perform useful work. Thus, thermal energy is converted to mechanical energy in engines. They are broadly classified in two types, Spark ignition engine and compression ignition engine.

1.2 Alternative Fuels

Major challenges for the future will be to reduce global emissions and crude oil consumption. Due to high emission rate of pollution by our conventional fuels, introduction of alternative fuels such as natural gas (NG), liquefied petroleum gas (LPG) and compressed natural gas (CNG) for internal combustion engines is likely to occur at an increasing rate. They are alternatives to conventional petrol and have the potential to reduce pollution. They do not contain toxic compounds, such as benzene, and they are simple compounds that do not form complex hydrocarbon by-products during combustion. However, their vehicle range is less and cost higher, especially during their initial use when modifications would be needed in the transportation infrastructure [1].

1.2.1 Liquefied Petroleum Gas

It is a by-product of petroleum refining and natural gas production. It consists mainly of propane stored in liquefied form at a pressure of 5-10 bars. The advantages of LPG are slightly lower emissions, mainly of carbon monoxide, hydrocarbons and have a higher octane number. The disadvantages of this are higher weight of tank, less space for luggage, slightly reduced performance and a shorter range compared with conventional gasoline [1].

1.2.2 Compressed Natural Gas

CNG (compressed natural gas), a gaseous form of natural gas, has been recognized as one of the promising alternative fuel due to its substantial benefits compared to gasoline and diesel. It is a naturally occurring mixture of hydrocarbons that exists in the gaseous state at normal temperature and pressure. Its chief constituent is methane, but other alkanes are also found in it. Natural gas is also being used developed as an alternative fuel for automobile because it is one of the cleanest-burning fuels. It emits about 70% less carbon monoxide and has much less ozone-forming potential than standard petroleum gasoline. It is also less expensive than gasoline. The biggest drawback of natural gas is that it must be compressed to fit in a car or truck or bus, so heavy tanks are required to store it, and the pressure required (200 – 300 bar) is high enough to place considerable safety demands on the system. The pressurized form of this gas is known as compressed natural gas (CNG).The infrastructure of distribution of CNG is also comparatively high [1].

1.3 Compress Natural Gas (CNG) Engines

Research in CNG engine essentially focused on three main areas: intake process, combustion system and exhaust treatment. CNG as an alternative fuel in an engine could be divided into three main types; Dual Fuel Diesel- CNG, Gasoline-CNG and Dedicated/Mono Fuel. The main problem to commercialize the CNG engine was the lack of engine performance. The CNG engine, either in dual fuel, bi-fuel or dedicated forms is lower performance compare to that of gasoline. Based on the Maxwell and Jones (1995) works, the average power and torque loss of CNG compared to gasoline is in the range of 3 to 19.7% and 1.6 to 21.6%, respectively. Several factors affecting the low engine power and torque, those are loses in volumetric efficiency, low flame speed. So, the manufacturers of natural gas IC engine need to make design modification to achieve a faster burn to optimizing the engine performance. These modifications should consider two effects: the mixing and the in-cylinder flow motion. Many works have been done in the in-cylinder flow motion such as the effect of swirl and tumble, combustion chamber geometry and spark plug locations [2].

1.4 Intake Manifold

An inlet manifold or intake manifold is the part of an engine that supplies the fuel/air mixture to the cylinder. The primary function of the intake manifold is to evenly distribute the combustion mixture (or just air in a direct injection engine) to each intake port in the cylinder head(s).



Fig. 1.2: Intake Manifold

The ideal intake manifold distributes flow evenly to the piston valves. Even distribution is important to optimize the efficiency and performance of the engine. It may also serve as a mount for the carburettor, throttle body, fuel injectors and other components of the engine. The intake manifold has historically been manufactured from aluminium or cast iron but use of composite plastic materials is gaining popularity. The intermittent or pulsating nature of the airflow through the intake manifold into each cylinder may develop resonances in the airflow at certain speeds. These may increase the engine performance characteristics at certain engine speeds, but may reduce at other speeds, depending on manifold dimension and shape [3].

1.4.1 Static Length Intake Manifold

Static intake manifolds for vehicles have fixed air flow geometry and static intake manifold. With a static intake manifold, the speed at which intake tuning occurs is fixed. A static intake manifold can only be optimized for one specific rpm [3].

1.4.2 Variable Length Intake Manifold

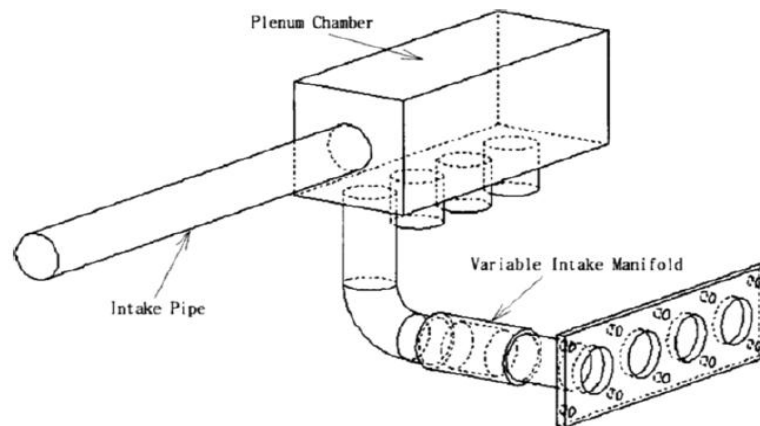


Fig 1.3: Variable length intake manifold

Variable length intake manifold technology uses the pressure variations generated by the pulsating flow due to the periodic piston and valve motion to produce a charging effect. By varying the intake length/volume, we can operate engine over a broad speed range. Various designs for variable intake geometry have met with varying degrees of success. The designs of the variable intake manifolds may be rather complex and expensive, to produce. Difficulty in servicing and a limited range of variable tuning may also be disadvantageous design results of variable intake manifolds [3].

1.5 Modification Scope of Intake Manifold

The main task of an Inlet Manifold is to distribute air inside the manifold runner uniformly, which is essential for an optimized inlet manifold design. The inlet manifold design has strong influence on the volumetric efficiency of the engine. An uneven air distribution leads to less volumetric efficiency, power loss and increased fuel consumption [4, 5]. Depending on the amplitude and phase of pressure waves inside the inlet manifold, filling of cylinders by air can be affected positively or negatively. The amplitude and phase of these pressure waves depend on inlet manifold design, engine speed and valve timing. The unsteady nature of the induction means and the effect of the manifold on charging is extremely dependent upon the engine speed. This is because the entry of

air inside the inlet manifold is a function of varying pulses. Therefore these pulses should be fine-tuned in engine manifolds to give required power [6, 7, 8].

1.6 CFD (Computational Flow Dynamics)



Fig 1.4: CFD Simulated intake manifold [9]

Computational fluid dynamics is a tool to find numerical solution of governing equation using high speed digital computer. So with the availability of powerful computers; the CFD prediction methods for in-cylinder flow of IC engines have become popular. They can give very useful information regarding the flow pattern and has the potential to reduce the total development time of the intake system of an IC engine. Engine manufactures require precise engine design to bring the end product to the market in a short time period and hence CFD codes play an important role in IC engine design. By using the CFD code, flow field can be predicted by solving the governing equations viz., continuity, momentum and energy. The renormalization group theory (RNG k- ϵ) turbulent model is used for analyzing the physical phenomena involved in the change of kinetic energy [9].

1.7 Conclusion

From above introductory part we learn that various factor like fuel selection and engine parts play a crucial role in optimize performance of engine. Compress natural gas give eco-friendly engine with less emission of carbon dioxide and other harmful hydrocarbon ,on other hand intake manifold can give better performance with refine design We also study that how Computational Fluid Dynamics approach simplify design approach for various engine part by solving difficult equation of flow in various part of engine

References

1. Rajbahak H. L, Joshi K. M , Ale. B. B, “Report on vehicular exhaust emission with reference to age of vehicles, road conditions and fuel quality aspects”, SOMEN Paper,(2001).
2. Rosli Abu Bakar , Azhar Abdul Aziz and Mardani Ali Sera, “Effect Of Air Fuel Mixer Design On Engine Performance And Exhaust Emission Of A CNG Fuelled Vehicles”, 2nd World Engineering Congress, Sarawak, Malaysia, july 22-25, (2002).
3. Ceviz M.A and Akın M., “Design Of A New SI Engine Intake Manifold With Variable Length Plenum”, (2010).
4. Safari M, Nasiritosi A and Ghamari M, “Intake Manifold Optimization by using 3D- CFD Analysis,” SAE paper, pp. 32-73, (2003).
5. Wangner Trindade. “Use of 1D-3D Coupled Simulation to Develop a Intake Manifold System,” SAE paper 01-1534, (2010).
6. Marcelo. R. C and Thomas. M.M, “Correlation between Numeric Simulation and Experimental Results on Intake Manifold Development,” SAE paper 36-0274, (2009).
7. Safari. M, “Intake Manifold Optimization by Using 3-D CFD Analysis.,” SAE paper 32-0073, (2003).
8. Negin. M, Reza. E and Siamac. H, “The Effect of Intake Manifold Runners Length on the Volumetric Efficiency by 3-D CFD Model”, SAE paper 32-0118, (2006).
9. Benny Paull and Ganesan V., “Flow field development in a direct injection diesel engine with different”, International Journal of Engineering, Science and Technology, Vol. 2, No. 1, pp.80-91, (2010).

Chapter-2

Literature Review

Introduction

In this chapter, discussion about literature review carried is presented. The literature is mostly related to topics of design effect of Intake Manifold on engine performances.

2.1 Study Categorization on the basis of

2.1.1 Computational fluid dynamics (CFD) analysis

2.1.2 Experimental analysis

2.1.3 Numerical approach analysis

2.1.4 Stress analysis

2.1.1 Basis of CFD simulation

S.Karthikeyan et al [1] In this paper, pressure waves for the intake manifold is simulated using 1D AVL-Boost software, to study the internal air flow characteristic for the 3-cylinder diesel engine during transient conditions. Based on the 1D simulation results, the intake manifold design is optimized using 3D CFD software under steady state condition.

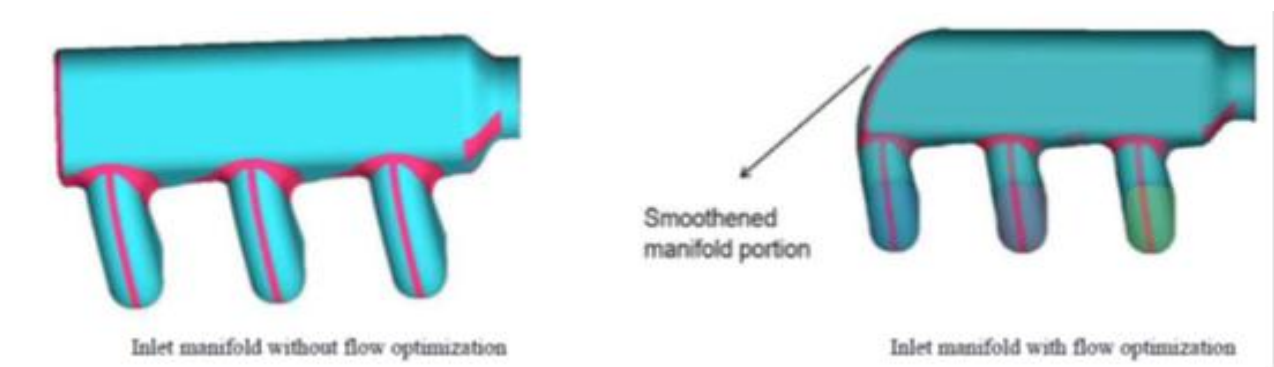


Fig 2.1: Inlet Manifold without and with optimization [1]

From the 1D AVL BOOST software, variation of pressure pulses with various crank angles is obtained for all the three runners at different engine speed conditions and obtaining graph shows that pressure variation is more due to sudden increase in the velocity of incoming air. Therefore intake manifold (IM) geometry near the corners should be made smooth to avoid sudden increase in the pressure waves. Manifold profiles near the corners can be made smooth to avoid the reflecting shock waves with higher velocity as the engine speed increases to 1250 rpm. CFD analysis show that during second cylinder opening, some amount of air is trying to enter into first and third cylinder due to eddies. Flow reversals are present in the plenum, which is the reason for causing an improper distribution of air to all the runners in the initial IM design. But after optimization of the

manifold the variations are reduced and almost uniform amount of air is entering the runners. From the CFD results, 76% mass fraction of air is observed for all the three runners at 1800 rpm. Further experimentally air pressure inside the runners are investigated and increased air pressure of 13% shows that flow of air has increased inside the runner for the optimized IM design. The reduced smoke level indicates better air mixing inside the engine using optimized manifold.

Benny Paul et al. [2] observed the effect of helical, spiral, and helical-spiral combination manifold configuration on air motion and turbulence inside the cylinder of a Direct Injection (DI) diesel engine motored at 3000 rpm. By using the CFD tool (FLUENT), they compared predicted CFD results of mean swirl velocity of the engine at different locations inside the combustion chamber at the end of compression and the turbulence modeled using RNG k- ϵ model stroke with experimental results available in the literature. They also compared the volumetric efficiency of the modeled helical manifold.

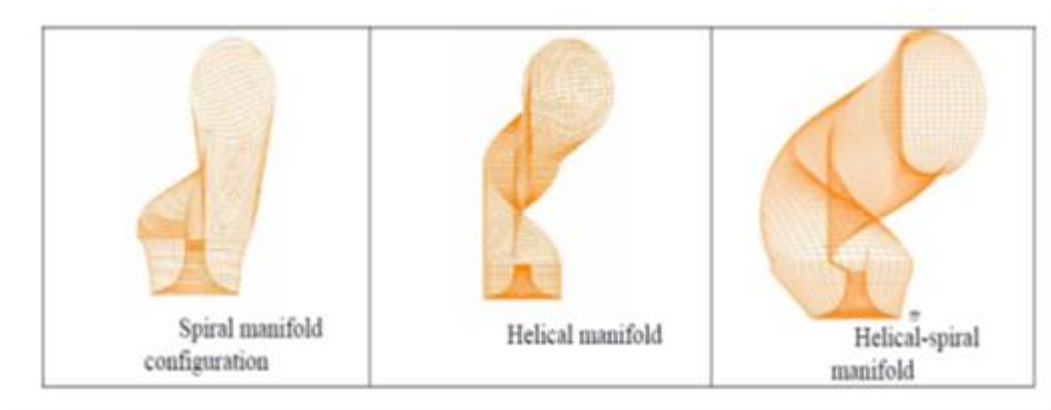


Fig 2.2: Modelled Spiral, Helical, Helical spiral manifolds [2]

After the analysis they notice various things like, the helical-spiral manifold geometry creates higher velocity component inside the combustion chamber at the end of compression stroke. Swirl ratio inside the cylinder and turbulent kinetic energy are higher for spiral manifold. Volumetric efficiency for the spiral-helical combined manifold is 10% higher than that of spiral manifold. Conclusion of result shows that Helical-spiral combined manifold creates higher swirl inside the cylinder than spiral manifold. Helical manifold provides higher volumetric efficiency. Helical-spiral combined manifold provides higher mean swirl velocity at TDC of compression. Hence, for better performance a helical-spiral inlet manifold configuration is recommended by them.

M. A. Jemni et al. [3] presents an investigation of mixture preparation in the intake manifold of a Diesel converted engine into LPG spark-ignition engine operation. Two manifold shapes are used in order to test the adequate design in view of flow and air-gas homogenization. The first is designed according the acoustic-wave-filling phenomena, and the second present an unspecified

design. The model of simulation done by solving Navier-Stokes and energy equations in conjunction with the standard k- ϵ turbulence model, using the 3D CFD code Flow Works.

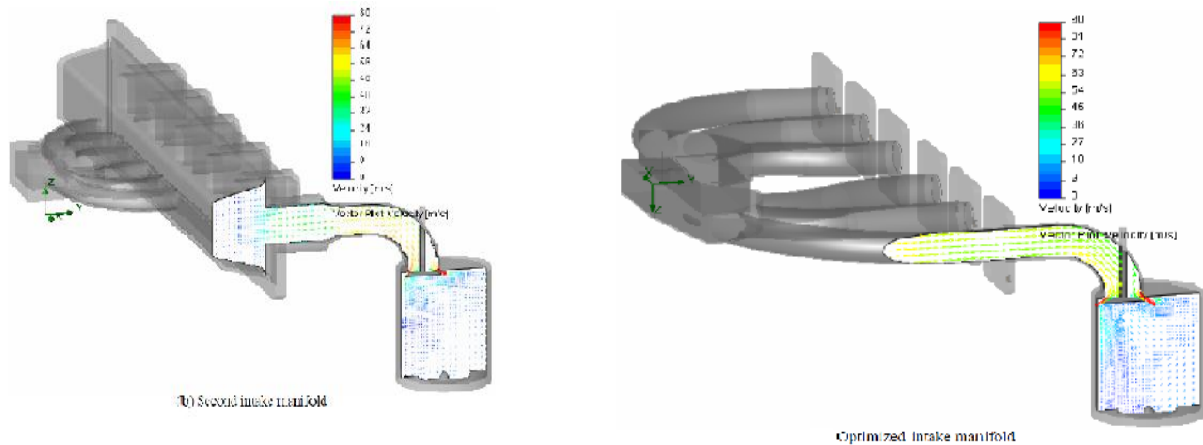


Fig 2.3: Mixer flow in without and without manifold [3]

In Optimized manifold the mixture velocity is nearly equal to 81 m/s passing through the valve and decreases less than 25 m/s, such velocity supports filling. Whereas, this isn't the case in the second manifold, 70 m/s and decrease below 16 m/s. This difference shows the manifold geometry influence on mixture velocity. In runners, a velocity discontinuity is noticed in the second manifold. Its origin is the presence of several dead zones in the geometry. Experiment tests were performed in order to study the intake manifold influence on the engine performance. The air-fuel ratio and the specific fuel consumption are measured and determined. With the optimized manifold, both AFR (air fuel ratio) and SFC (specific fuel consumption) are improved by 7 % and 28 % respectively.

Min-Ho Kim et al. [4] In this, the internal flow characteristics in the intake manifold of a six-cylinder diesel engine are investigated computationally for the variation of spacer and chamber width under steady state.

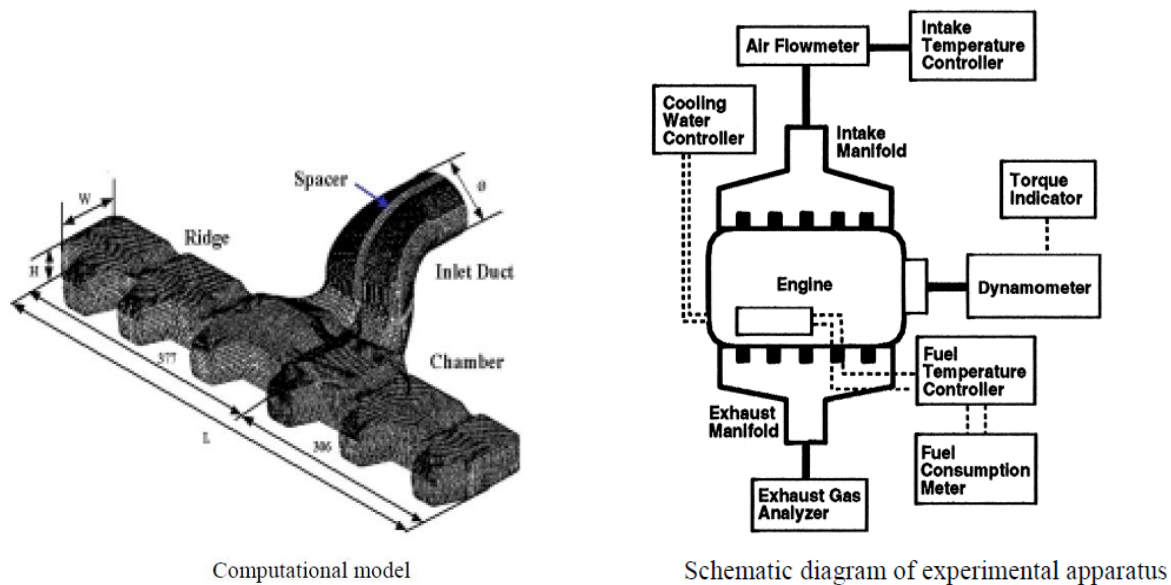
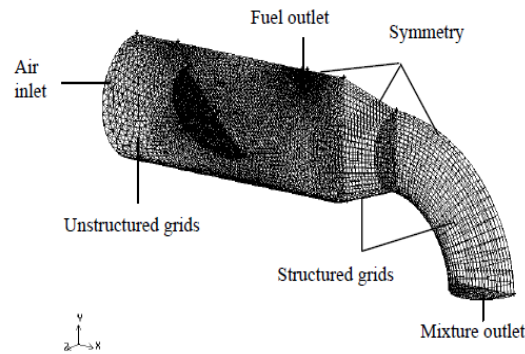


Fig 2.4: Computational modelled of six cylinder engine and schematic diagram of experimental apparatus [4]

Analysis result of relative air distribution, the distribution rate of all ports was in the range of approximately 14%~19%, and the air distribution rate into port No.4 was the least one. Model with spacer is more efficient than the other model without spacer. In the case of the engine performance test, with regards to the fuel consumption rate and smoke at low speed, the case of the model without the spacer decreased more than the model with the spacer. But at high speed, it shows a tendency to increase, contrary to the finding at low speed. In case of the model with the spacer, as the chamber width increased at low speed, the fuel consumption and the smoke level decreased, but increased at high speed. Therefore, in order to develop a high efficiency, low emission engine at high speed, the attachment of a spacer inside the intake manifold and the reduction of the chamber width are required for optimum results.

Luo Ma-ji et al. [5] This paper presents a KIVA-3 code based numerical model for three-dimensional transient intake flow in the intake port-valve-cylinder system of internal combustion engine using body-fitted technique, which can be used in numerical study on internal combustion engine with vertical and inclined valves, and has higher calculation precision. A numerical simulation (on the intake process of a two-valve engine with a semi-sphere combustion chamber and a radial intake port) is provided for analysis of the velocity field and pressure field of different plane at different crank angles. The results revealed the formation of the tumble motion, the evolution of flow field parameters and the variation of tumble ratios as important information for the design of engine intake system.

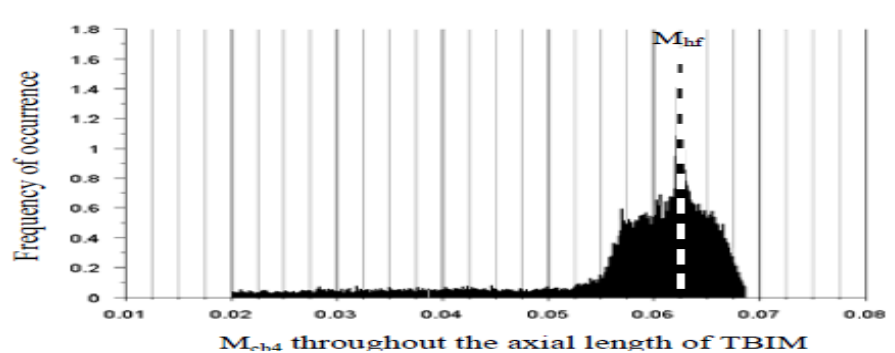
Yvonne S. H. Chang et al. [6] In this work we studied the effect of injection frequency on the mixing in Throttle Body Injection Mixer (TBIM) for a CNG motorcycle through CFD simulation. Injection frequencies of 1, 2, 4, 5 and 7 injections per engine cycle had been investigated using the RNG k- ϵ turbulent model.



Computational mesh system and boundary conditions of TBIM for CFD simulation

Fig 2.5: Mesh of throttle body injection mixer [6]

In addition, the quality of mixing was also investigated through the mixing homogeneity (H_m) in TBIM. The (H_m) was defined as the ability of air and fuel to mix with a uniform mass fraction of methane (M_{ch_4}) in TBIM. So form the effect of various injection frequencies on the mixing quality of TBIM in terms of highest frequency (M_{hf}) and H_m had been studied in this research. A good mixing was that with M_{hf} closed to M_{ch_4} .s and the best H_m at the same time, which was shown by a single contour of M_{ch_4} throughout the mixing region during simulation.



Histogram of M_{ch_4} used to determine M_{hf}

Fig 2.6: Histogram of M_{ch_4} used to determine M_{hf} [6]

Although the H_m was not improved remarkably, the M_{hf} was, however, enhanced dramatically with a varying injection frequency. It was found that the injection frequency of 4 injections per engine cycle was the most optimum one throughout the case studies.

J. N. Kim et al. [7]. In this paper, four strategies were applied for controlling the swirl intensity of intake air. The variation of the intake valve lift induces different swirling and tumbling intensities. A fully three-dimensional model was used to investigate the optimal value for intake valve lift in a CAI (controlled auto ignition) engine. The purpose of this study is to examine the effects of intake port swirl on the overall performance of the CAI engine.

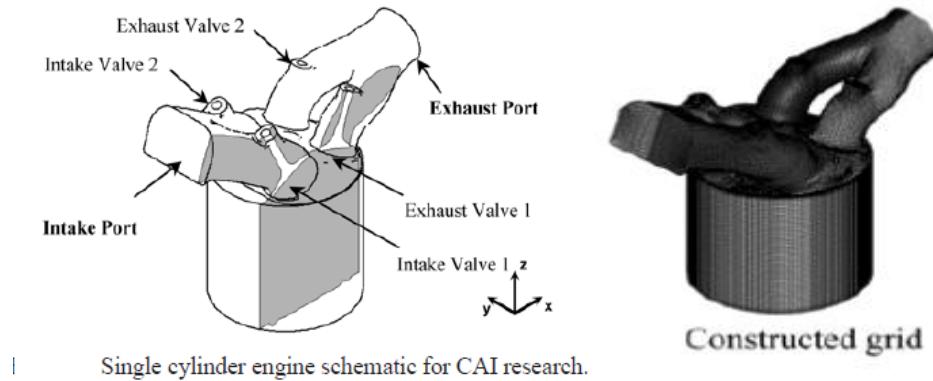


Fig 2.7: Constructed Grid and single cylinder schematic for CAI (control auto ignition) research [7].

A numerical simulation was conducted by using 3D unsteady RANS (Reynolds-Averaged Navier-Stokes), a turbulent Eulerian-Lagrangian particle tracking model. Experimental data for pressure and temperature was provided with other necessary initial and boundary conditions for the fully 3D computation. The experimental data show that some areas with a high internal EGR (exhaust gas recirculation) mass fraction inside the cylinder correspond to relatively high temperature areas. We also found that high fuel concentration and the auto-ignition spots affected each other, and that this effect is especially prominent when the equivalence ratio is low. So with the most homogeneous mixture, the best combustion efficiency is yielded. However, the higher temperature increased the amount of nitric oxide (NO) emissions.

2.1.2 Experimental analysis

Jae-soon Lee et al. [8] A study for the optimal design of the intake system has been performed by varying the factors which can influence the volumetric efficiency, such as the volume of the plenum chamber, the length of the intake manifold and the pipe length between the surge tank and the plenum chamber. Experimental tests have also been carried out to obtain pressure history in the intake manifold & volumetric efficiency over the various engine speeds.

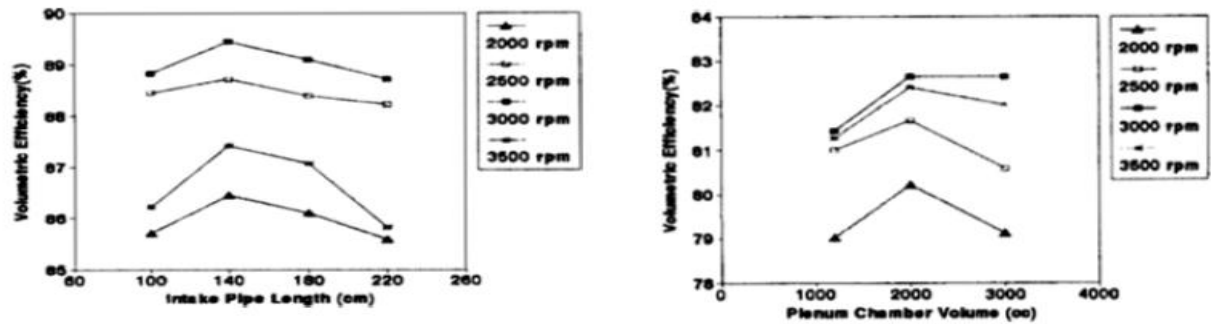


Fig: 2.8 Volumetric efficiency at various speed w.r.t pipe length or plenum volume chamber

The optimum dimensions for the intake system of the test engine are determined as: 140cm for the length of the intake pipe, 2000cc for the volume of the plenum chamber and 90cm for the length of the intake manifold. The volumetric efficiency of the engine with the optimum intake system obtained through this study is about 4 percent higher than that of the original system.

B. Murali Krishna et al. [9] The main objective of this work is to study the in-cylinder fluid flow field characteristics of a single-cylinder engine to see the effect of intake manifold inclination at equivalent rated engine speed using Particle Image Velocimetry (PIV) under various static intake valve lift conditions. From the results, it is seen that the in-cylinder flow structure is greatly influenced by the intake manifold inclinations irrespective of intake valve lift. Maximum Turbulent Kinetic Energy (TKE) was highest at full intake valve lift irrespective of the inclination. Also, the maximum TKE was the highest for 600 intake manifold inclination compared to other inclinations irrespective of the intake valve lift at equivalent rated engine speed.

A. Martínez-Sanz et al. [10] The objective of this work was to develop a new design of a high performance intake manifold through a combination of CAD and FEM. First a FEA model was done, which included a complete thermal and structural analysis of the new intake manifold and the contact area between the aluminum coupling, using the combined tools of CATIA, ANSYS WORKBENCH, MATHCAD. Then several composite prototypes were made and analyzed. New materials field also in this idea was developed in order to study the different possibilities available to build an intake manifold. Aluminum was finally decided to be used due to its great thermal properties and the low weight in comparison with some other materials like steel. A new problem appeared when it was needed to calculate the way of joining this intermediate coupling to the runners. The right solution of problem was to join the both parts with an adhesive. In this case, the contact stress is minimum and the fatigue calculation is suitable for the implementation.

D. V. Boikov et al [11] The design of the intake passage has a considerable influence on organization of the processes of mixture formation and combustion in an engine. In the course of operation of either diesel or carburetor engines, carbonaceous deposits are formed in the intake ports of the cylinder heads and in the fillets of the intake valves. These deposits distort the profile of the intake passage, with adverse effects on its characteristics and on the operability of the engine. After various test we studied direct discharge of fuel combustion products from the cylinder into the intake passage is not the dominant factor determining the quantity of carbonaceous intake deposited and it depend upon the pressure of intake manifold and the crankcase.

Gary D. Bourn et al. [12] Objective was to investigate the perceived imbalance in airflow between power cylinders in two-stroke integral compressor engines and develop solutions via manifold redesign. A laboratory GMVH-6 engine and virtual 2 stroke software used for simulation and design. Several conceptual manifold designs and retro-fits to the existing manifolds were developed. Development of these designs was driven by results from GMVH-6 engine test results which show the perceived air imbalance to not be as great as originally presumed. Therefore, two concepts were offer for potential air balance improvement and be insensitive to random geometric variations. The first concept was a side branch absorber retro-fit to the exhaust manifold. The second concept was an intake manifold modification or redesign that would improve flow to each cylinder. Simulation and geometric analysis results indicated that a large portion of the perceived air imbalance was caused by geometric variation .After experiment, the GMVH-6 test engine has exhibited an 11 percent difference in compression pressure between the highest and lowest cylinder. A one-dimensional simulation model was constructed for the GMVH-6 engine using Virtual 2-Stroke® software. The model was validated to measured data from cylinder 1L and used for analysis and design. The model was used for sensitivity studies of the geometric variations and found they account for approximately 50 to 60 percent of the compression pressure spread

Rosli Abu Bakar [13]In this paper research will focus on developing an advanced intake system for CNG fuelled engine. This study comes up with a design of mixer and a swirl-device that produced the combination of pressurized and turbulent flow in the intake process. A research mixer that combined a venturi-burner principles with three variables; 2,4,8 and 16 number of hole surrounding the mixing arena, input angles (300, 400,500 and 600) and output angles (200, 300, 400 and 500). A swirl-device has two variable; numbers of revolution (1, 1.5, and 2) and angle of plane (150, 300, 450 and 600). All models then fabricated and tested in a CNG engine performance test rig. Other than this they study turbulent flow and finds that tumble is simpler system compare

than that of swirl. Turbulent flow produced by squishing also improved the burning rates, which resulted in improvement of thermal efficiency (Evan). Their conclusion on different things are, The venturi-burner mixer is approved to increase the intake pressure hence improve the combustion performance resulted in advanced the engine power. The combination of 600 of inlet angle and 300 of outlet angle with 8 holes is proven to increase the engine performance to up to 5% that made it closer to the gasoline standard engine performance. The swirl-device located at the intake port is verified to generate the swirl flow that improve the combustion performance and improved intake pressure flow and enlarged the combustion flame speed in intake system increase of 8% of power output. Exhaust Emission of CNG is very less compared to that of gasoline.

Mardani Ali Sera et al. [14] In this report , experiments were carried out to investigate the effect of air/fuel mixer on the engine performance and exhaust emission of a CNG fuelled engine. Three types of mixers were fabricated to create the turbulent effect of an air-fuel mixture. The modification is based on the mixing characteristics and turbulent coefficient. In this investigation, the CNG fuelled engine is not optimized. In order to get the optimum results, the CNG operation required some specific condition such as: high compression ratio, advance ignition timing, supercharge or turbocharge condition, intake valve close timing and a suitable air fuel ratio. Three types of mixers are shown below.

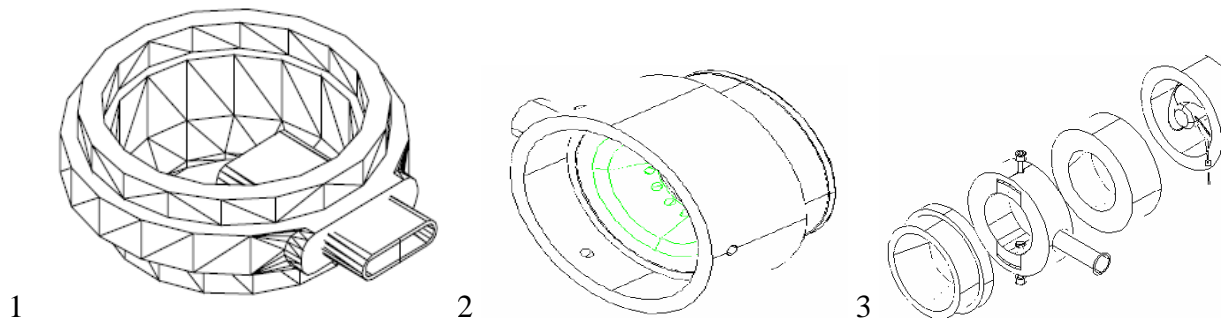


Fig 2.9: Mixer [14]

The experimental results showed that Mixer 3 has the highest pressure rise compared to Mixer 1 and 2, respectively. Mixer 2 was slightly lower compared to Mixer 1. The experiment proved that the petrol has a higher engine performance, hence pressure rise, compared to CNG operation. Difference between these happens due to lower density effect and un-appropriate operating conditions. This phenomena may happens due to, The turbulent flow increased the homogenous mixture that affected the better combustion performance and in the case of Mixer 2, with smaller outlet area it has given the lower fuel supply that produces the lower pressure rise. The experiments also showed that the air fuel ratio affected the CNG engine performance. The highest air fuel ratio gives the highest pressure rise, hence the highest engine performance. Higher air fuel ratio also increased the thermal efficiency of the engine. Since CNG fuel has a higher flammability,

implementation of higher air fuel ratio, in some cases even lean and ultra-lean burn will make a higher benefit.

M.A. Ceviz et al. [15] This paper investigates the effects of intake plenum length/volume on the performance characteristics of a spark-ignited engine with electronically controlled fuel injectors. In the engine with multipoint fuel injection system using electronically controlled fuel injectors has an intake manifold in which only the air flows and, the fuel is injected onto the intake valve. Since the intake manifolds transport mainly air, the supercharging effects of the variable length intake plenum will be different from carbureted engine. Engine performance characteristics such as brake torque, brake power, thermal efficiency and specific fuel consumption were taken into consideration to evaluate the effects of the variation in the length of intake plenum.

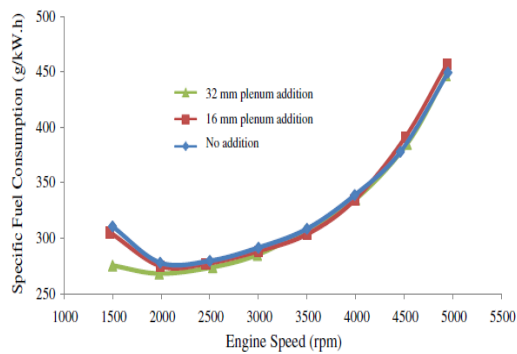
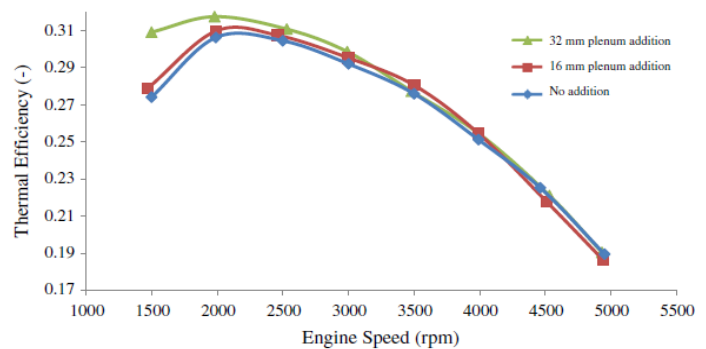


Fig. 3. Variation of specific fuel consumption with engine speed for three different intake plenum volumes.



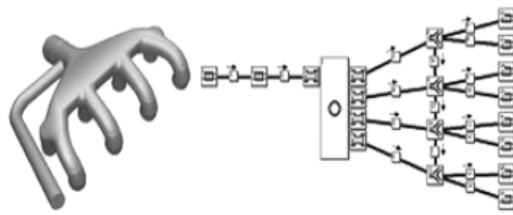
Variation of thermal efficiency with engine speed for three different intake plenum volumes.

Fig 2.10: Variation of specific fuel consumption and thermal efficiency with engine speed for three different intake plenum volumes[15]

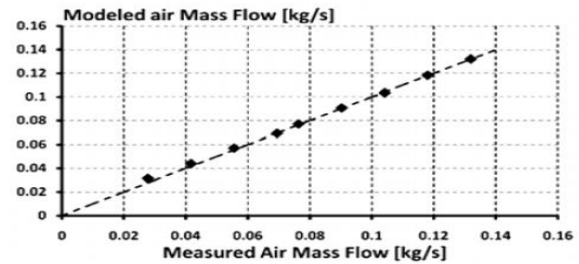
The results showed that the variation in the plenum length causes an improvement on the engine performance characteristics especially on the fuel consumption at high load and low engine speeds. According to the test results, plenum length must be extended for low engine speeds and shortened as the engine speed increases.

A. J. Torregrosa et al. [16] presents a methodology for diesel engine intake line analysis that combines specific element tests and modeling. The purpose of this methodology is to determine the impact of intake lines, or newly designed intake elements, on the volumetric efficiency of internal combustion engines while avoiding expensive on-engine tests. The preliminary design for an intake line should be based on keeping pressure losses to a minimum. Intake manifold tuning can increase the air mass flow without increasing the boost pressure, thus mitigating all of the aforementioned problems. Methodology proposed in this paper for obtaining the intake line model and the approach used for the model assessment. This paper proved that it is possible that the simple flow and

impulse tests of the elements composing an intake line are sufficient to characterize the behavior of the whole system.



1 Engine 1 manifold.



Modeled vs. measured air mass flow through engine 1 manifold.

Fig 2.11: Engine manifold and modelled vs. measured air mass flow through engine manifold[16]

The presented methodology can also be used to assist in the redesign process of any element in the intake line. It is possible to test the prototype in the impulse and flow test rig and to integrate the models in the engine model, thus allowing estimation of the effect on engine breathing. Finally, this paper showed the modeling solution to different intake system elements, such as resonators, intercoolers and manifolds.

Zuoyu Sun et al.[17]. Swirling is very important phenomena used for efficient burning of fuel. Generally swirling is needed at the end of intake manifold.so introducing good swirler at the end of intake manifold increases the performance of the engine. In this paper, the authors design four types of swirler including one straight-shaped swirler and three arc-shaped swirlers. In order to research the fundamental characteristics of swirler, the authors make series of experiments researches. The total researches can be divided into three stages: in the first stage, steady flow tests are carried for researching the swirl capability and the discharge capability of swirler from the macro-level; in the second stage, flow fields in the cylinder are measured by Particle Image Velocimetry (PIV) technique in the water analog tests for researching the swirl performance from the micro-level; at last stage, the tested swirler is installed on a certain type of actual diesel engine for studying whether swirler can improve the engine operation performance noticeably. The results show that this new device can induces intake swirl efficiently and can improve fuel economy at on an optimized swirl ratio.

AwangIdris et al.[18]Investigated the fluid characteristic effect in the engine cylinder of four-stroke direct injection diesel engine converted to port injection dedicated compressed natural gas (CNG) engine spark ignition using computational engine model for steady-state and transient simulation. The simulation results of fluid characteristics are shown the characteristics of in

cylinder volumetric efficiency profile, percent burned mass, fuel/air ratio, fuel flow profile, total fuel consumption and total fuel energy entering to cylinder in variations engine speeds. After the study air-fuel characteristics results shown that increasing engine speed in port injected CNG engine will be decrease the air-fuel characteristics such as cumulative mass fuel injected, cylinder volumetric efficiency,

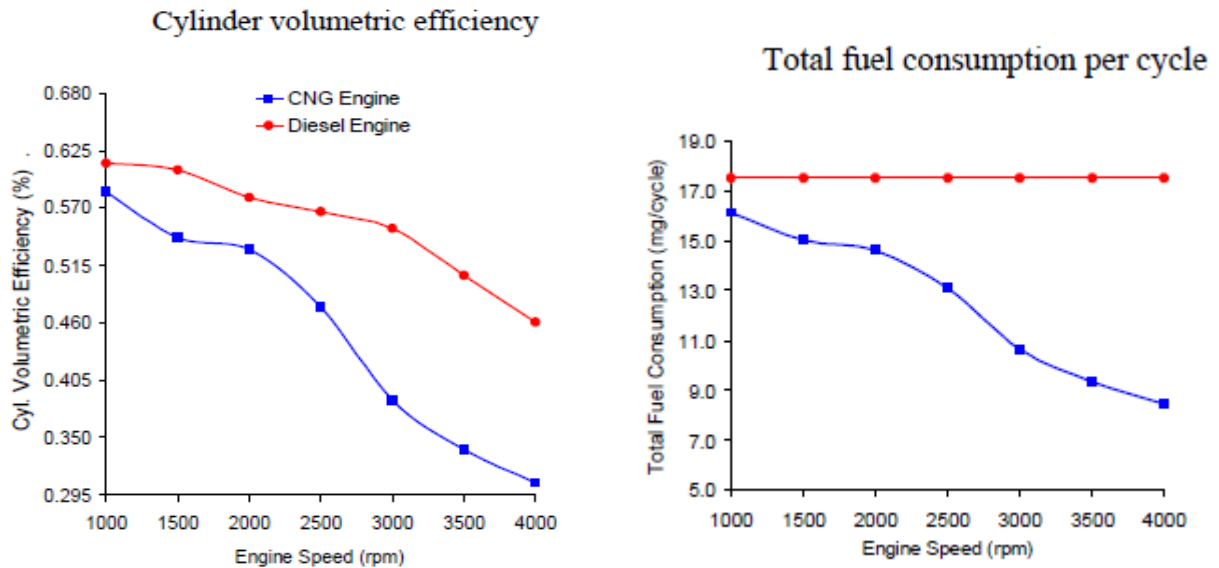


Fig 2.12: Cylinder volumetric efficiency and total fuel consumption per cycle for CNG and diesel engine[18]

Increasing engine speed in port injected CNG engine will be increase the air-fuel characteristics such as mass flow rate from intake valve, percent burned mass at cycle start and fuel/air ratio in cylinder. The air-fuel performance characteristics in cylinder of port injection CNG engine commonly is lower than the base diesel engine, but the percent burned mass.

2.1.3 Numerical analysis

David Chalet et al. [19] Simulation of pressure waves in inlet and exhaust manifolds of internal combustion engines remains challenging. In this paper, a new model is presented in order to analyze these pressures waves without the use of a one-dimensional description of the system. It consists on studying the system using a frequency approach. The principle of the dynamic flow bench used here is to create an initial steady flow rate through the tested part and then to interrupt the flow very quickly in approximately 0.5 m/s. The inlet system is then characterized by its geometrical characteristics as well as the fluid characteristics. The new model is then used in order to simulate the pressure waves into a 1-m pipe which is connected to a driven engine acting as a pulse generator. Inlet and exhaust manifolds can be studied by a one-dimension approach by solving the Euler equations. The analysis of the volumetric efficiency of an internal combustion

engine can also be obtained by the means of a frequency analysis .After studying the result, it appears that in the previous parts the gas temperature and the gas velocity have a significant impact on the pressure wave evolution and as a consequence on the model. A new model equation is given,

$$p = p_{atm} + p_{loss} + \bar{p}$$

$$\frac{d^2\bar{p}}{dt^2} + 2\frac{1}{1-\frac{u}{as}}\varepsilon\left(1-\left(\frac{u}{as}\right)^2\right)\sqrt{\frac{T}{T_{ref}}}\omega_o\frac{d\bar{p}}{dt} + \left[\left(1-\left(\frac{u}{as}\right)^2\right)\sqrt{\frac{T}{T_{ref}}}\omega_o\right]\bar{p} = \Gamma\frac{du}{dt}$$

This is a direct link between the air flow velocity and the pressure. This new approach gives the possibility to reduce the computational times. Further investigations can be made in order to describe a complete inlet manifold of a multi-cylinders engine.

Han Wenyan et al.[20] In this paper the effects of both intake manifold length and valve timing on the torque, volumetric efficiency and fuel consumption are investigated To overcome the conflicts between low speed and high speed engine performance, variable valve timing(VVT) strategy is also investigated.. In modeling process, Wiebe's law for heat release behavior in the cylinder and Woschni's correlation for heat transfer to cylinder wall are modeled separately in simulation. Designing the intake system by taking into account the gas dynamic effect can result in the considerable torque improvement and it's called tuned induction. With the increase of intake manifold length, the maximum volumetric efficiency tends to lower speed and decreases earlier at high speed .So it conclude that Intake manifold length has a significant effect on volumetric efficiency and torque, long manifold increases them at middle speed but decreases at high speed. Backflow during valve overlap period occurs at high Speed problem overcomes variable valve timing (VVT).Matching valve timing with intake manifold length using gas dynamic effect can obviously improve engine torque and BSFC at low and middle speed.

Hyoun-Jin et al. [21].Proposes an optimal design scheme to reduce the noise of the intake system by using support vector regression (SVR) techniques. In general, the intake noise is low frequency noise below 500Hz. The booming noise generated by the intake noise transferred to the interior of the vehicle has an uncomfortable impact on riding quality. The length and radius of each component of the current intake system were selected as input variables and the L_{18} table of orthogonal arrays was adapted as a space-filling design $L_{18}(2^1 \times 3^7)$. The simulation of parameter design utilized an orthogonal array design. In order to evaluate the design and levels, the experiments satisfying the condition were done. With these simulated data, we can estimate parameters in support vector regression by solving a nonlinear problem and finding an optimal level for the intake system by using support vector regression.

Table 2.1

Condition	Overall TL(Transmission Losses) (dB)
Current	34.83
SVR	38.87

Support vector regression (SVR) as an alternative technique for approximating complex engineering analyses. Therefore, we consider support vector regression, which is suitable for computer experiments, to improve the performance of the system with a low cost and time savings. SVR can be applied to solve highly correlated and nonlinear problems. Therefore, SVR is suitable for this reduction of the intake noise. SVR gives noticeable results and is a preferable way to analyze the intake system. The overall level of transmission loss (TL) by the optimal designs using SVR with the meta-heuristic method was increased by 4.04 (dB) as compared with the current designs.

V. V. NAGA DEEPTHI et al.[22]. This paper aims at studying the effect of air swirl generated by directing the air flow in intake manifold on diesel engine performance. The turbulence was achieved in the inlet manifold by grooving with a helical groove of size of 1mm width and 2mm depth of different pitches to direct the air flow in inlet manifold. The tests are carried with different configurations by varying the pitch of the helical groove from 2 mm to 10 mm in steps of 2 mm inside the intake manifold. The measurements were done at constant speed of 1500 rpm. The results are compared with normal engine (without helical groove). The results of test show an increase in air flow, increases the brake thermal efficiency, mechanical efficiency and decrease in HC and Co emissions. On the other hand the volumetric efficiency is dropped by about 5%.

Martin Musial [23]-In this we study the how the plenum and runner design effect our engine system and what design parameters we have to considered when choosing a car or design a car engine. According to design it should be plenum volume at least 1.5 to 2 time the engine displacement example 2 liter engine need intake manifold with plenum chamber of 3 to 4 liter displacement. Other side engine need different air requirement at different speed (RPM).For large ports and runner slower the velocity, large ports can flow more air but at the expense of velocity. Runner shape and length determine velocity and correlate to ramming effect. Ramming effect increase volumetric efficiency and in turn horse power and torque. Tapering the runner increase the efficiency of engine , by experiment it study that the air thorn entry and 2.5 deg tapered runner

fared much better than the radius entry 5 deg tapered runner making almost 22 hp more and overall 18 lb –ft torque at only 14 psi.

2.2 Formulae Work:

Volumetric Efficiency (η_v):-It indicates the breathing ability of the engine. How much air an engine can take it and utilization of the air is what going to determine the power of the engine, Mathematically it is defined as the volume flow rate of air into the intake system divided by the rate at which the volume is displaced by the system

$$\eta_v = \frac{m_a}{\rho_a V_{disp} N/2} \quad (i)$$

Where ρ_a is the inlet density

For petrol engines η_v is between 80% to 85 % where as for diesel engine it is between 85% to 90%. Gas engines have much lower η_v since gaseous fuel displaces air and therefore the breathing capacity of the engine is reduced.

2.3 Gap analysis:

On the basis of various papers studied it is found that the geometry of intake manifold put huge impact on the engine performance. Proper or adequate turbulence during mixing give good working result of engine. Pressure in the intake manifold very important factor for even distribution of Charge in all four cylinders. For this, geometry of intake manifold to be improved, steps are taken to improve this uneven distribution, but after doing lot of works there is still gaps in design of intake manifold those are need to be improve for proper even distribution of fuel in cylinders.

References:

1. Karthikeyan S, Hariganesh R, Sathyanadan M, Krishnan S, “ Computational Analysis Of Intake Manifold Design And Experimental Investigation On Diesel Engine For LCV”, ISSN: 0975-5462, vol. 3 no. 4, (March 2011).
2. Benny Paul, Ganesan V, “Flow Field Development In a Direct Injection Diesel Engine With Different Manifolds”, IJEST: Vol. 2, No. 1, pp. 80-91, (2010).
3. Jemni M .A, Kantchev G, Abid M. S, “Intake Manifold Design Effect On Air Fuel Mixing And Flow For An LPG Heavy Duty Engine”, IJEE:Vol. 3, Issue 1, pp.61-72, , (2011).
4. Min Ho Kim, Woo In Chung, In-Bum Chyun, “Three-dimensional Flow Characteristics and Engine Performance for the Geometry Modification of Intake Manifold in Multi-cylinder Diesel Engine”, Seoul 2000 FISITA World Automotive Congress, June 12-15, (2000).
5. Luo Ma-Ji, Chen Guo-Huo and MA Yuan-Hao, “Three Dimensional Transient Numerical Simulation For Intake Process In The Engine Intake Port Valve Cylinder System” , ISSN 1009 - 309.5 Journal of Zhejiang University SCIENCE V.4, No.3, PP .309- 316, May- June, (2003).
6. Yvonne S. H. Chang, Z. Yaacob and R. Mohsin, “Computational Fluid Dynamics Simulation of Injection Mixer for CNG Engines”, San Francisco, U.S.A, WCECS 2007, October24-26, (2007).
7. Kim J.N, Kim H.Y, Yoon S.S, S. D. SA, “Effect of Intake Valve Swirl on Fuel-Gas Mixing And Subsequent Combustion In a CAI Engine”, Vol. 9, No. 6,pp. 649–657 , (2008).
8. Jae-soon Lee, Keon-Sik Yoon, “A Numerical and Experimental Study on the Optimal Design for the Intake System of the MPI Spark Ignition Engines” , KSME Journal, Vol 10, No. 4, pp.471-479, (1996).
9. B. Murali Krishna, A. Bijucherian, and J. M. Mallikarjuna, “Effect of Intake Manifold Inclination on Intake Valve Flow Characteristics of a Single Cylinder Engine using Particle Image Velocimetry” , World Academy of Science, Engineering and Technology 68 (2010).

10. Martínez-Sanz A., Sánchez-Caballero S, Viu A. and Pla-Ferrando R. , “ Design And Optimization Of Intake Manifold In A Volkswagen Car” ANNALS of the ORADEA UNIVERSITY. Fascicle of Management and Technological Engineering, Vol X (XX) ,NR2, (2011).
11. Boikov and M. A. Grigorev. “Fouling Of Diesel Engine Intake Passage With Carbonaceous Deposits” , Chemistry and Technology of Fuels and Oils, Vol.33,No.3,(1997).
12. Gary D. Bourn, Ford A. Phillips and Ralph E. Harris, “Technologies To enhance The Operation of Existing Natural Gas Compression Infrastructure Manifold Design For Controlling Engine Air Balance, DOE Award No. DE-FC26-02NT41646, (2002).
13. Rosli Abu Bakar, “Design and Development of a New CNG (compressed natural gas) Engine”, Vol. 72351, (2002).
14. Mardani Ali Sera, Rosli Abu Bakar and Azhar Abdul Aziz, “Effect Of Air Fuel Mixer Design On Engine Performance And Exhaust Emission Of A CNG Fuelled Vehicles”, WEC 22-25 (July2002).
15. Ceviz M.A and Akin M., “Design of a new SI engine intake manifold with variable length plenum” ELSEVIER JOURNAL, (2009).
16. Torregrosa A. J, Galindo ., Guardiola C and Varnier O, “Combined Experimental And Modeling Methodology For Intake Line Evaluation In Turbocharged Diesel Engines International Journal of Automotive Technology, Vol. 12, No. 3, pp. 359–367,(2011).
17. Zuoyu Sun, Xiangrong Li, Wei Du, “Research on Swirler for Intake Induced Swirl in DI Diesel Engine” , 2011 International Conference on Computer Distributed Control and Intelligent Environmental Monitoring, , DOI 10.1109/CDCIEM.2011.525 ©2011 IEEE, (2011).
18. AwangIdris, Semin, Abdul Rahim Ismail and Rosli Abu Bakar, “Engine Cylinder Fluid Characteristics of Diesel Engine Converted to CNG Engine” ISSN 1450-216X Vol.26 No.3, pp.443-452, (2009).

19. David Chalet, AlexandreMahe, JérômeMigaud and Jean-François Hetet, “A frequency modelling of the pressure waves in the inlet manifold of internal combustion engine” ELSEVIER JOURNAL,(2011).
20. Han Wenyan, Xu Sichuan and Deng Xiao, “Optimization Design of Intake Manifold and Valve Timing of Gasoline Engine Based on AMESim Code” IEEE (2011).
21. Hyoun-Jin Sim, Sang-Gil Park, Yong-Goo Joe and Jae-Eung Oh, “Design of The Intake System for Reducing The Noise In The Automobile Using Support Vector Regression” Journal of Mechanical Science and Technology 22 pp.1121-1131, (2008).
22. Prasad S. L. V, Pandurangadu V, Prathibha Bharathi V. V. and Naga Deepthi V. V., “Experimental Study Of The Effect Of Air Swirl In Intake Manifold On Diesel Engine Performance” International Journal of Multidisplenary Research and Advances in Engineering (IJMRAE), ISSN 0975-7074, Vol. 3, No. I pp. 179-186 (January 2011).
- 23 Martin Musial , “Intake manifold design and testing”. Modified Magazine, pp.117-120.

CHAPTER 3

OBJECTIVE

From the literature review and past development in the field of engines, there are still some areas where improvement can be done for achieving good performance. Intake manifold plays very crucial role in achieving high efficiency as well as in emission control. Compressed natural gas engine has low volumetric efficiency due to gaseous nature of fuel, Due to this drawback CNG engine have low performance then gasoline engine.

In intake manifold of CNG engine due to geometry there is variation in pressure, which in turn affect the flow velocity of Charge in runners of intake manifold, in all runners we have different velocity and as a result mixture distribution is not uniform.

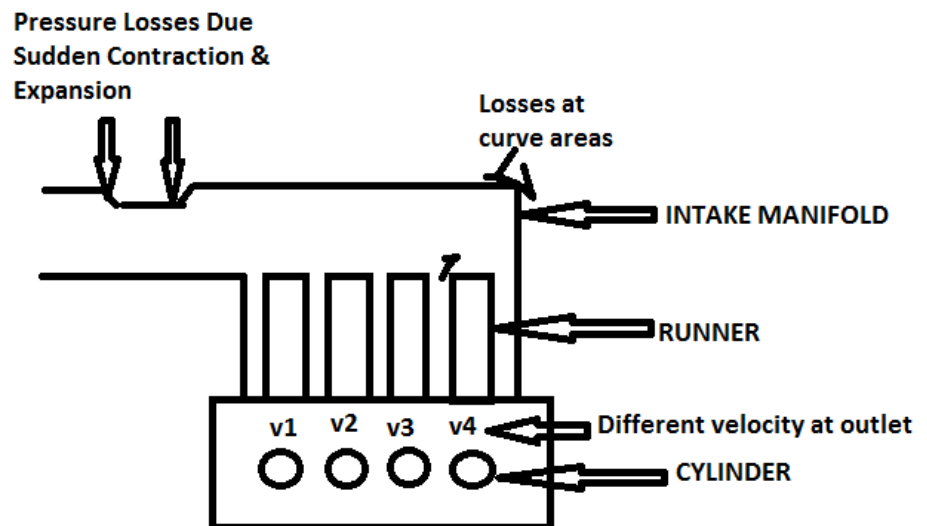


Fig 3.1: Losses comprising figure of intake manifold

So objectives of research are:

- To reduce the pressure losses in intake manifold,
- To achieve equal velocity of flow in all runners of intake manifold, and
- To propose a good geometry model for intake manifold to improve the performance of engine.

CHAPTER 4

METHODOLOGY

To achieve a best intake manifold of compressed natural gas engine, a methodology is proposed as given below:

- Experimental analysis of intake manifold,
- Modelling-Creating prototype of given intake manifold in Design software (Pro-E) for stress analysis,
- CFD analysis of the intake manifold,
- Comparison of experimental and CFD analysis, and
- Propose modifications for a given intake manifold.

4.1 Experimental analysis of intake manifold:

All the petrol engines can be converted into CNG engine using CNG kit so that component of these two (petrol/CNG) engines is not different too much except some modification if necessary. After the survey it is found that there is not much difference in the geometry of intake manifold system of Maruti Wagnor except the way of charging the engine that's why for experimental setup, the intake manifold of Maruti Wagnor is selected for the study and shown in Fig.5.1



Fig.4.1: Intake Manifold

4.1.1 Tools and Instruments:

For making experiment setup various instruments are required like Anemometer(Fig 4.2) to measure the air flow, U-tube manometer(Fig 4.4) to check the pressure at inlet and outlets ,Blower (Fig 4.3) ,Regulator (Fig 4.6) to control the flow of air, Thermometer (Fig 4.7) and various attachments example pressure taps, pipes attachments(Fig 4.5) etc.



Fig: 4.2 Anemometer



Fig: 4.3 Blower

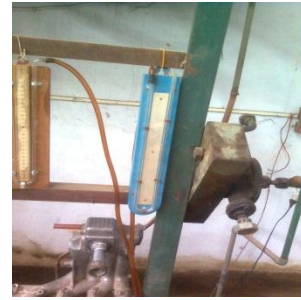


Fig: 4.4 U tube manometer

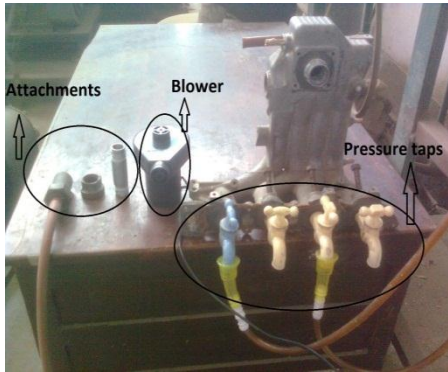


Fig 4.5 Pressure taps, pipe attachments

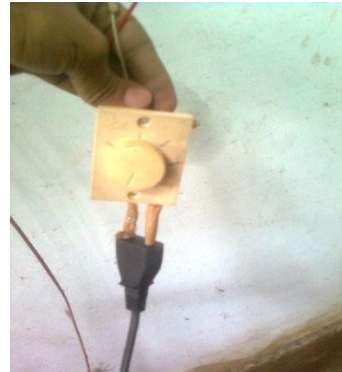


Fig: 4.6 Regulator



Fig 4.7 Thermometer

4.1.2 Experimental setup:

The setup shown below (Fig 4.8) is for taking out the reading at outlets of intake manifold with Anemometer and U-tube manometer.



Fig: 4.8 Experiment setup

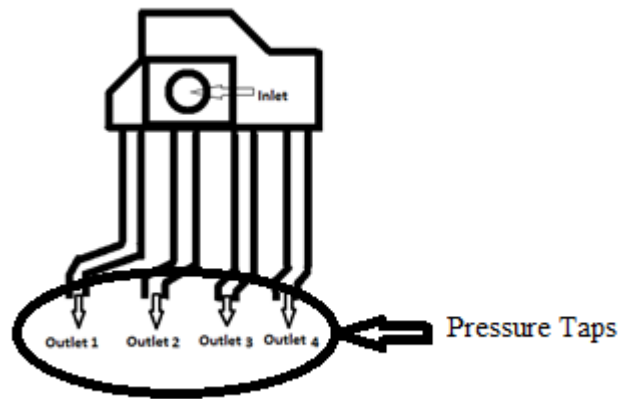


Fig 4.9: Intake manifold block diagram

With attachments:

Intake diameter= 20mm

Outlet nozzle diameter= 5mm

4.1.3 U-tube manometer:

This device (Fig 4.10) used to measure the pressure at various pressure taps of intake manifold. We have here four cylinder intake manifold, so pressures corresponding these runners outlet lead us to measure the mass flow rate and velocity at outlet.

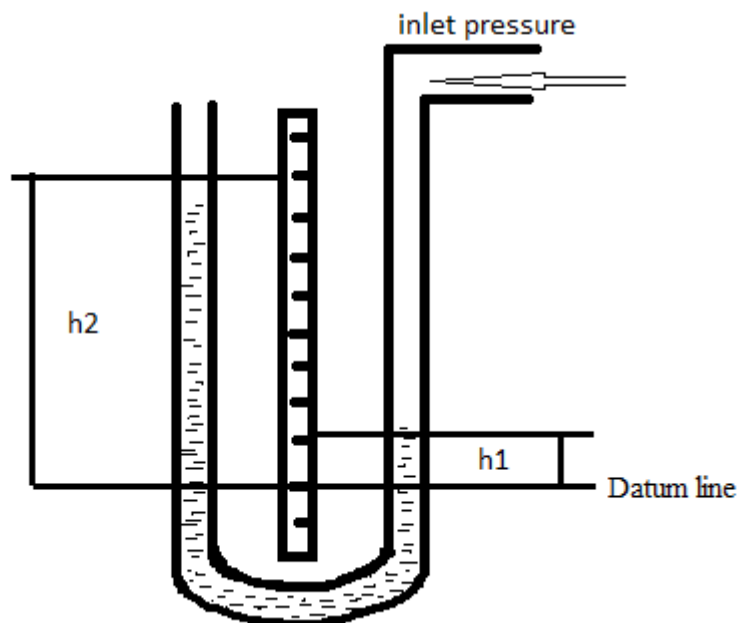


Fig: 4.10 Measurements in U-Tube Manometer

Formula used:-

As the pressure is same for horizontal surface, there for pressure above the horizontal datum line in the left column and in the right column of U-tube manometer should be the same.

$$\text{Pressure in left column} = P + \rho_1 \times g \times h_1$$

$$\text{Pressure in right column} = \rho_2 \times g \times h_2$$

Equating to pressure we get

$$P = \rho_2 \times g \times h_2 - \rho_1 \times g \times h_1 \quad (i)$$

P=Gauge pressure

h_1 =Height of light liquid above the datum line

h_2 =Height of heavy liquid above the datum line

ρ_1 =Density of light liquid

ρ_2 = Density of light liquid

Experimental consideration:

Air density is much lower value than the water so the density of air is neglected compared to water. so the density ρ_2 equal to ρ_1 and that is density of water.

Some other formulas used:

i) Area(A)

$$A = \pi r^2$$

r = Radius

(ii)

ii) Mass flow rate (Q)

$$Q = \rho AV$$

A=Area

(iii)

iii) Pressure (P)

$$p = \rho RT$$

ρ = Density

R=Gas constant=287 j/(kg×k) for air

T=Temperature (K)

p =Pressure

iv) Bernoulli's equation:

$$\frac{P_1}{\rho_1 g} + \frac{v_1^2}{2g} + z_1 = \frac{P_2}{\rho_2 g} + \frac{v_2^2}{2g} + z_2 + \text{losses} \quad (iv)$$

By applying the above operation we can calculate the velocity at inlet and different velocity at outlet

4.2 Modelling of Intake manifold system:

We Model 3-D geometry of an intake manifold (Fig 4.11) in design software and getting modelled part for an analysis.

Physical appearance of intake manifold:

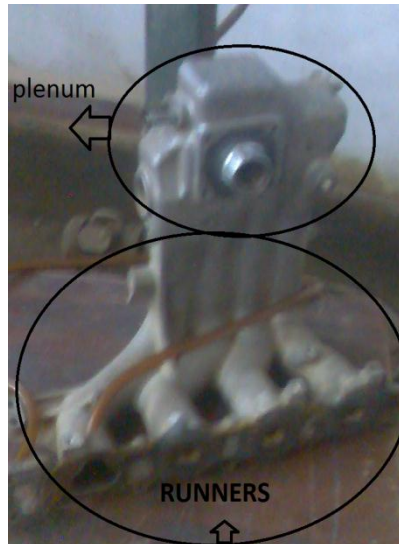


Fig: 4.11 Physical appearance of Intake manifold

Modeller don't have the classified geometry of the intake system there for by using the reverse engineering process the geometry is modelled in software as precise as possible for exact similarity to our physical model. Here In reverse engineering process modeller simply measures the various dimensions of intake system and draws the geometry first then created model in software.

4.2.1 Destructive testing:



FIG: 4.12 Destructive test of intake manifold

For exact modelling it necessary to examine the interior design of manifold that's why destructive test (Fig 4.12-4.13) also perform on manifold to see the various hidden projection and curves inside of manifold.



Fig: 4.13 Hidden inside projection

4.2.2 Dimensioning of manifold:

The dimensions of a simple intake manifold are taken. The manifold has been tested by blowing air at different velocities through it and when we have the results from its physical testing we can compare these results by using these basic dimensions.

Basic dimension of intake manifold system are:

Table: 4.1

Section	Dimension (Diameter)
Intake	38 mm
Outlet 1(inner diameter)	30 mm
Outlet 2 (inner diameter)	30 mm
Outlet 3 (inner diameter)	30 mm
Outlet 4 (inner diameter)	30 mm
Thickness	2.5 mm

4.2.3 Prelim design drawing:

Design and modelling software (Pro-E) used to draw model of intake manifold system similar to physical one. The drawing of modelled is shown in Fig 4.14 and final design is shown in Fig 4.15.

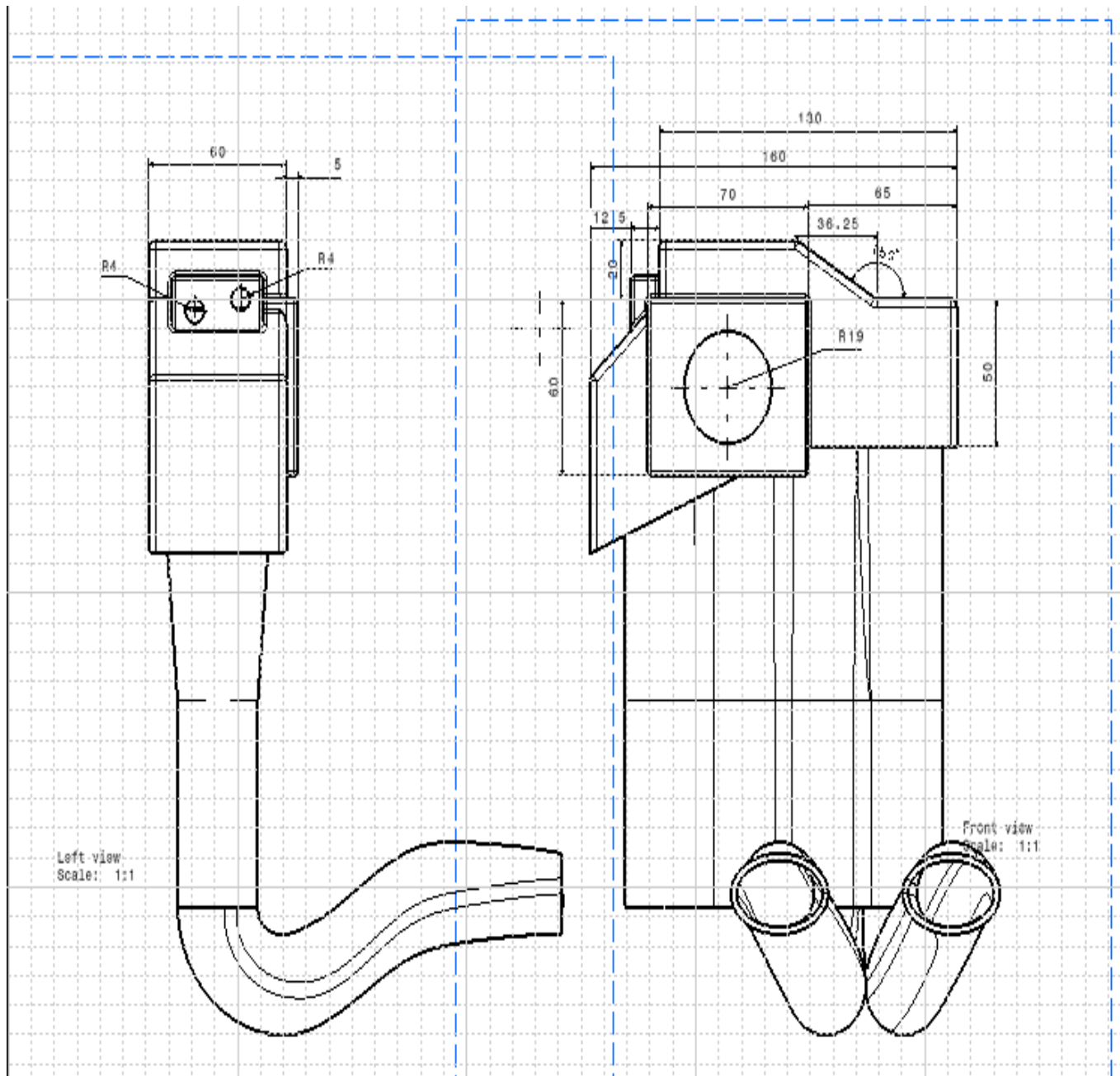


Fig: 4.14 Prelim design drawing of original intake manifold

4.2.4 Final model drawing:

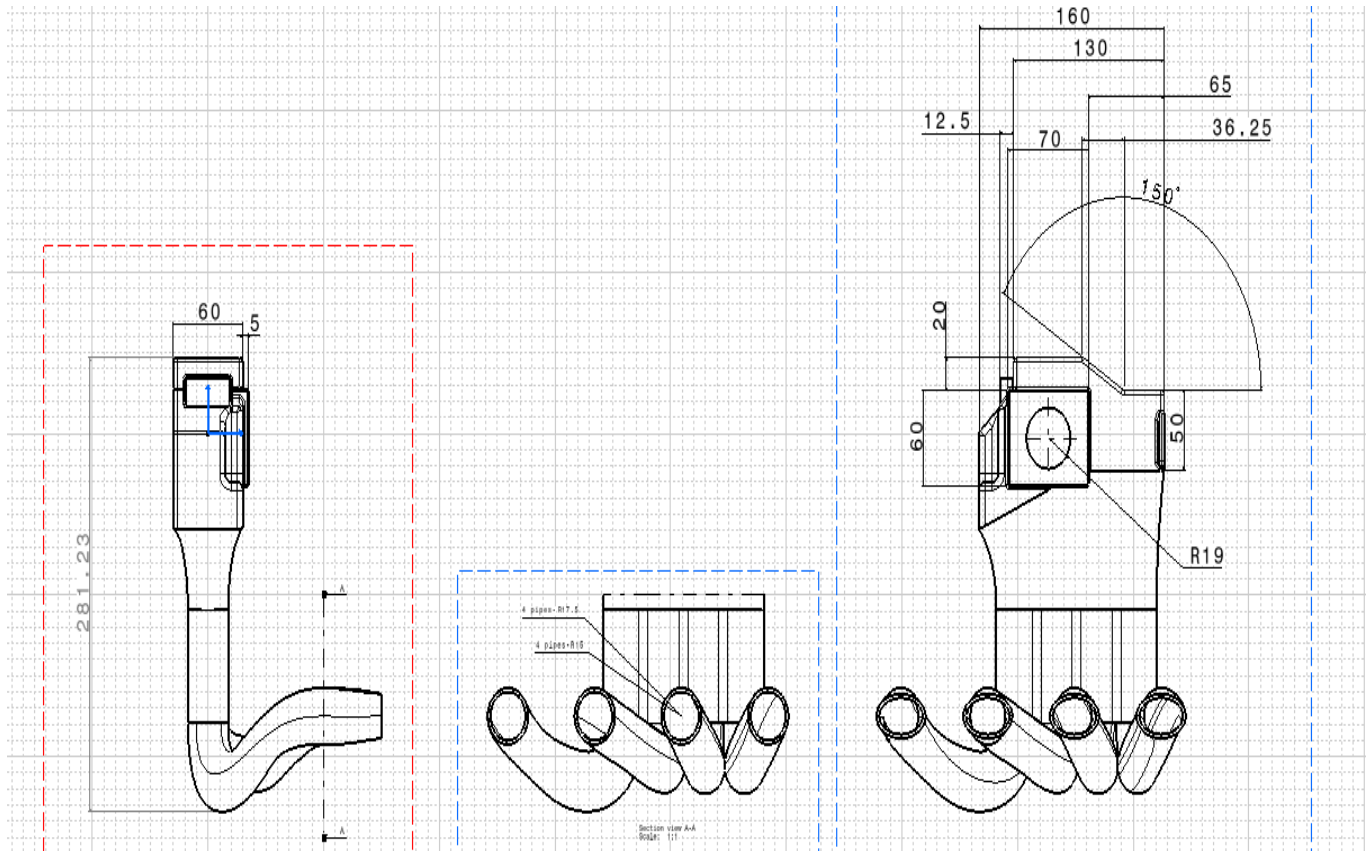


Fig: 4.15 complete Drawing of intake manifold

4.2.5 3-D view of final model of intake manifold:

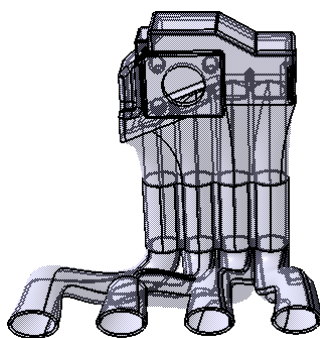


Fig: 4.16 Front view

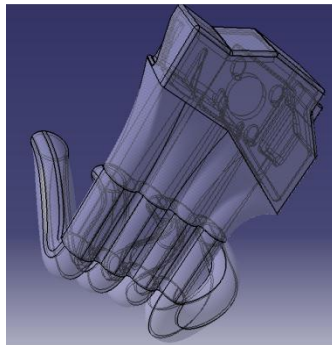


Fig: 4.17 Back view

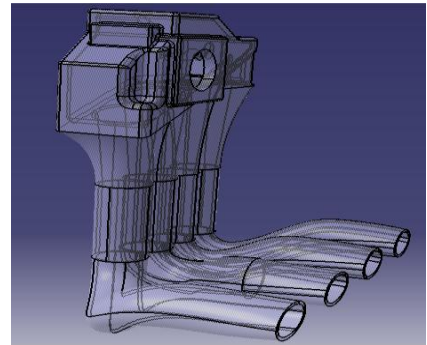


Fig: 4.18 Left side view

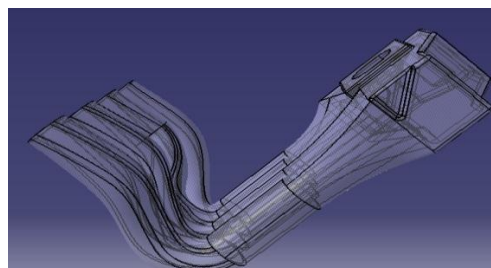


Fig: 4.19 Right side view of intake manifold

4.2.6 Stress Analysis of Model:

Under certain circumstances which could potentially create a high-pressure impulse inside the manifold or backfire due to the mistimed spark events occur that why it is necessary for a designer that its design is suitable for tolerating the effect of backfire because due to back fire a huge amount of pressure is built up in the intake manifold and chance of bursting of intake manifold increases. Manifold geometry is a factor in the magnitude of a backfire event. Simple four cylinder log type manifolds at atmospheric pressure typically generate pressures of approximately five bar. Pressures of eight bar have been seen with complex manifolds incorporating long runners and multiple plenums under the same conditions. Intake material properties are very important factor while choosing a intake manifold for car, most of IM (intake manifold) manufacturer using aluminium alloys due to its high strength and high temperature resistance properties[3].Some time ribs and fillets are used in intake manifolds but ribs and fillets to the model gave no improvement to the stress state, so it is necessary to review all parameters in manufacturing process [2] There are number of alloys of aluminium exist but best one suited for intake manifold are:

- 1) 2xx.x alloy (Aluminium + copper alloy) :Ultimate tensile strength of 130-450 MPa [1][5].
- 2) 3xx.x alloy (Aluminium + manganese + copper): Ultimate tensile strength of 130-275 MPa [1][5].
- 3) 6xx.x alloy(Aluminium + magnesium + silicon): These alloy are best suited for intake manifold and there ultimate tensile strength is 125-400 MPa.[1][5],

For 2xxx to 8xxx, the last two digits identify different aluminium alloy of group. The second digit indicates alloy modification. A second digit of zero indicates the original alloy and integer 1 to 9 indicate consecutive alloy modification [5].

Yield Strength=the stress which give a permanent deformation of 0.2%.

Ultimate Strength=the stress which give rupture.

4.2.6.1) Mathematical stress analysis:

$$p = \frac{2s \times t}{D_o \times S.F} \quad (i)$$

P=Max Working pressure

S=Material strength

T=Wall thickness

D_o =Outside diameter

S.F=Factor of safety (1.5 to 10)

S=130-450 MPa

T=2.5mm

$D_o=35.5\text{mm}$

S.F=2

1bar= 10^5 pascal= 10^5 N/m^2

$$p = \frac{2 \times 450 \times 2.5}{35.5 \times 2} = 31.69 \text{ N/mm}^2 = 31.69 \times 10^6 \text{ N/m}^2$$

From above result we can say that our design is in permissible stress condition .Above design can tolerate the pressure of 5 bar without bursting.

b) Computational Stress analysis of intake manifold:

The main aim of stress analysis here is to check the thickness and material (Fig 4.20) suitability of intake manifold against bursting pressure in bad conditions, so except doing the analysis of whole geometry we considered one runner (Fig 4.21) of intake manifold for analysis.

Bursting force =3 bar

Thickness of intake manifold=2.5 mm

Materials.1

Material	Aluminium
Young's modulus	7e+010N_m2
Poisson's ratio	0.346
Density	2710kg_m3
Coefficient of thermal expansion	2.36e-005_Kdeg
Yield strength	9.5e+007N_m2

Fig: 4.20 Material detail

Static Case
Boundary Conditions

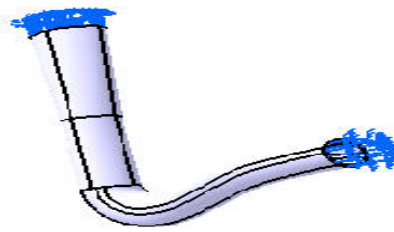


Fig: 4.21 Static case of one runner of intake manifold

After applying internal pressure results are:

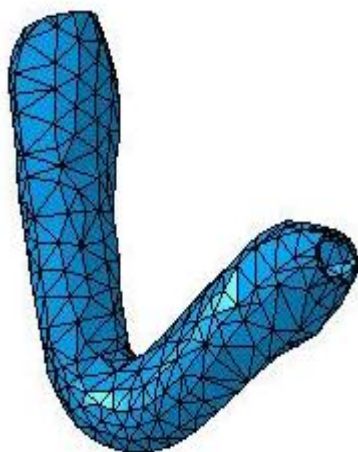


Fig: 4.22 Deformed mesh

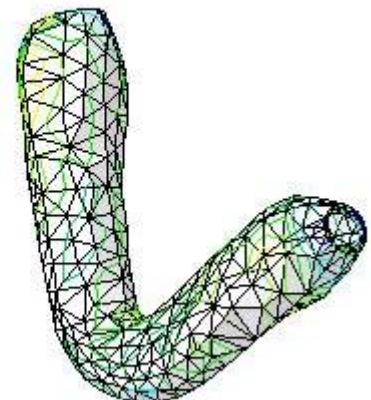
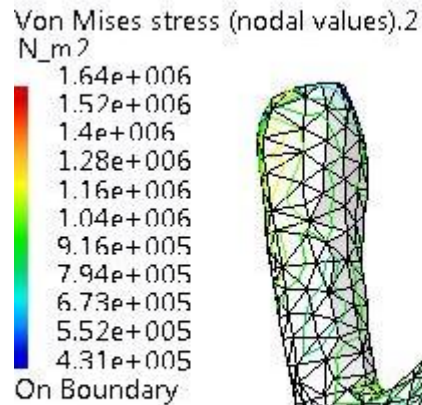


Fig: 4.23 Von miss stress analysis

Result of stress analysis:

From above both mathematical and computational analysis (Fig 4.22-4.23) it is noticed that the thickness of given intake manifold is far greater than required thickness to bear the pressure of 3 to 5 bar that is even for very extreme cases. But the intake manifold is manufacture through the sand casting technique which has manufacture low limit of .15 in. (4mm),but thickness as little as 1.00 in. to 0.090 in. (2.5mm to 2mm) can be achieved[4], That's why the thickness is not go more below to the 2.5 mm.

Conclusion:

The thickness of given intake manifold already at its lowest casting limit (2.5mm),if the thickness is go below from it the casting defects become more prominent and various pressure losses occurred in design.

References:

- 1) Introduction to Aluminum Alloys and Tempers ,chapter 6 “Applications for Aluminum Alloys and Tempers.
- 2) Curioni S, Lanzellotto T, Minak G, Zucchelli A, Caridi D. A, “Bursting Tests Of A Short Fibre Reinforced Composite Air Intake Manifold” DIEM Alma Mater Studiorum – Università di Bologna, (2008).
- 3) Raetech corperation “Composite Intake Manifold Backfire Testing” 4750 Venture Dr. Suite 100 Ann Arbor, MI 48108.
- 4) John Gilbert Kaufman and Elwin L Rooy, “Aluminium Alloy Casting: Properties, Processes and Applications” , December (2004).

Website:

- 5) www.azom.com/aticle.aspx?ArticleID=2863, “Aluminium-Specification, Properties, Classification and Class, Supplier Data by Aalco, Source:Aalco, Date Added: May 17, 2005| Updated: Aug 11, (2011).

4.3 CFD analysis of intake manifold:

In CFD simulation following steps is follow:

1. Simplifying the geometry.
2. Setting up the model.
3. Meshing of the model which includes decomposition of complex geometry.
4. Post processing (analysing meshing quality).
5. Defining boundary conditions (for CFD solver).

Meshing: The accuracy of the results depends highly upon the meshing quality. Thus the choice of meshing scheme (grid pattern) is very important for fluent to provide accurate results. For doing simulation of the intake manifold model we have to do first meshing ,in this technique the flow domain is converted or split into various subdomain primitives like hexahedral and tetrahedral. Care must be taken to ensure proper continuity of solution across the common interfaces between two subdomains, so that the approximate solutions inside various portions can be put together to give a complete picture of fluid flow in the entire domain. We use the tetrahedral mesh for this purpose which imposed on model.

4.3.1 Strategy for study of intake manifold:

For finding out losses and optimized geometry, study will take place on following three models of same intake manifold with small modifications:

- 4.3.1.1 Model 1(Fig 4.24)- Flow model of original geometry.
- 4.3.1.2 Model 2(Fig 4.25) - Model without internal projection at plenum
- 4.3.1.3 Model 3(Fig 4.26) - Model without projection at plenum and without curve at end of runners

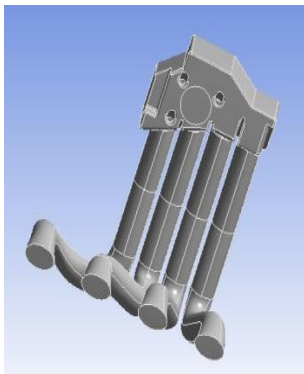


Fig: 4.24 Model-1

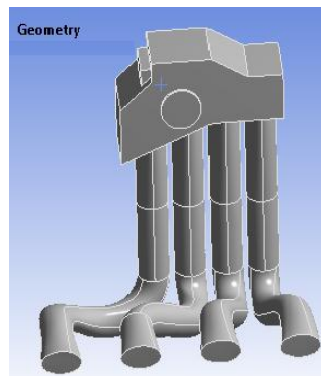


Fig: 4.25 Model-2

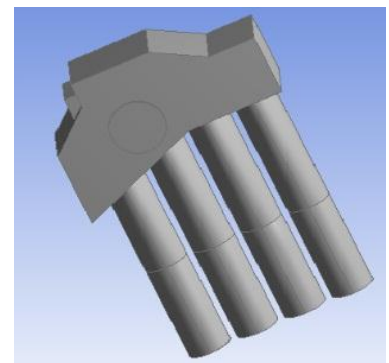


Fig: 4.26 Model-3

Internal projection
In flow model

4.3.1.1 Actual flow model (Model-1):

a) Geometrical Model:

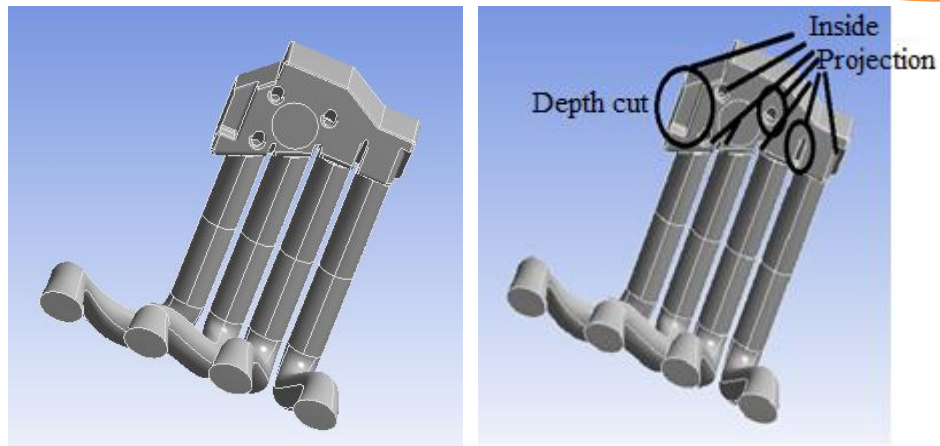


Fig: 4.24 Model-1 (Actual Flow Model of Geometry)

b) Meshing of model-1:

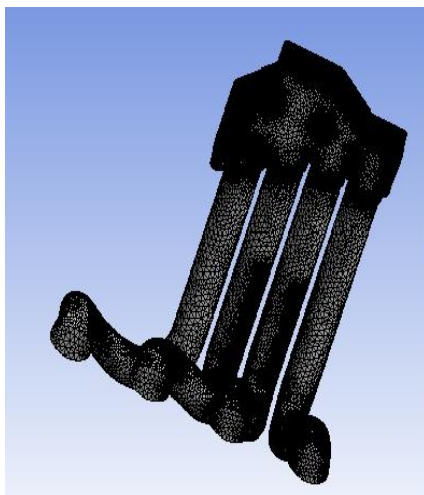


Fig:4.27 Meshing of flow domain (Model-1)

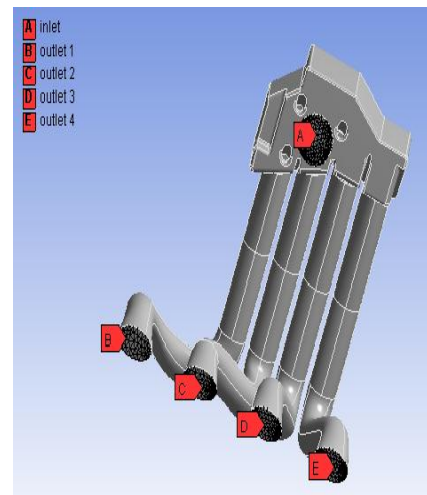


Fig :4.28 Name selection(Model-1)

Model-1(Fig 4.24) is compared with the other model to check the losses at various part of original geometry. After doing the meshing (fig 4.27) and named selection (fig 4.28), it show that the tetrahedral meshing is employed on the model and in what manner part of model is used for inlet and outlet The skewness, no of nodes and no of element is always checked for better quality of results.

Meshing properties of model -1:

Table 4.2

Nodes	483849
Elements	2593187

c) **Simulation result:**

In order to achieve a more accurate solution it required to increase the criteria for convergence from a default value of 0.001 to $e-04$ so as to reduce the possibilities of errors by a vast percentage. Iteration take lot of time due complicated geometry and high turbulence in flow model.

At Inlet velocity-18 m/s

Residual plot:

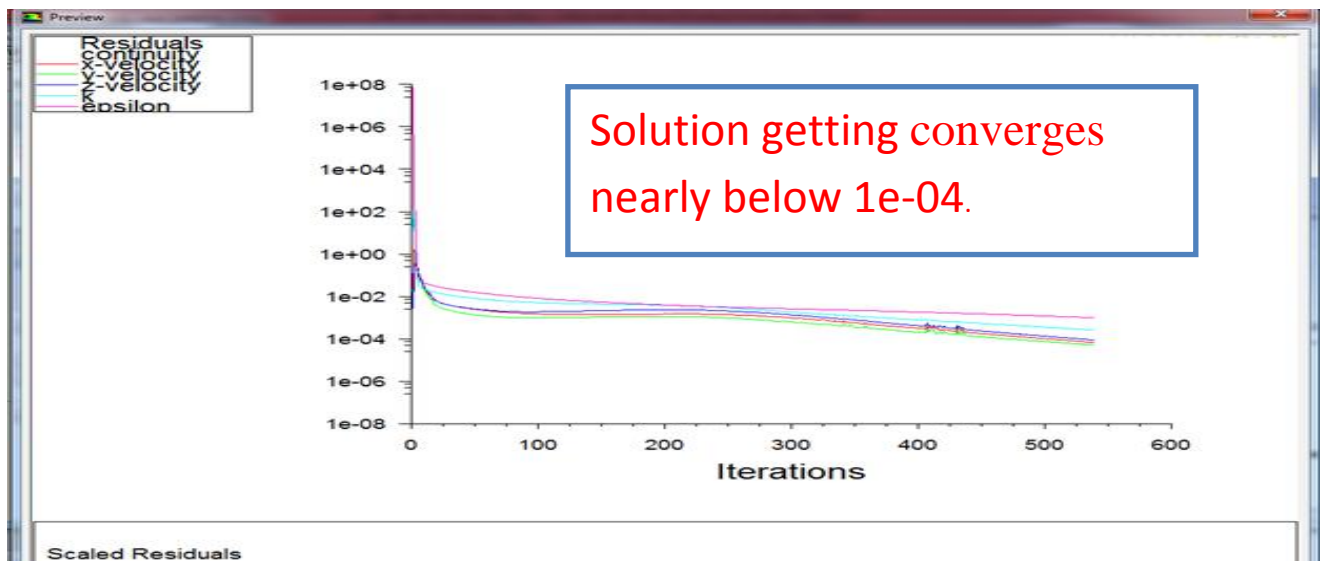


Fig 4.29 (a) Residual plot (Model-1,18m/s)

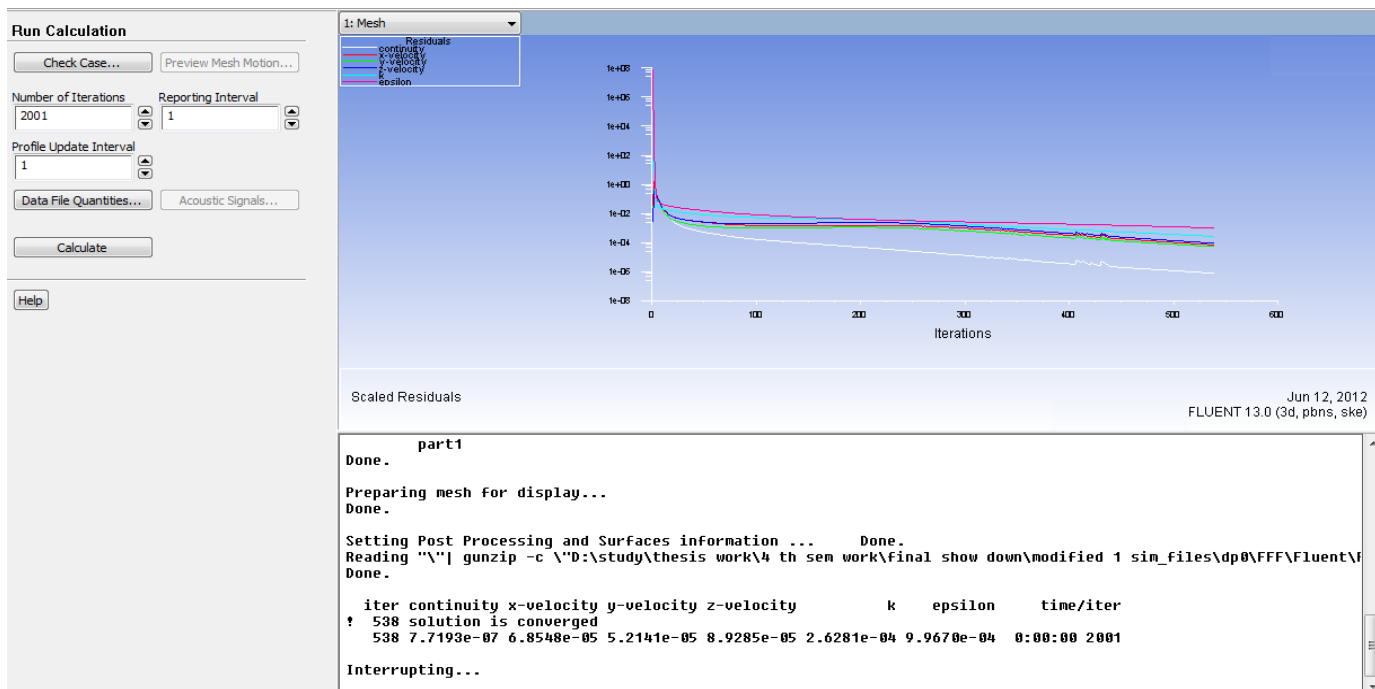
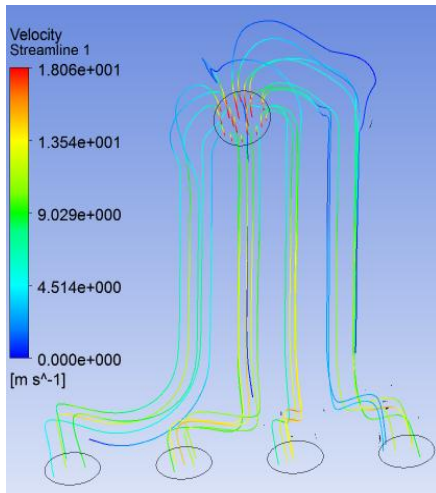


Fig: 4.29 (b) Convergence of Residual Plot (Model-1,18m/s)

The solution is converged (Fig4.29 a-b) after the 538 no of iteration in between $e-04$ to $e-06$

Front view



Back view

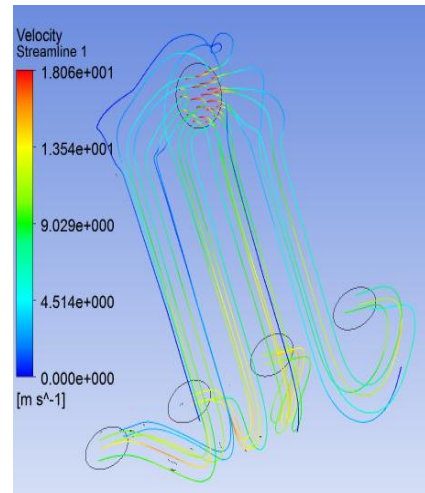


Fig: 4.30 Velocity streamlines Front view and Back view (Model-1,18m/s)

Velocity streamline view (fig 4.30) tells how the velocity streamlines flow inside the intake manifold and in which side or part more and less velocity of stream occurs.

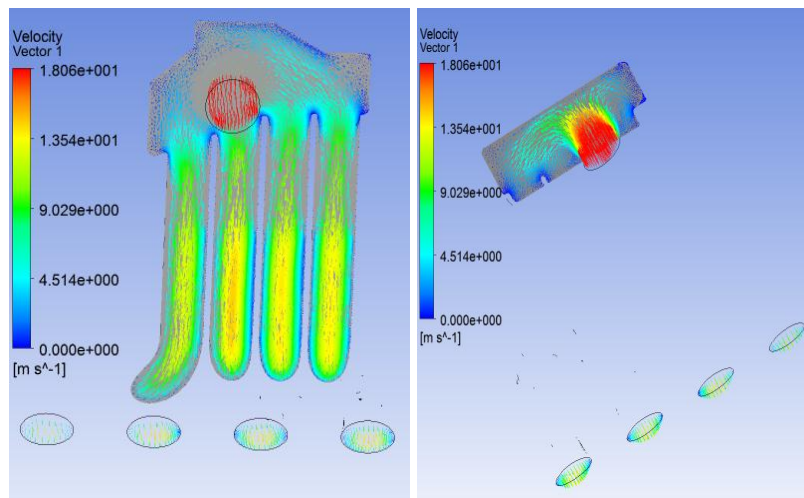


Fig: 4.31 Velocity vector (Model-1,18m/s)

Velocity vector (Fig 4.31) give the good idea of velocity distribution inside the intake manifold, where is a velocity loss occur and where is velocity is more. It clearly visible that velocity at the surface and at the runners stiffener is very less. The velocity losses occur at the unwanted projection inside of plenum.

Fluent result at outlet are

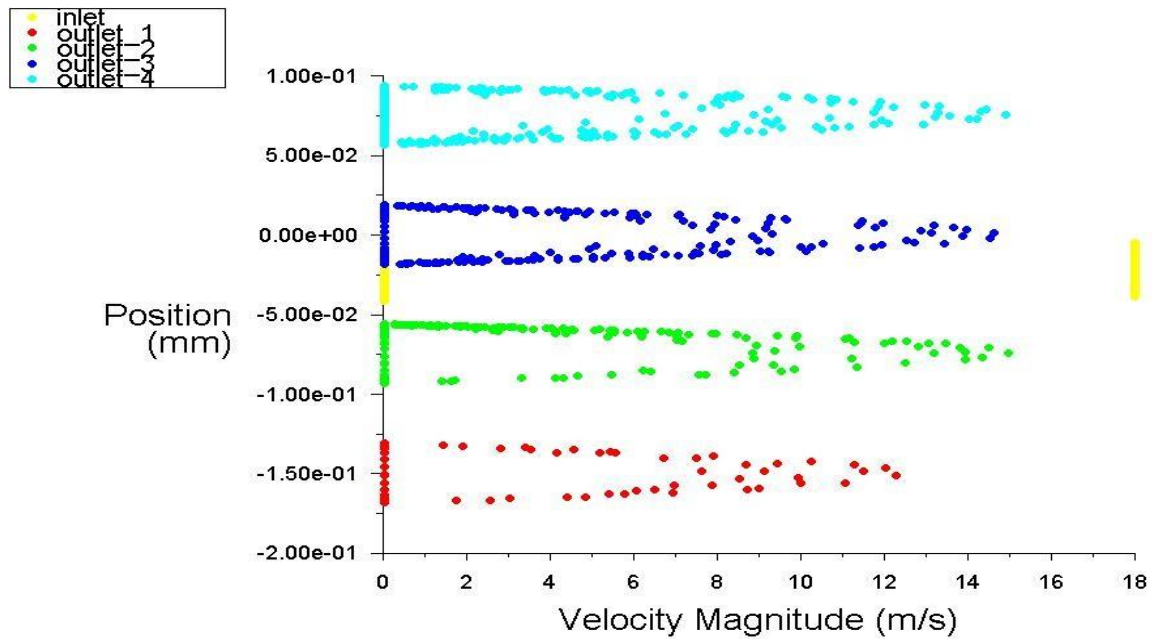


Fig 4.32(a): Velocity profile at different outlets (Model-1,18m/s)

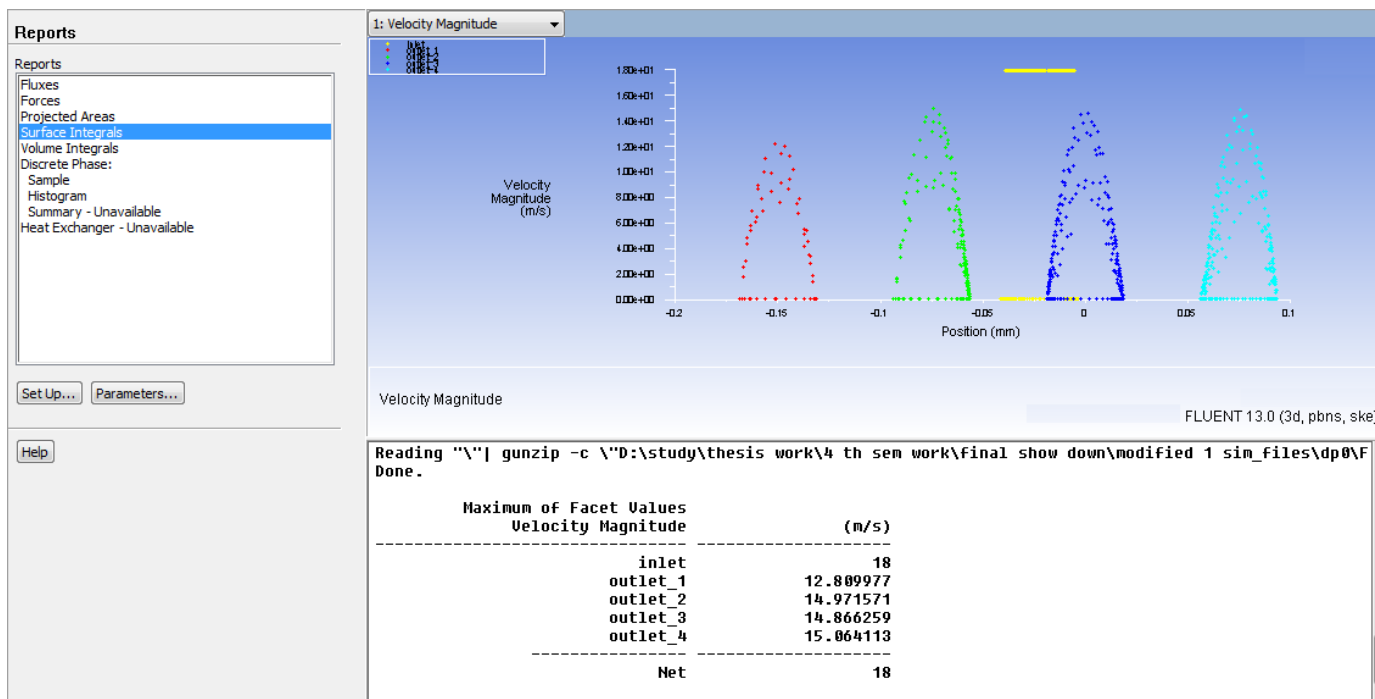


Fig: 4.32 (b) Velocities values at different outlets (Model-1,18m/s)

Fig 4.32 (a)-(b) show the velocity profile at the outlets of intake manifold. The variations in velocity at outlets are easily visible. Velocity at outlet-1 is lowest while at outlet-4 it highest.

Results:

Inlet (m/s)	Outlet 1 (m/s)	Outlet 2 (m/s)	Outlet 3 (m/s)	Outlet 4(m/s)
18	12.1811	14.93	14.83	15.05

At Inlet velocity=15 m/s

Residual plot: Solution is converges after 510 iterations.

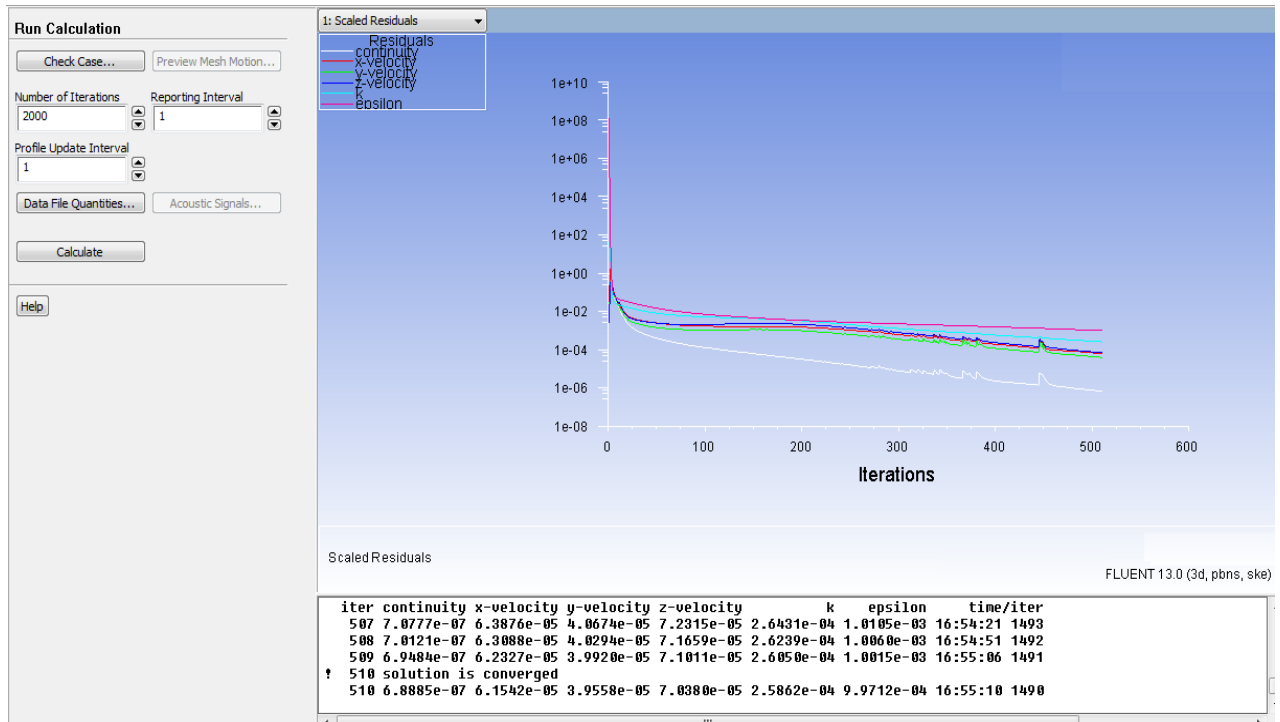


Fig: 4.33 Residual Plot (Model-1,15m/s)

At inlet velocity 15 m/s for model -1 the residual plot (Fig 4.33) converge below the 1e-06 ,it show that the it greatly reduces the chance of error in the results of output.

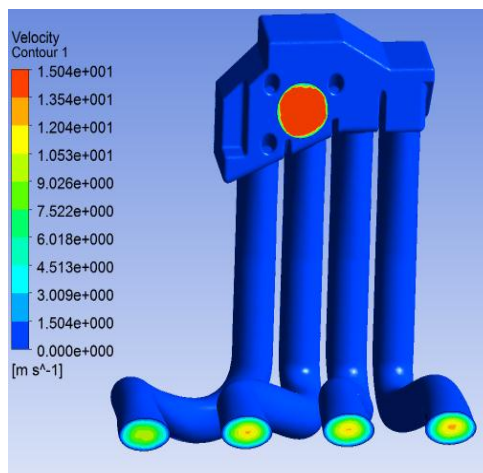
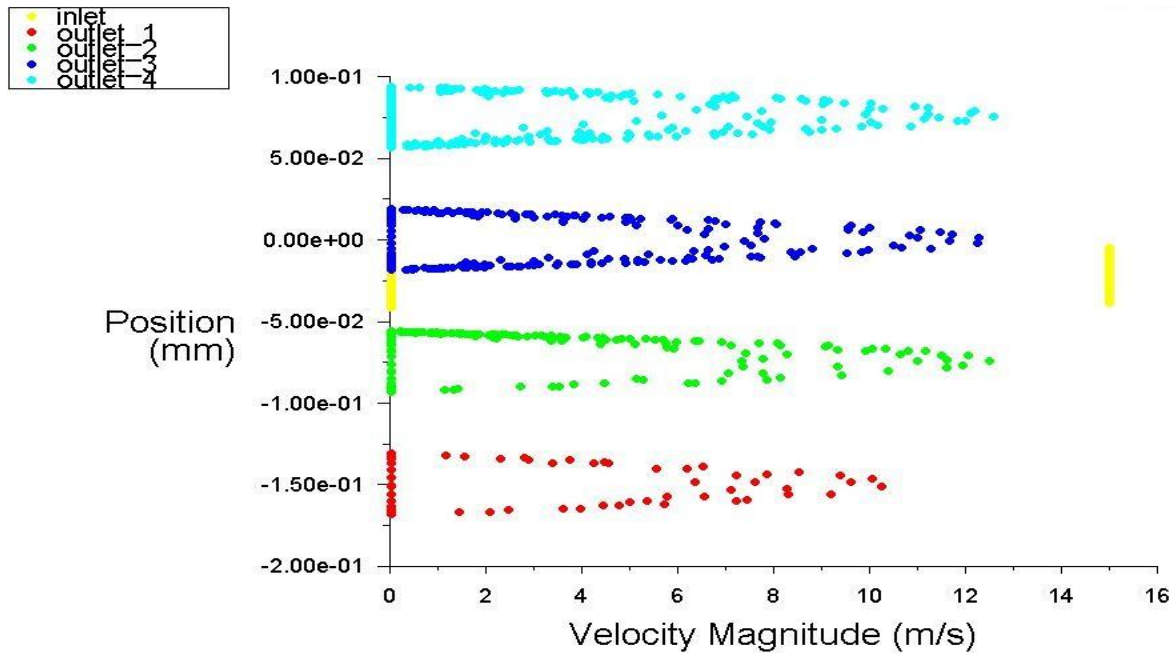


Fig: 4.34 Velocity contour (Model-1,15m/s)

According to Fig 4.34 velocity is more in output-4 compare to other three outlets .Outlet-1 show lowest velocity in all.

Fluent result at outlet is:



Velocity Magnitude

FLUENT 13.0 (3d, pbns, ske)

Fig: 4.35 Velocities profile at different outlets (Model-1,15m/s)

Fig 4.35 shows the velocity profile at different outlets at 15 m/s inlet. The velocity profile is nearly same as above (Fig 4.32) profile for 18 m/s inlet, this show velocity drop occurs in same manner for both inlet velocities for Model-1.

Result (Model-1):

Inlet (m/s)	Outlet 1 (m/s)	Outlet 2 (m/s)	Outlet 3 (m/s)	Outlet 4(m/s)
15	10.81	12.4499	12.4934	12.7307

Similarly simulation results at following velocities are:

Inlet(m/s)	Outlet 1 (m/s)	Outlet 2(m/s)	Outlet 3(m/s)	Outlet 4 (m/s)
13	9.59	10.85	10.55	11.4114
11	8.17	9.15	9.0194	10.1

4.3.1.2) Model without internal projection at plenum (Model-2):

a) Geometrical Flow model:

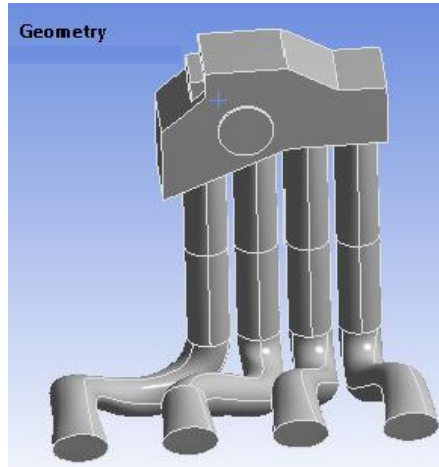


Fig: 4.25 Model-2 (Flow model of geometry without internal projection at plenum)

b) Meshing of model-2:

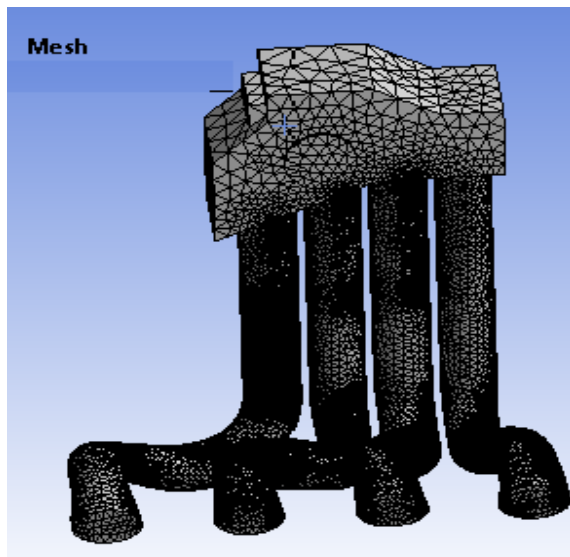


Fig: 4.36 Meshing (Model-2)

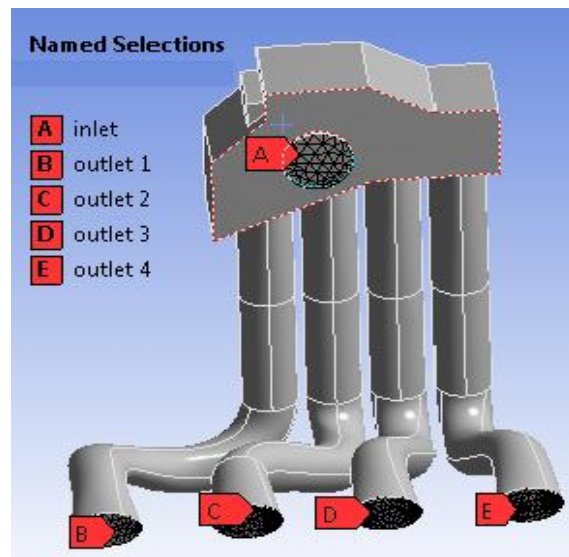


Fig: 4.37 Name selections (Model-2)

Model-2 (Fig 4.27) has been used to check the losses in plenum of intake manifold. Fig 4.36 and Fig 4.37 show meshing and named selection for model -2. The meshing at the curve part of runner is very high as compared to plenum. To achieve desired good result the tetrahedral meshing is done and maximum skewness is kept between .87 to .89.

Meshing properties of model-2:

Table: 4.3

Nodes	213274
Elements	1125037

c) **Simulation result of model -2:**

At Inlet velocity =18 m/s

Residual plot: Solution is converges after 459 iteration.

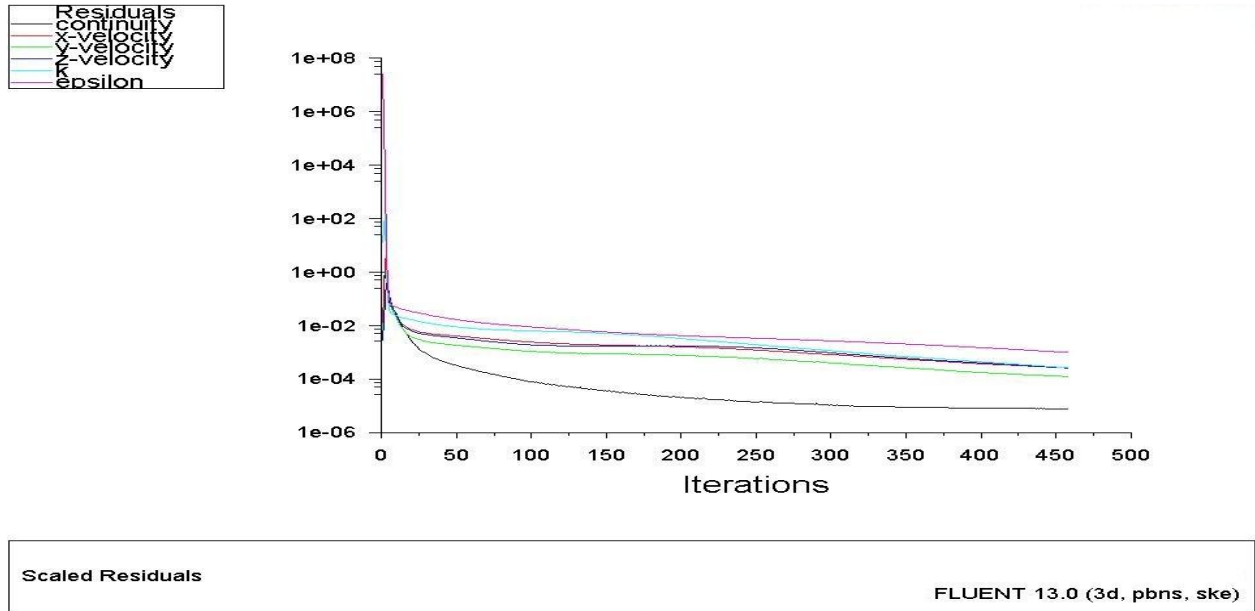


Fig: 4.38 (a) Residual Plot (Model-2,18m/s)

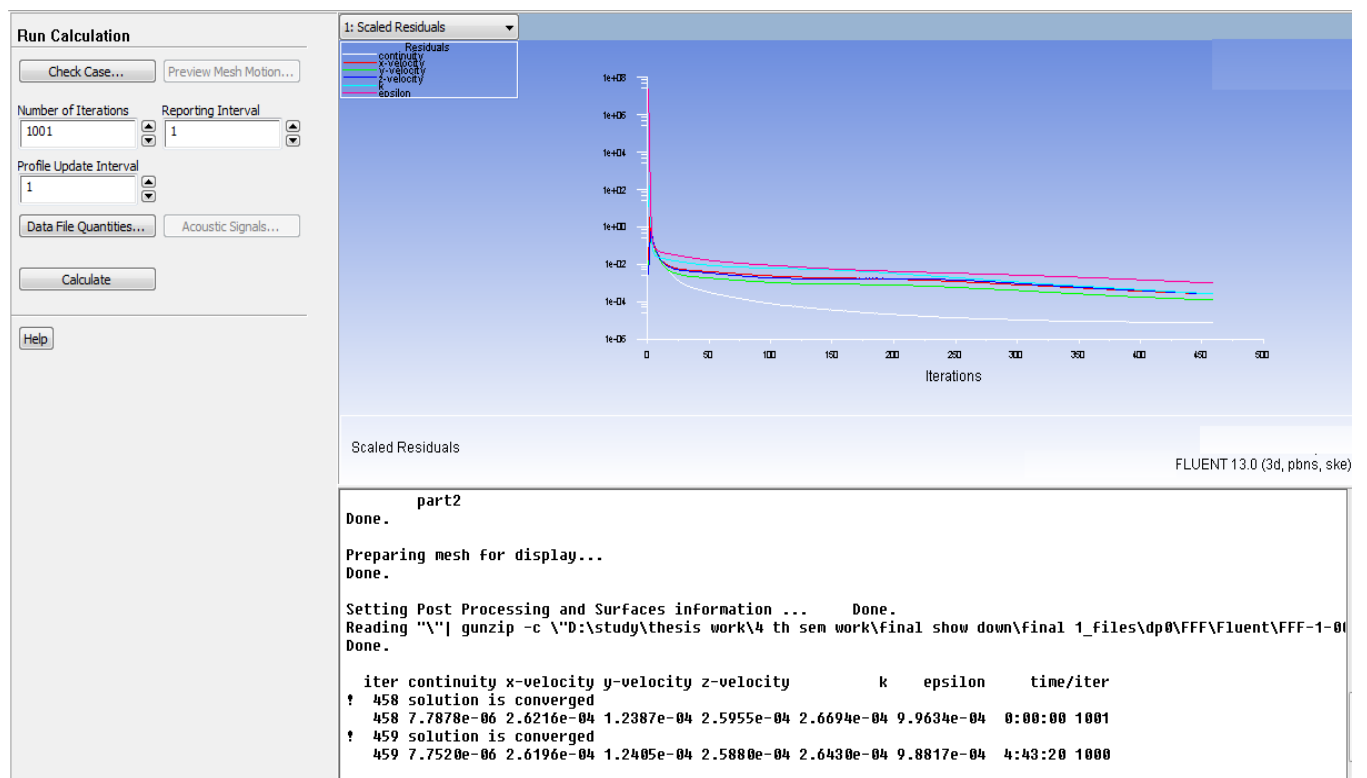


Fig: 4.38 (b) Convergence of Residual plot (Model-2,18m/s)

Fig 4.40 (a- b) show the convergence for model-2 also take place at the $1e-05$, it show that the results of model-2 are more error free.

Velocity streamlines:

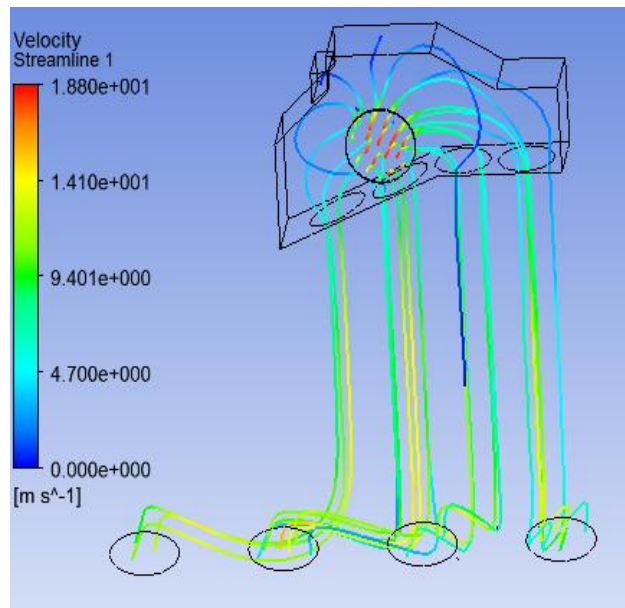


Fig: 4.39 Velocity streamline (Model-2,18m/s)

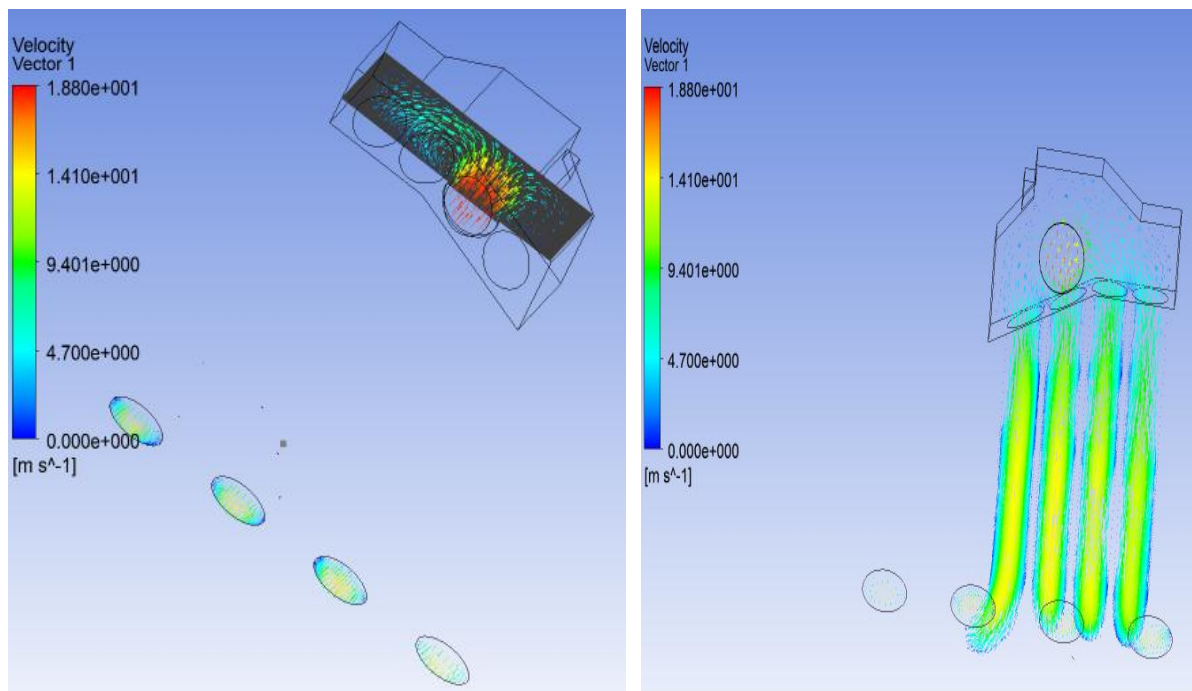


Fig: 4.40 Velocity vector in different plane (Model-2,18m/s)

In Fig 4.39 and Fig 4.40 show the velocity at outlets of model-2, velocity vector clear the idea the distribution of air in plenum, the salient cut at the plenum at the side of outlet 4 sucks the air from inlet readily and distribute more air in outlet-4 and outlet-3 .

Fluent results at outlets are:

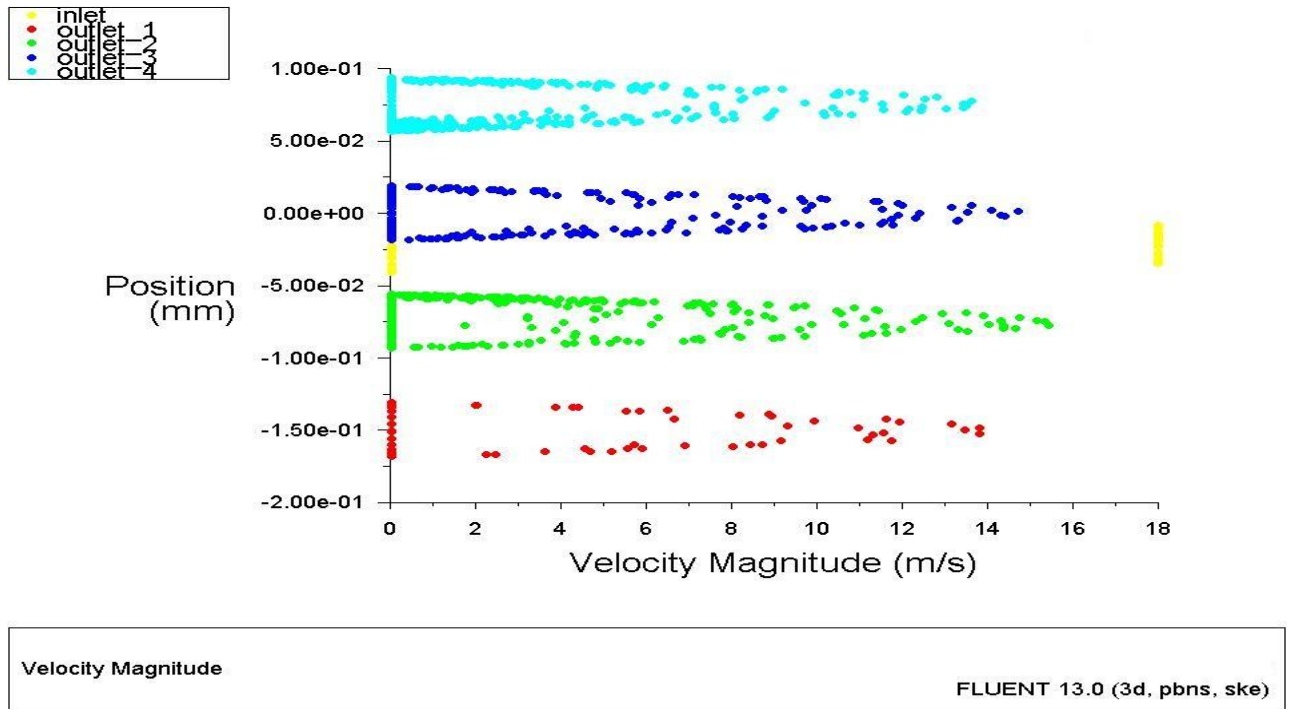


Fig : 4.41(a) Velocities profile at different outlets (Model-2,18m/s)

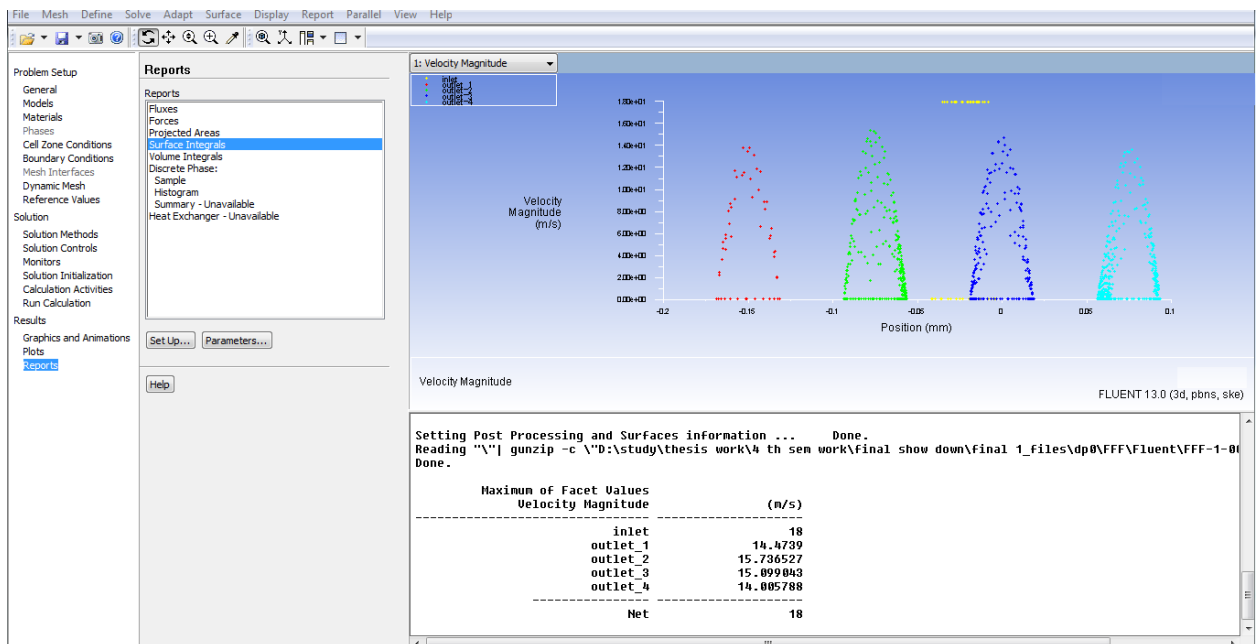


Fig: 4.41 (b) Velocities values at different outlets(Model-2,18m/s)

In Fig 4.41(a) and Fig 4.41 (b) the velocity profile at outlets for model 2 is shown ,in the profile it visible that velocity is more in outlets-2 and outlet-3 comparison with the model-1 where is velocity is more in outlet-4.

Result:

Inlet (m/s)	Outlet 1 (m/s)	Outlet 2 (m/s)	Outlet 3 (m/s)	Outlet 4(m/s)
18	14.47	15.7486	15.0876	14.8862

At Inlet velocity-15 m/s

Residual plot: Solution converges after 438 iterations.

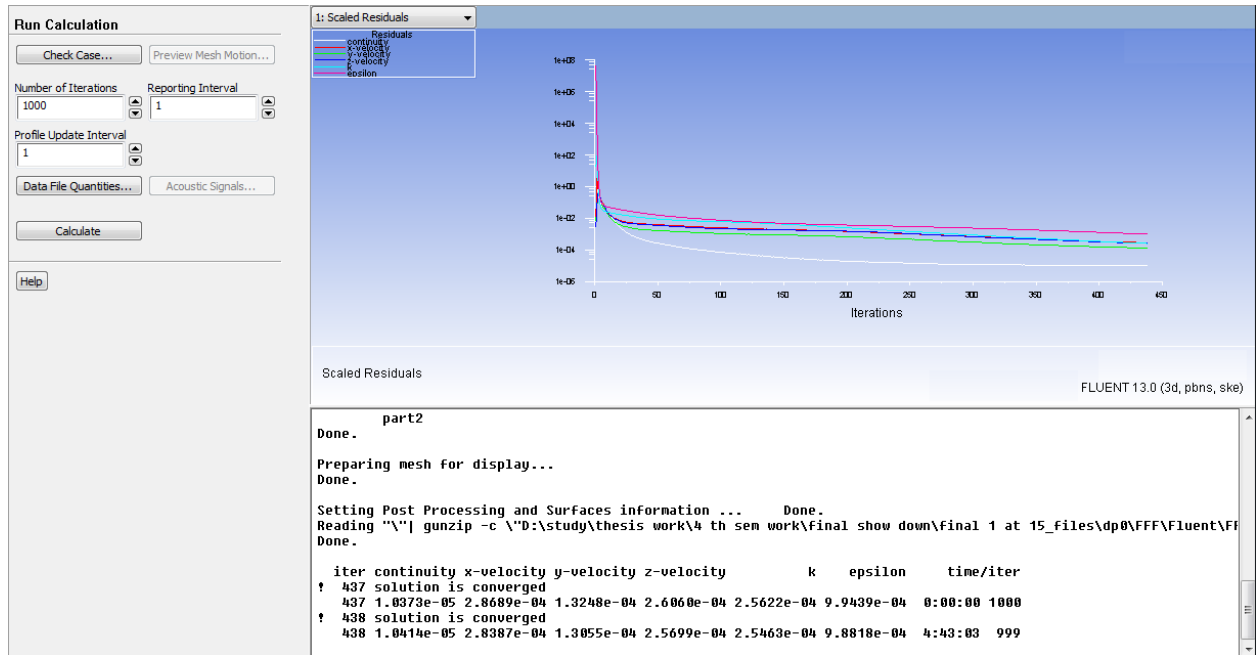


Fig: 4.42 Converge point of residual plot (Model-2,15m/s)

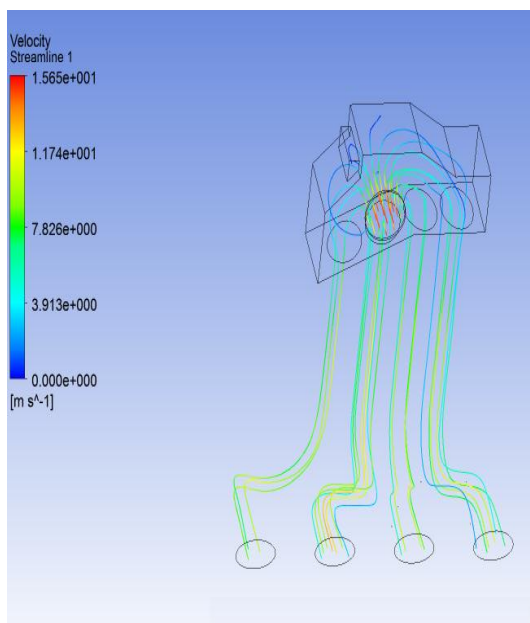


Fig: 4.43 Velocity streamline (Model-2,15m/s)

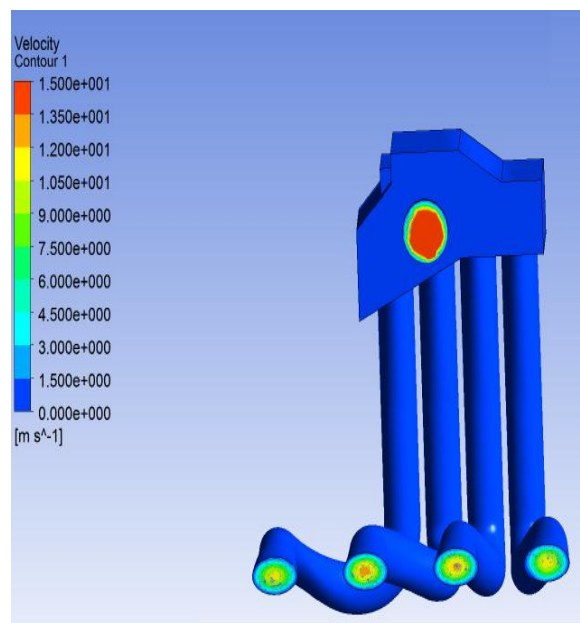


Fig: 4.44 Velocity contour (Model-2,15m/s)

Fig 4.42 shown convergence criteria for model-2 at inlet velocity 15 m/s. Fig 4.43 and Fig 4.44 show the velocity stream in four runner and velocity contour at four outlets of runners.

Fluent results at outlets are:

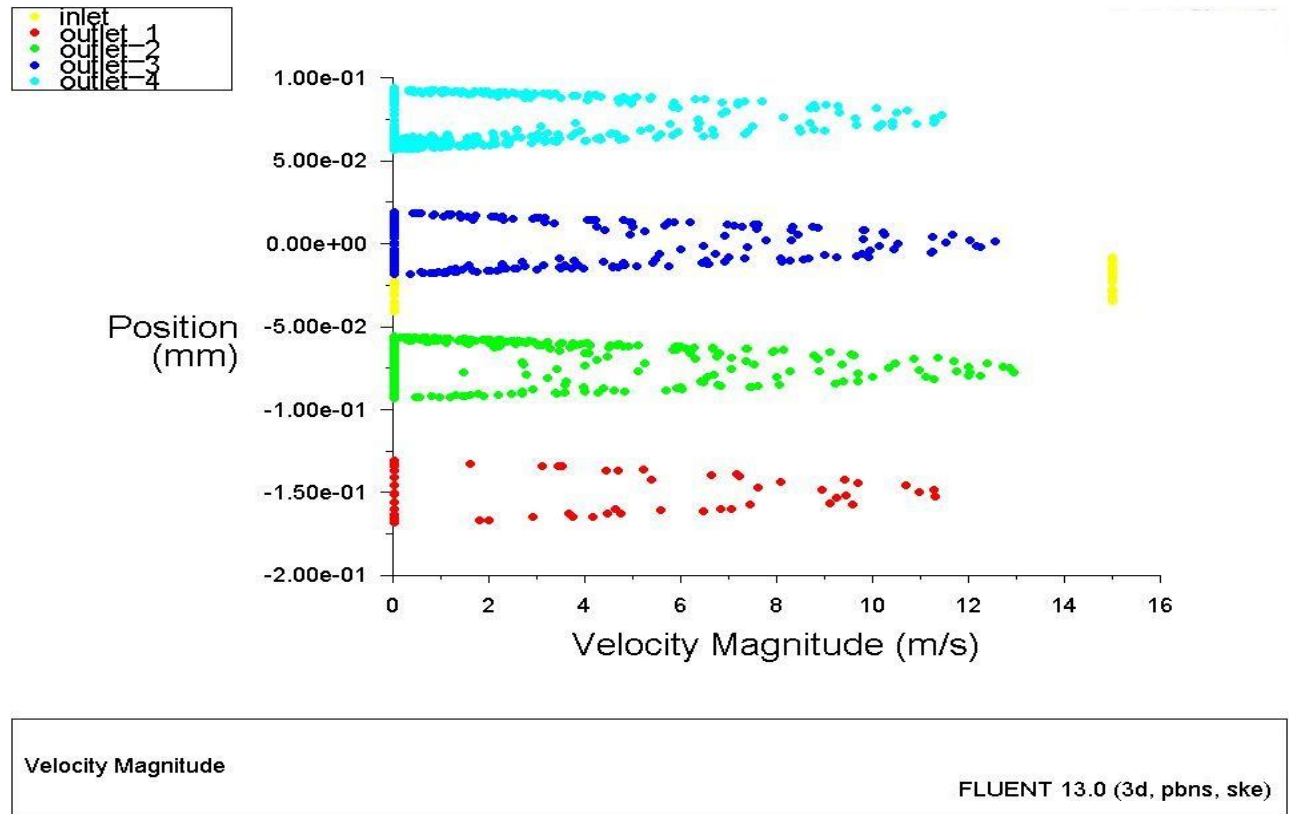


Fig: 4.45 Velocities profile at different outlets (Model-2,15m/s)

In Fig 4.45 velocity distribution profile for model 2 at inlet 15 m/s show more velocity at outlet 2-3, and tell how velocity vary in four outlets of intake manifold.

Result (Model-2)

Inlet (m/s)	Outlet 1 (m/s)	Outlet 2 (m/s)	Outlet 3 (m/s)	Outlet 4(m/s)
15	11.823	13.21	12.85	12.03

Similarly results at following velocities are:

Inlet(m/s)	Outlet 1 (m/s)	Outlet 2(m/s)	Outlet 3(m/s)	Outlet 4 (m/s)
13	10.095	11.4714	11.29	10.82
11	8.443	10.136	9.794	8.7458

4.3.1.3) Model-3 (Model without internal projection at plenum and curves at runner):

a) Flow model of Geometry without projections at plenum and curves part of runner:

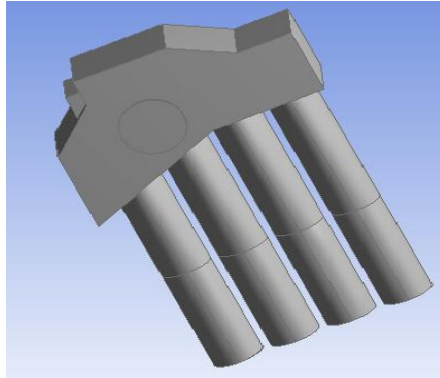


Fig: 4.26 Model-3(Geometry without projection at plenum and without curve part of runner)

b) Meshing of model-3:

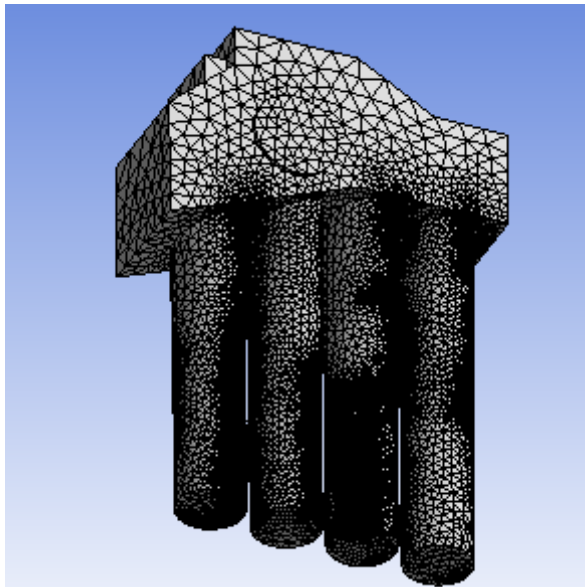


Fig: 4.46 Meshing (Model-3)

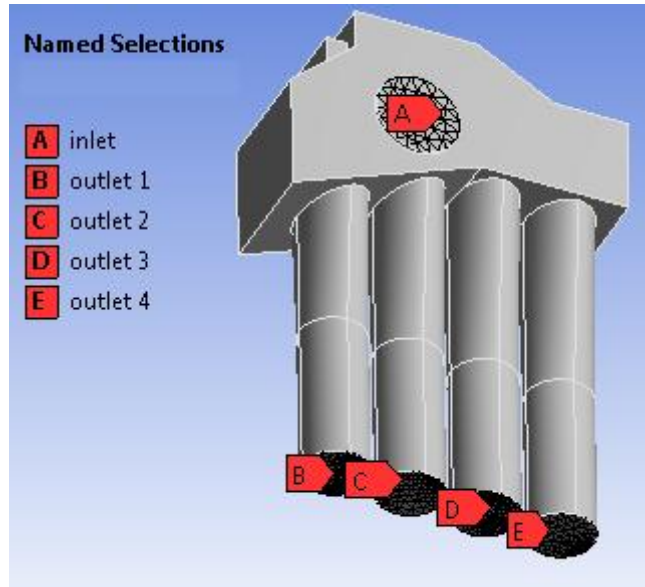


Fig: 4.47 Named selections (Model-3)

To check the losses in various part of intake manifold we have divided the original geometry of the model in three parts, model -3(Fig 4.26) is used to check the effect of curves at the end of runner. Fig 4.46 and Fig 4.47 show the tetrahedral meshing is employed and in what manner part of model is used for inlet and outlet.

Meshing properties of model-3:

Table 4.4

Nodes	121252
Elements	639373

c) **Simulation results:**
Inlet velocity-18 m/s

Residual plot:

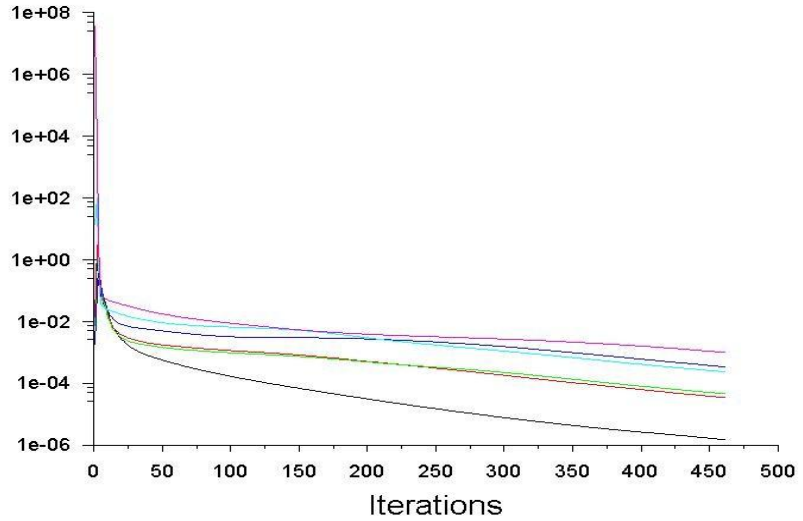


Fig 4.48 (a) Residual Plot (Model-3,18m/s)

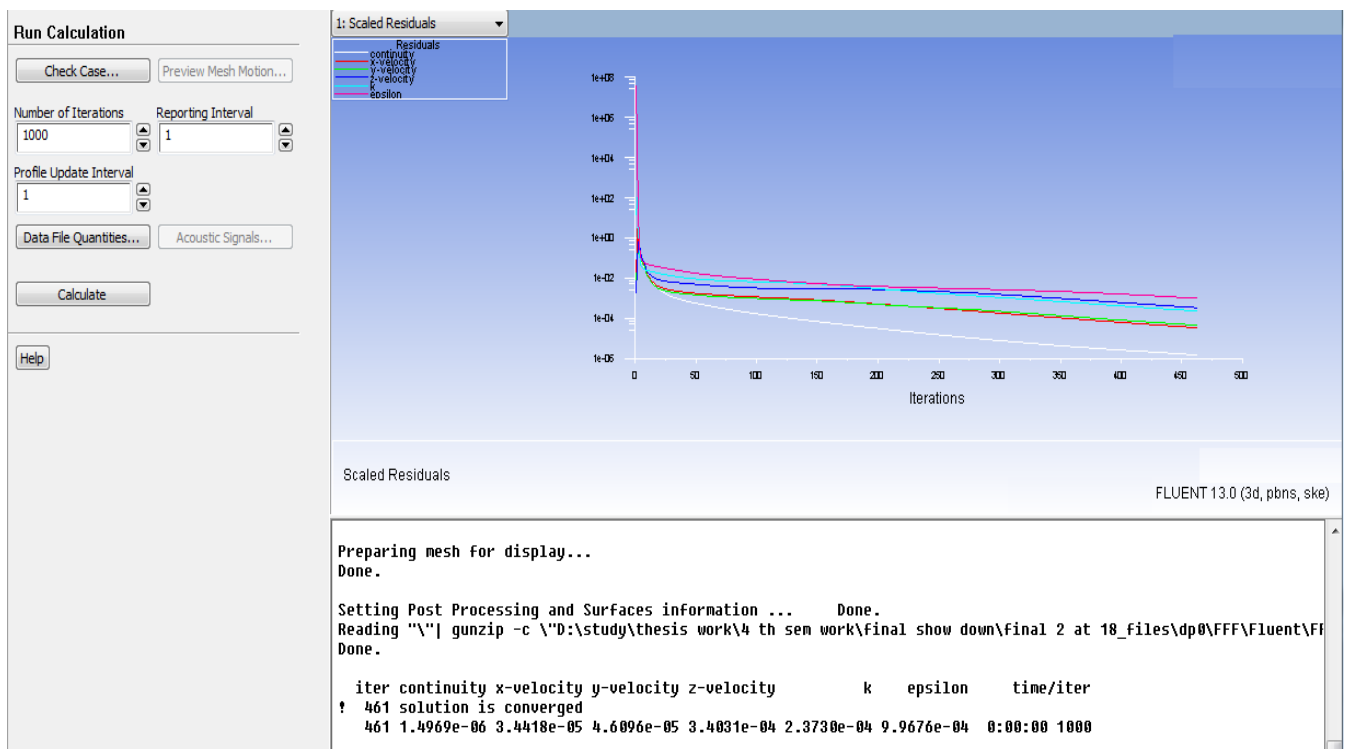


Fig: 4.48 (b) Convergence of Residual plot (Model-3,18m/s)

Model -3 is converged Fig (4.48 a-b) after 461 iteration near $1e-06$ which is very good for error free result.

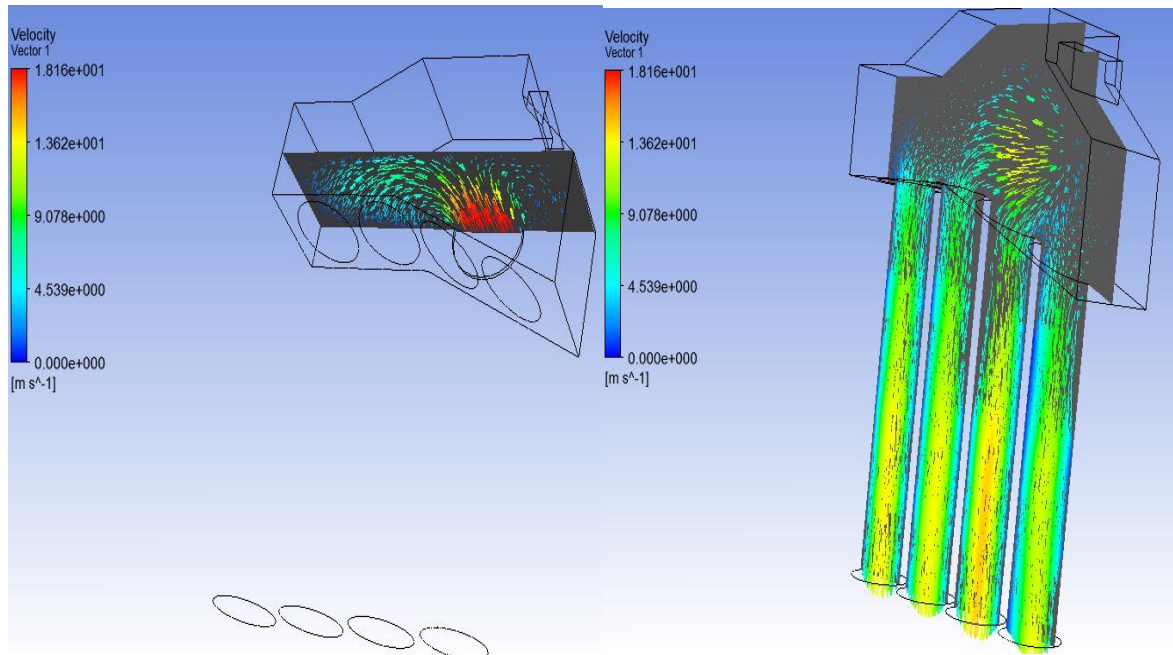
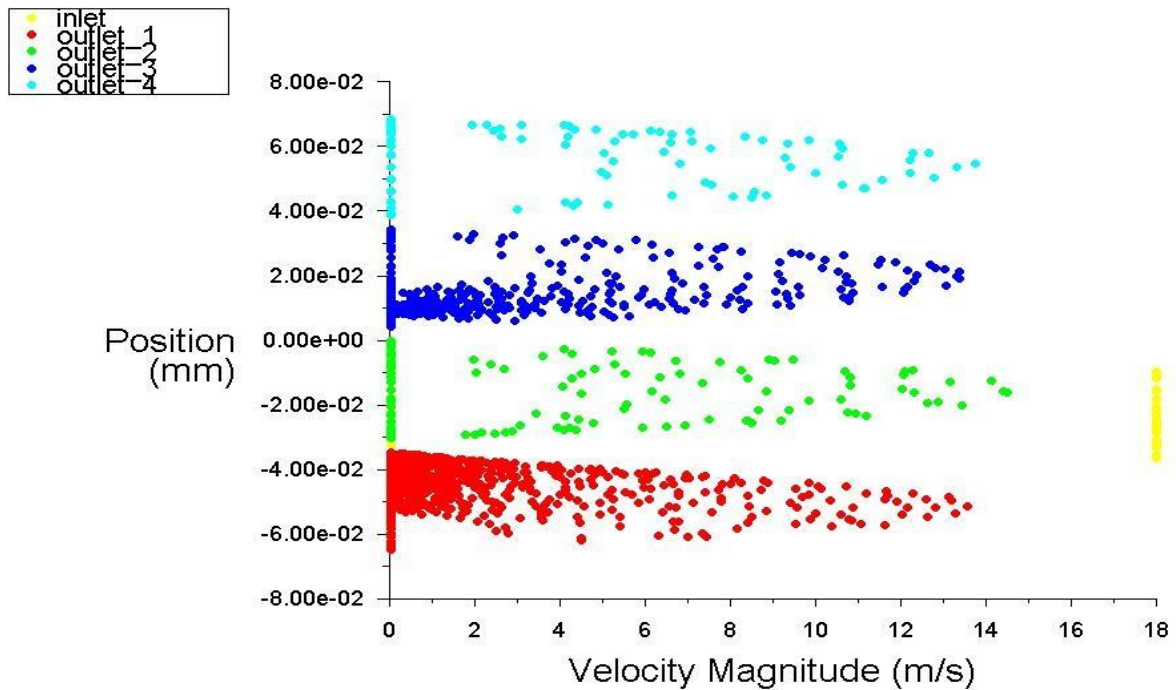


Fig: 4.49 Velocity vector in different plane(Model-3,18m/s)

Fluent result at outlets are:



Velocity Magnitude

FLUENT 13.0 (3d, pbns, ske)

Fig 4.50(a) Velocities Profile at different outlets (Model-3,18m/s)

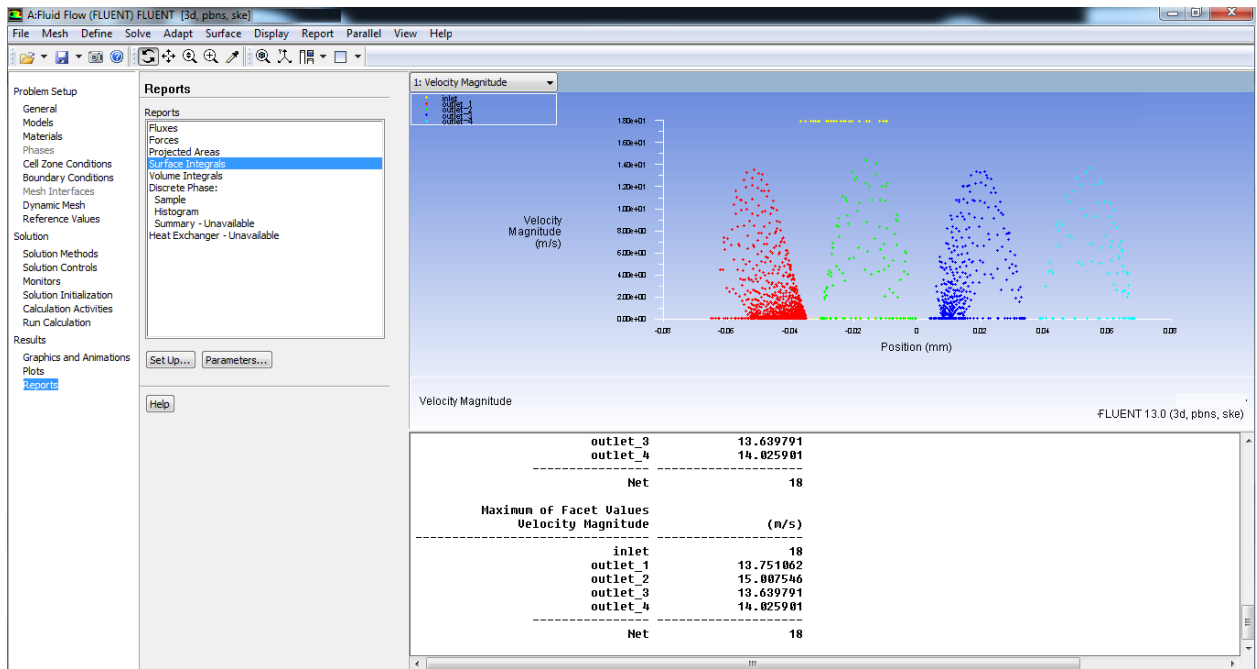


Fig: 4.50(b) Velocities values at different outlets (Model-3,18m/s)

Fig 4.52 (a-b) show slightly different velocity profiles as compared to other two models. Velocity distribution of air at outlet is become more uneven without curve.

Inlet (m/s)	Outlet 1 (m/s)	Outlet 2 (m/s)	Outlet 3 (m/s)	Outlet 4(m/s)
18	13.73	15.022	13.64	14.074

At inlet velocity =15m/s

Residual plot: The iteration is converges after 441.

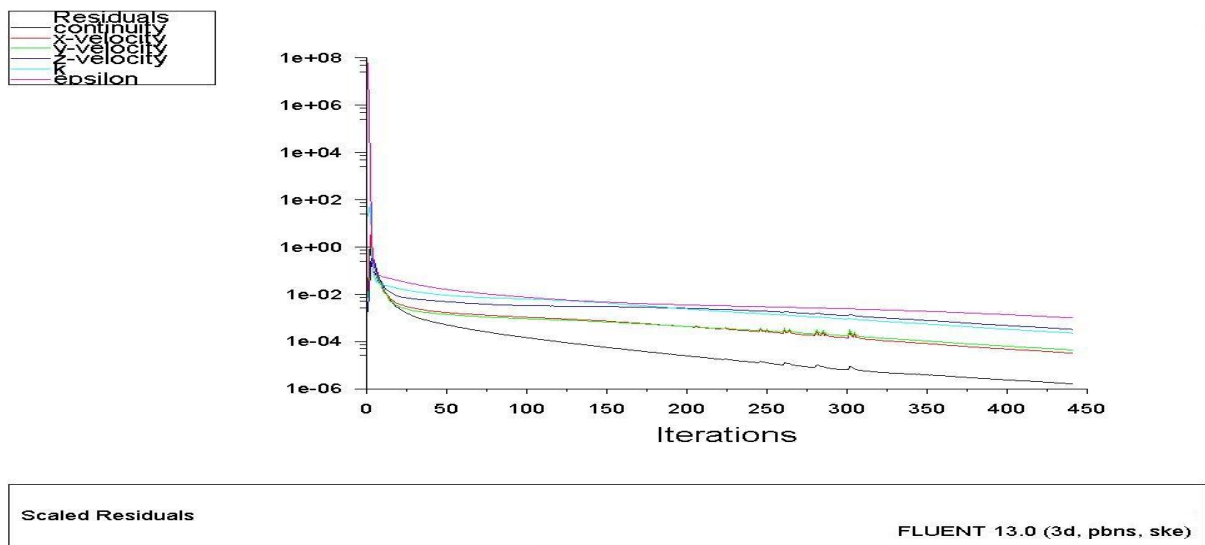


Fig 4.51 Residual plot (Model-3,15m/s)

Fluent result at outlet are:

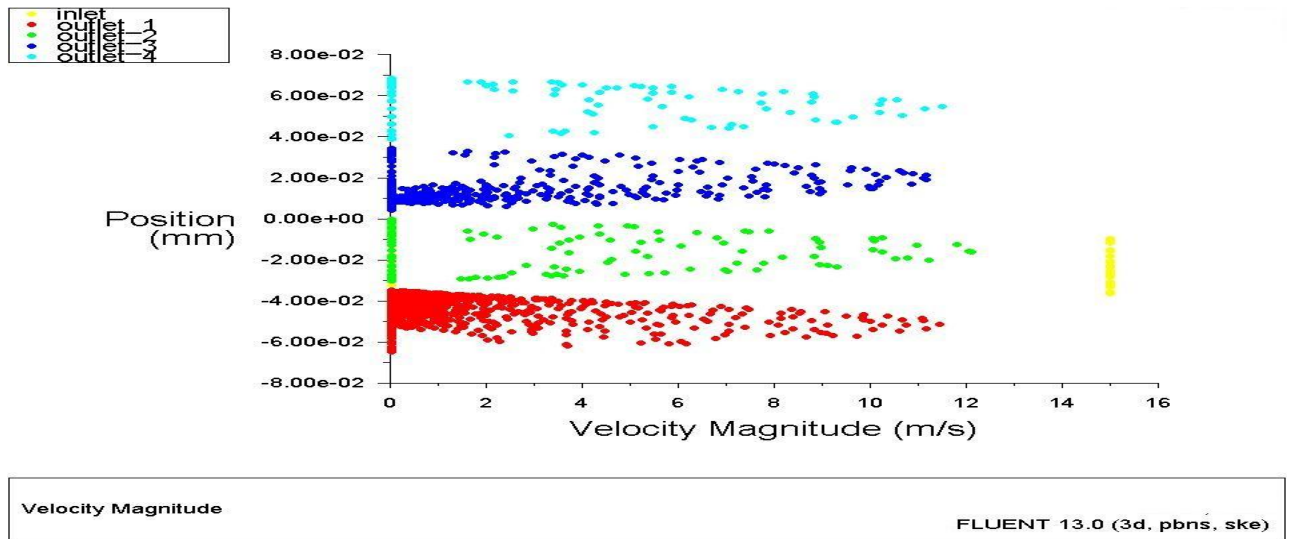


Fig:4.52(a) Velocities profile at different outlets (Model-3,15m/s)

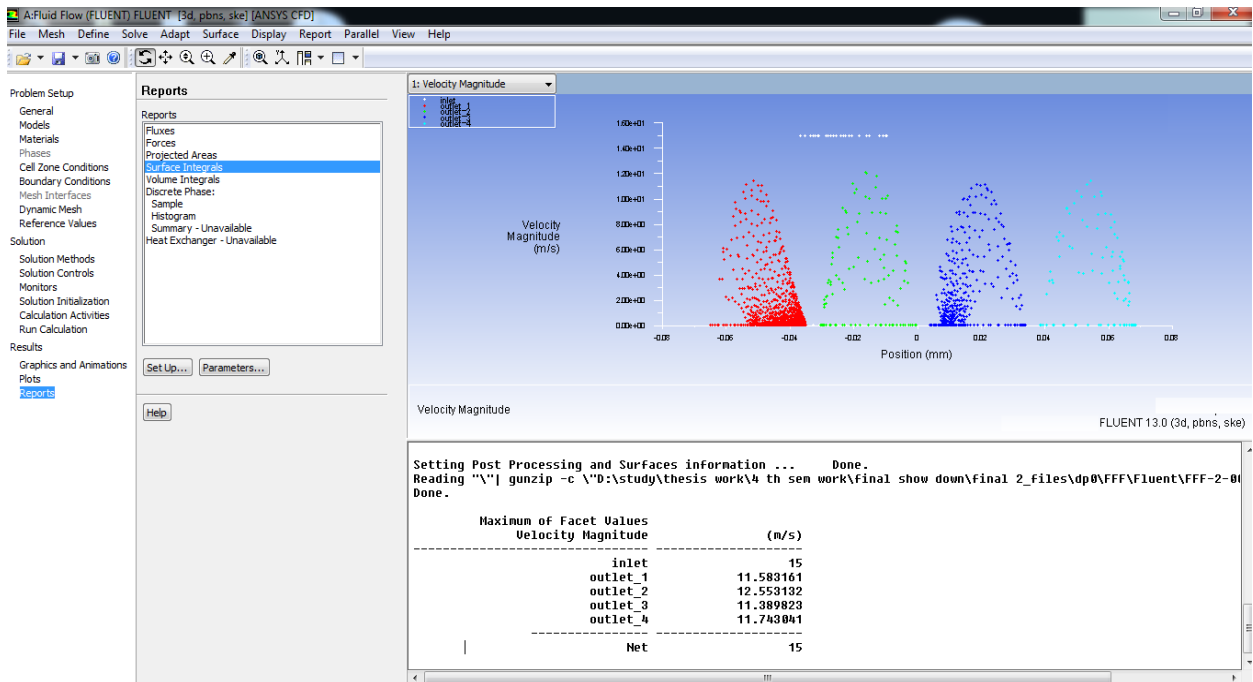


Fig: 4.52(b) Velocity at different outlets (Model-3,15m/s)

Velocity profile (Fig 4.52(a-b)) at lower inlet speed for model 3 show slight change in uneven distribution of air in outlets.

Inlet (m/s)	Outlet 1 (m/s)	Outlet 2 (m/s)	Outlet 3 (m/s)	Outlet 4(m/s)
15	11.57	12.55	12.09	11.73

Inlet(m/s)	Outlet 1 (m/s)	Outlet 2(m/s)	Outlet 3(m/s)	Outlet 4 (m/s)
13	10.408	11.074	10.537	10.421
11	9.245	9.596	9.484	9.345

CHAPTER 5

RESULTS AND DISCUSSION

From the above experimental and CFD analysis the following results are observed at various runners outlets of the intake manifold

5.1 Experimental result of Intake manifold:

5.1.1 Anemometer:

5.1.2 U-Tube manometer

5.1.1 Experimental data of Anemometer.

Table 5.1

INLET(m/s)	Outlet 1(m/s)	Outlet 2 (m/s)	Outlet 3(m/s)	Outlet 4(m/s)
5	1.5	1.9	1.7	2.4
8.4	3.1	3.5	3.2	3.93
11.2	3.2	4.0	3.7	4.43
12.5	3.5	4.5	4.2	4.93
14	4.1	4.8	4.6	5.0

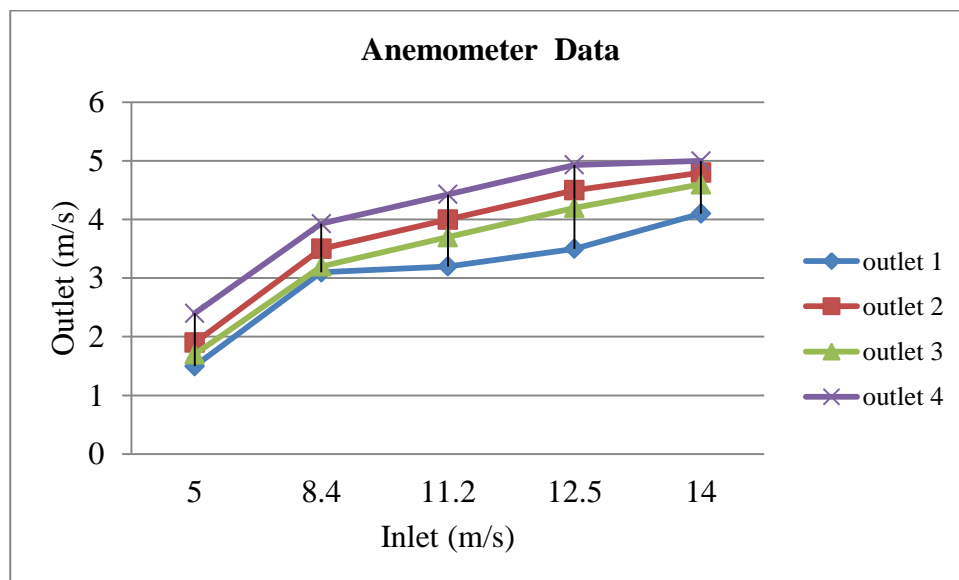


Fig: 5.1 Velocities at outlets with variable inlet velocities(Anemometer readings)

From above (Fig 5.1) results it shows that the velocity is minimum in outlet 1 and maximum in outlet 4. so more velocity losses take place in the outlet 1 side.

5.1.2 Experimental Data of Intake manifold by U-tube manometer:

Here inlet velocity of anemometer data mention, just to refer that measurement is taken at different mass flow rate by varying the speed of blower by flow regulator.

At inlet velocity=14 m/s

Temperature=300 kelvin

Table: 5.2

	Outlet 1 (cm)	Outlet 2 (cm)	Outlet 3 (cm)	Outlet 4 (cm)
h_2	27.7	27.3	27.5	27.1
h_1	2.8	3.2	3	3.5
P(Gauge press)	2440.2	2361.4	2401	2312.2

At inlet velocity=12.5 m/s

Temperature=300 kelvin

Table: 5.3

	Outlet 1(cm)	Outlet 2 (cm)	Outlet 3 (cm)	Outlet 4 (cm)
h_2	26.4	25.8	26	25.6
h_1	3.9	4.5	4.1	5
P(Gauge press)	2205	2087.4	2146.2	2018.2

At inlet velocity=11.2 m/s

Temperature=300 kelvin

Table: 5.4

	Outlet 1 (cm)	Outlet 2 (cm)	Outlet 3 (cm)	Outlet 4 (cm)
h_2	23.4	23.1	23.2	23
h_1	6.8	7.1	7	7.2
P(Gauge press)	1626.8	1568	1587.4	1548.4

At inlet velocity=8.5 m/s

Temperature=300 kelvin

Table: 5.5

	Outlet 1 (cm)	Outlet 2 (cm)	Outlet 3 (cm)	Outlet 4 (cm)
h_2	19.1	19	18.9	18.9
h_1	11.11	11	10.8	10.8
P(Gauge press)	783.02	784	793.8	793.8

Inlet velocity below 8.5 m/s give not any considerable difference in pressure at outlets because velocity is low and surrounding losses also take place on the experiment setup.

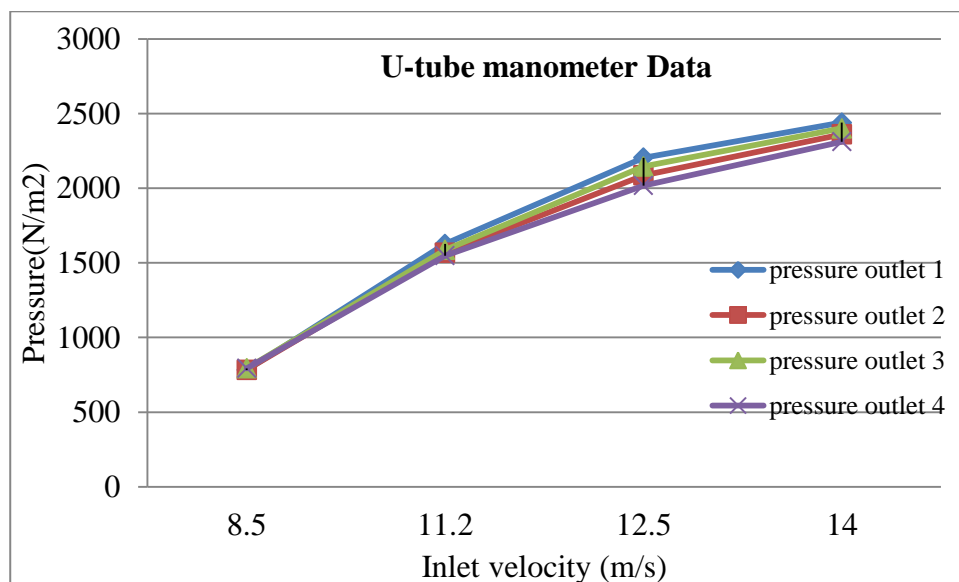


Fig: 5.2 Pressure at outlets on variable inlet velocities

5.2 Density variation analysis for compressible air flow at outlets

5.2.1 At NTP condition

5.2.2 At Experimental data of intake velocity 14 m/s

5.2.1 At NTP condition:

Temperature (T)= 293 kelvin

Pressure (P) =1 atm= 101325 N/m^2

Gas constant(R) = 287.05 J/Kg/K

$$P = \rho RT = \rho \times 287 \times 293$$

$$\rho = \frac{101325}{287.05 \times 293} = 1.204 \text{ kg/m}^3$$

5.2.2 At Experimental data of intake velocity 14 m/s

Inlet velocity=14 m/s

Outlet 1:

$$P=101325+2440.2=103765.2$$

Temp=300K

$$\rho = \frac{103765.2}{287.05 \times 300} = 1.204 \text{ kg/m}^3$$

Outlet 2:

$$P=101325+2361.4=103686.4$$

Temp=300K

$$\rho = \frac{103686.4}{287.05 \times 300} = 1.232 \text{ kg/m}^3$$

Outlet 3:

$$P=101325+2401=103726$$

Temp=300K

$$\rho = \frac{103726}{287.05 \times 300} = 1.233 \text{ kg/m}^3$$

Outlet 4:

$$P=101325+2312.2=103637.2$$

Temp=300K

$$\rho = \frac{103637.2}{287.05 \times 300} = 1.2034 \text{ kg/m}^3$$

From above calculation it may concluded that change in density of air are negligible. The change in pressure in each runners is very low so density difference is very low.

5.3 CFD Simulation result:

5.3.1 Model-1 (Actual Flow Model)

5.3.2 Model-2 (Model without internal projections at plenum)

5.3.3 Model-3 (Model without curve at the end of runner part and projection at plenum)

5.3.1 Model-1 results:

Simulation results

Table 5.6

Inlet(m/s)	Outlet 1 (m/s)	Outlet 2(m/s)	Outlet 3(m/s)	Outlet 4 (m/s)
18	12.811	14.93	14.83	15.05
15	10.81	12.4499	12.4934	12.7307
13	9.59	10.85	10.55	11.4114
11	8.17	9.15	9.0194	10.1
9	7.1	7.8794	7.65	8.34

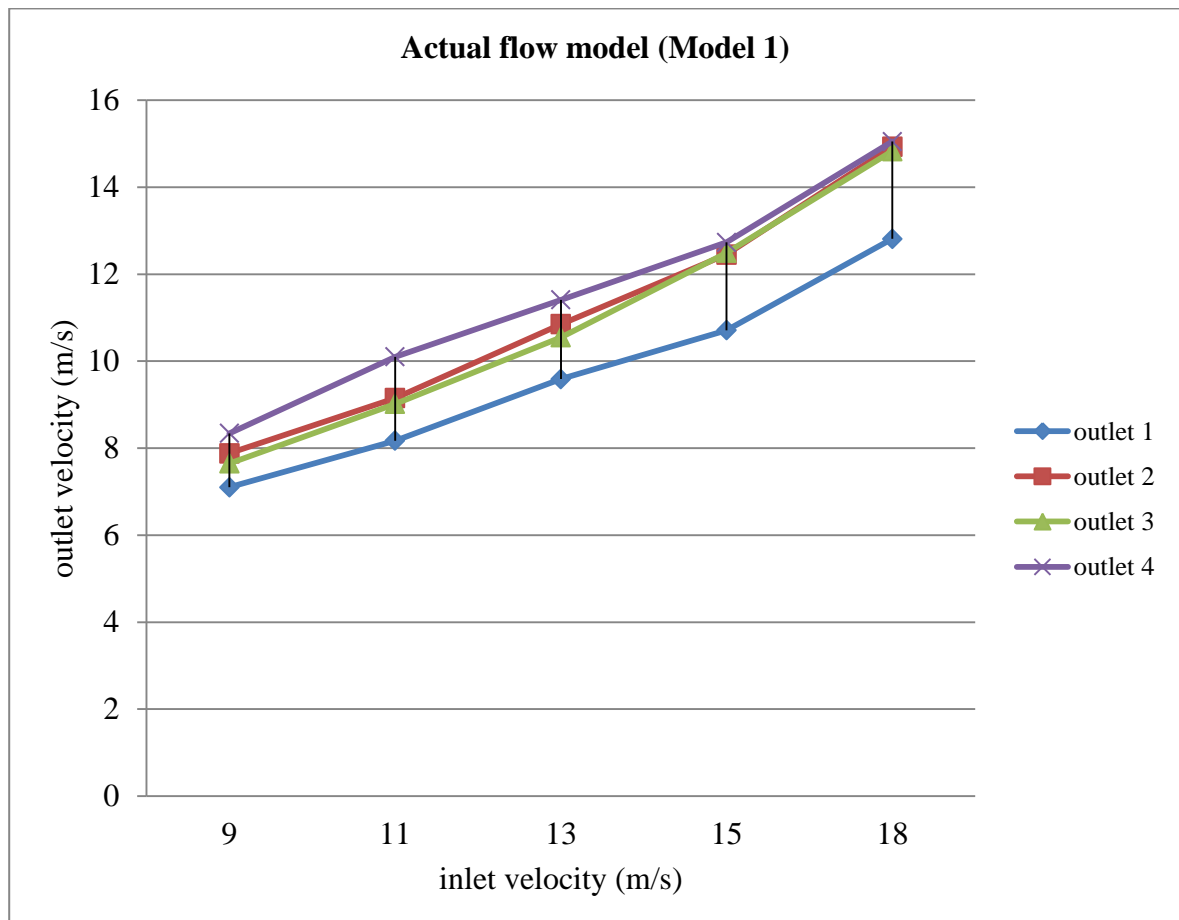


Fig: 5.3 Velocities at outlets with variable inlet velocities (CFD Simulation of Model-1)

5.3.2 Model-2 results:

Simulation results:

Table 5.7

Inlet(m/s)	Outlet 1 (m/s)	Outlet 2(m/s)	Outlet 3(m/s)	Outlet 4 (m/s)
18	14.47	15.7486	15.0876	14.8862
15	11.823	13.21	12.85	12.03
13	10.095	11.4714	11.29	10.82
11	8.443	10.136	9.794	8.7458
9	6.6168	8.33	8.16	7.003

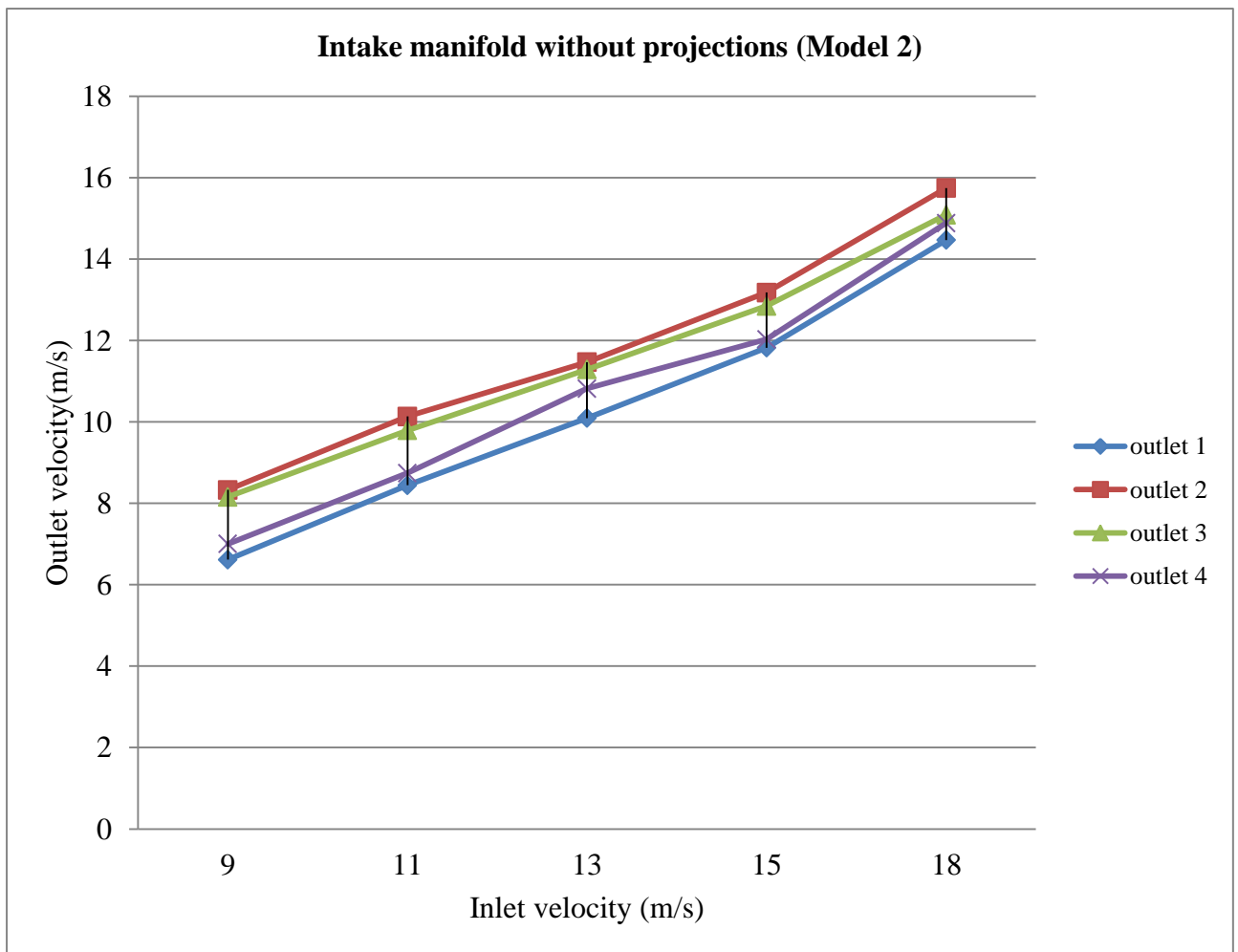


Fig: 5.4 Velocities at outlets with variable inlet velocities(CFD Simulation of Model-2)

5.3.3 Model-3:

Simulation result

Table 5.8

Inlet(m/s)	Outlet 1 (m/s)	Outlet 2(m/s)	Outlet 3(m/s)	Outlet 4 (m/s)
18	13.73	15.022	14.64	14.074
15	11.57	12.55	12.09	11.73
13	10.408	11.074	10.537	10.421
11	9.245	9.596	9.484	9.345
9	8.031	8.802	8.621	8.318

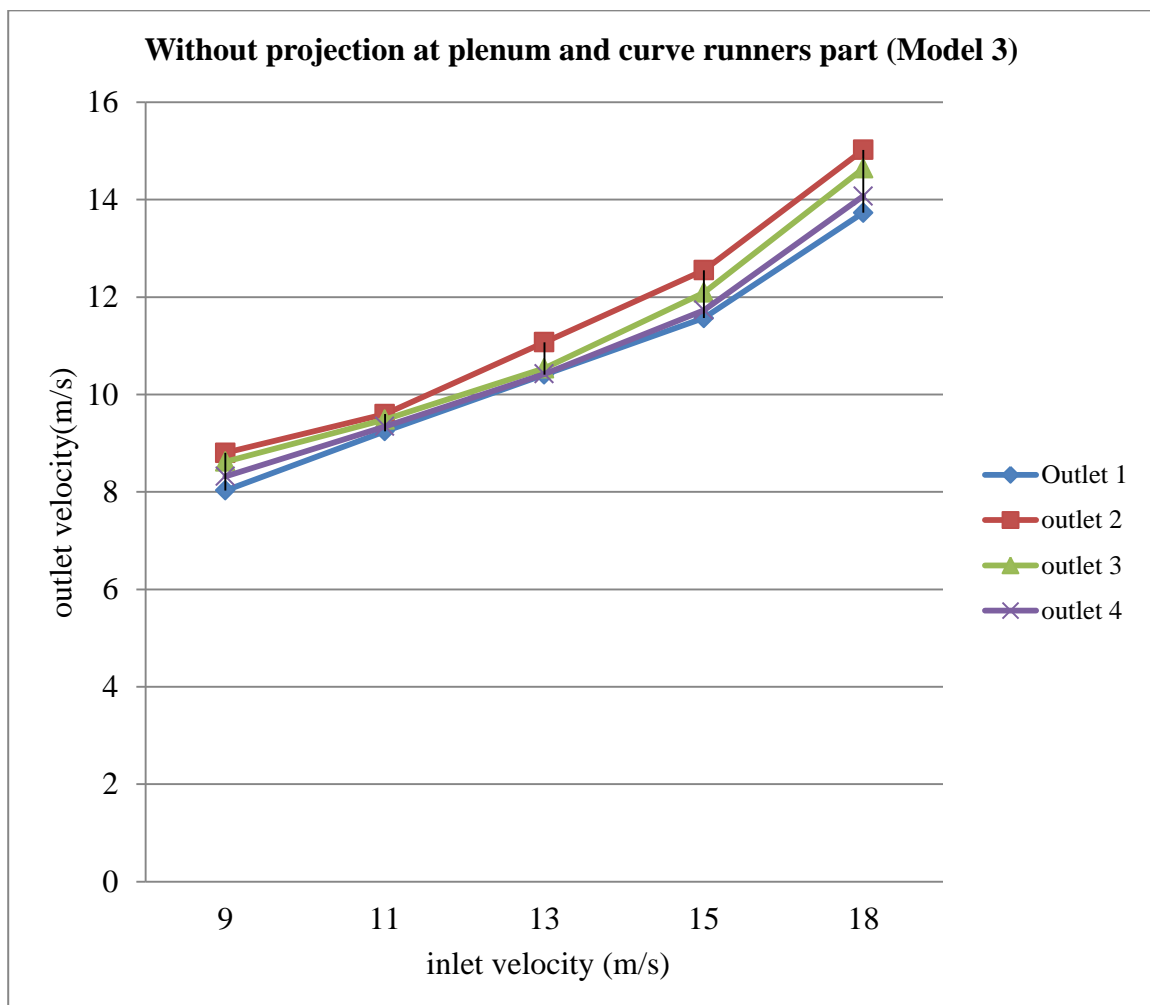


Fig: 5.5 Velocities at outlets with variable inlet velocities (CFD Simulation of Model-3)

From above three graph (fig 5.3,5.4,5.5) of the velocity of different models we conclude that the outlet velocity in runner two(outlet-2) and three(outlet-3) is nearly equal ,the variation in velocity is seen at outlet-1 and outlet 4.At outlet-4 velocity is maximum while on other hand the velocity at outlet-1 is minimum.

5.4 Validation:

5.4.1 Experimental model validation:

5.4.2 CFD model validation with experimental model

5.4.1 Experimental model validation

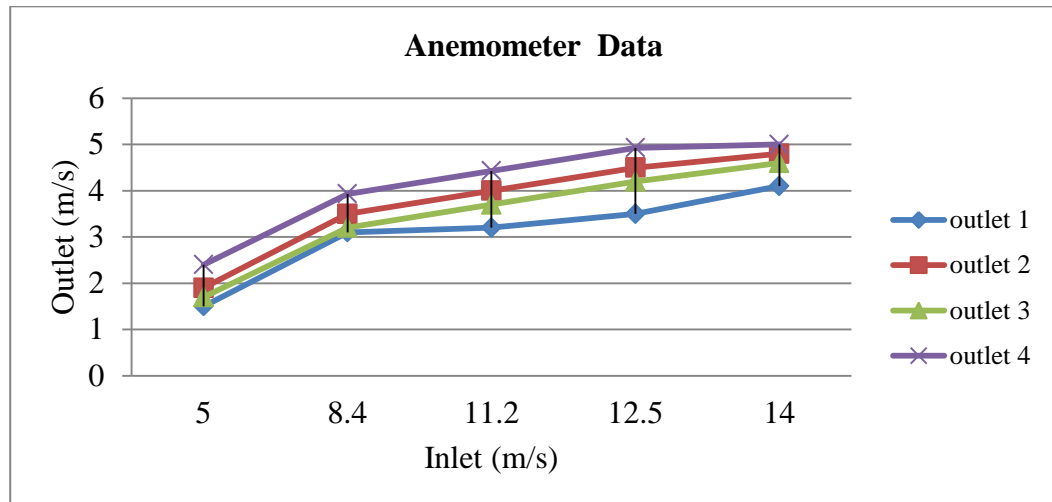


Fig: 5.1 Velocities at outlets with variable inlet velocities(Anemometer readings)

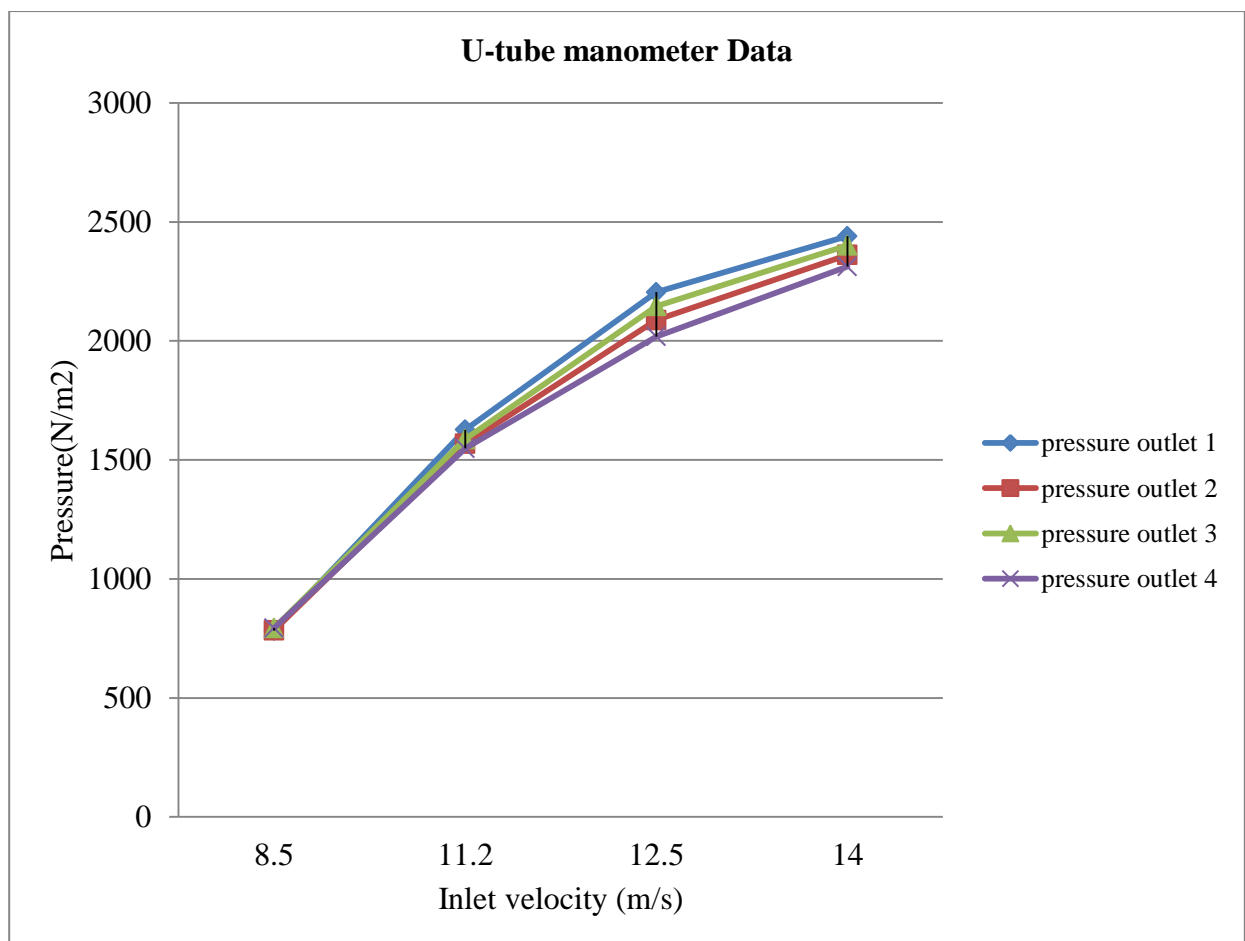


Fig: 5.2 Pressure at outlets on variable inlet velocities

Velocity and pressure are inversely proportional to each other if one is greater than other one is low From the two experimental data (anemometer and U-tube manometer) of the intake manifold it validate that outlet-1 has less velocity than other outlets and more pressure losses at outlet-1 side.

5.4.2 CFD model validation with experimental model:

Experimental results:

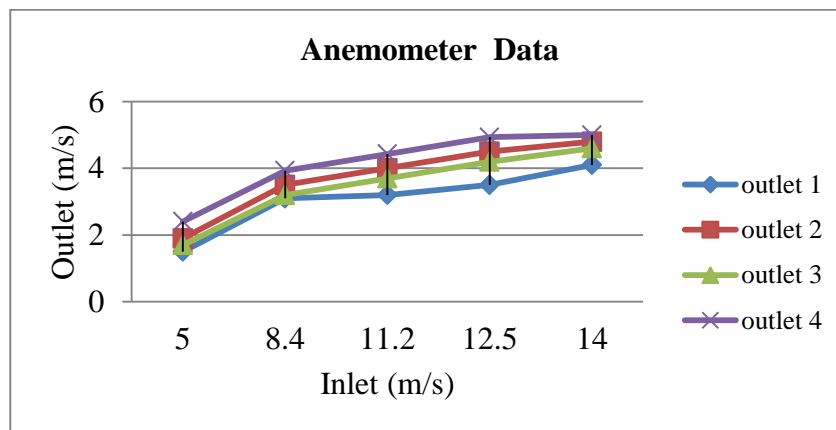


Fig: 5.1 Velocities at outlets with variable inlet velocities(Anemometer readings)

Simulation results:

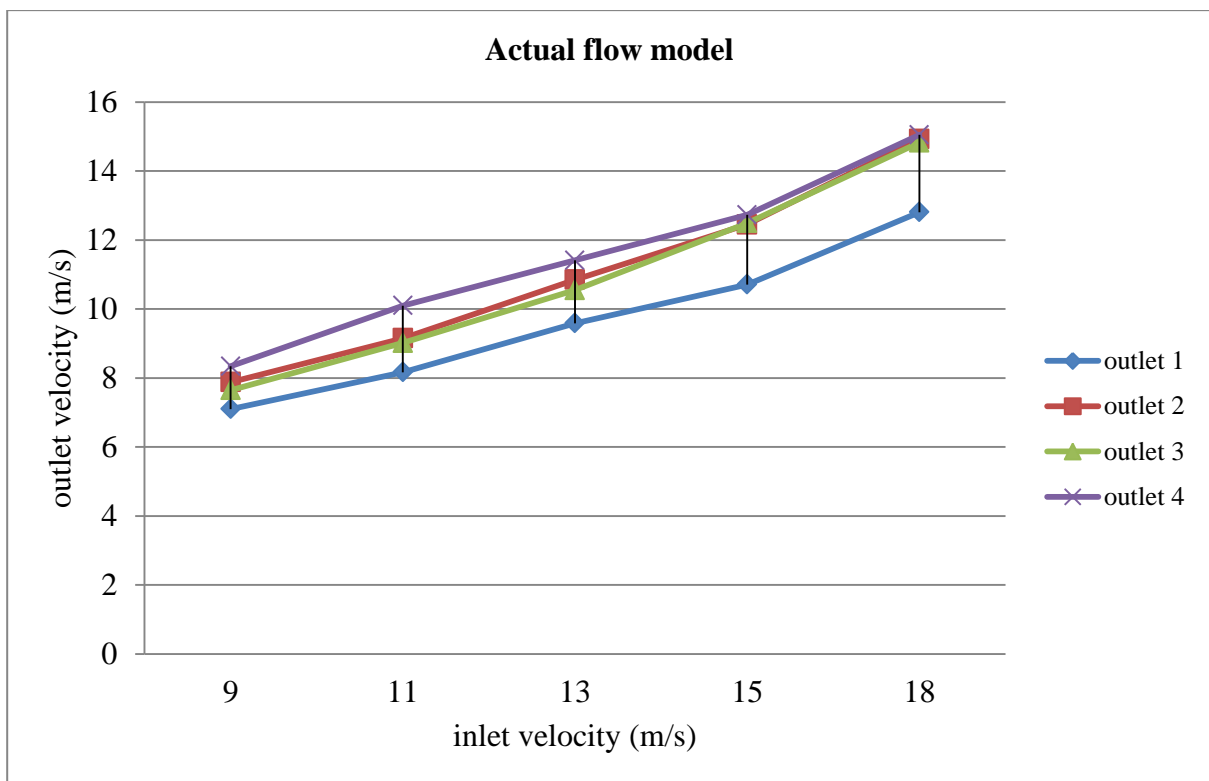


Fig: 5.3 Velocities at outlets with variable inlet velocities (CFD Simulation of Model-1)

The velocity at outlet-2 and outlet-3 are nearly same in both while velocity at outlet-4 highest and velocity at outlet-1 lowest in both model. The variation in graph structure is due to experimental losses.

5.5 Examine the three models at different outlets:

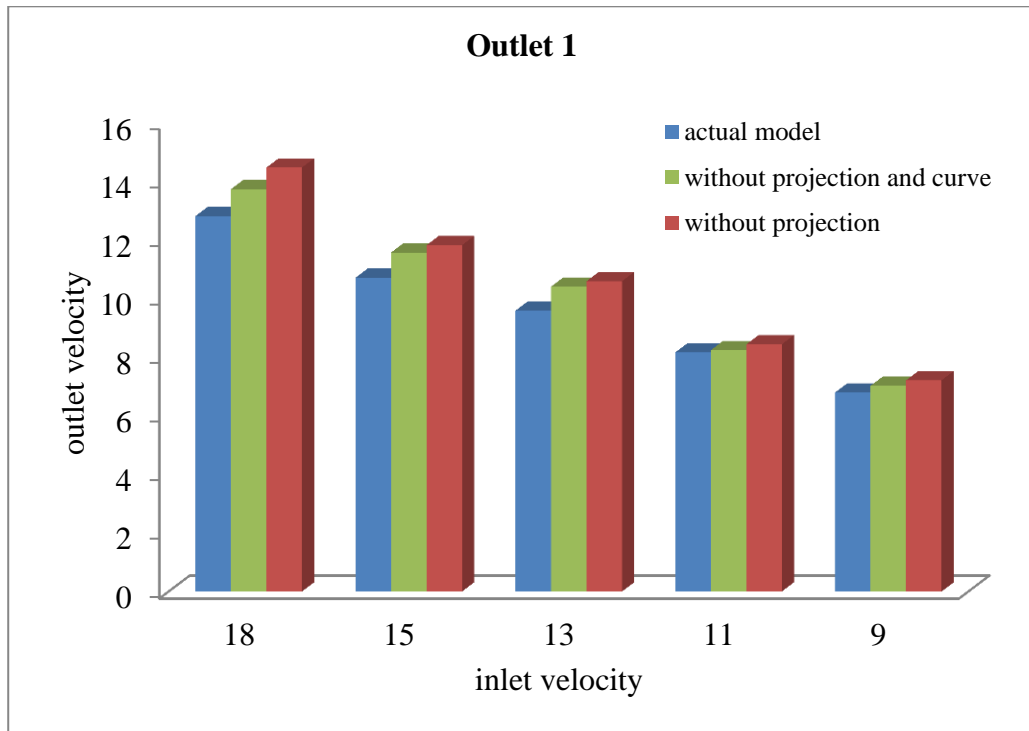


Fig: 5.6 Outlet vs. inlet velocities at outlet-1 of all 3 Models

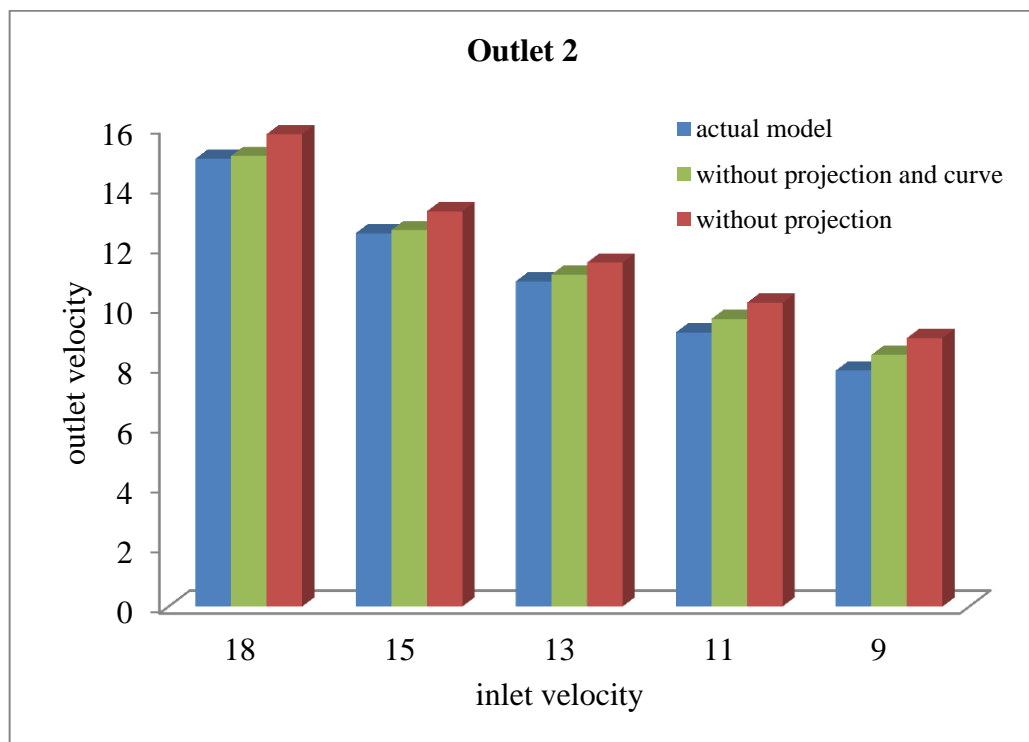


Fig: 5.7 Outlet vs. inlet velocities at outlet-2 of all 3 Models

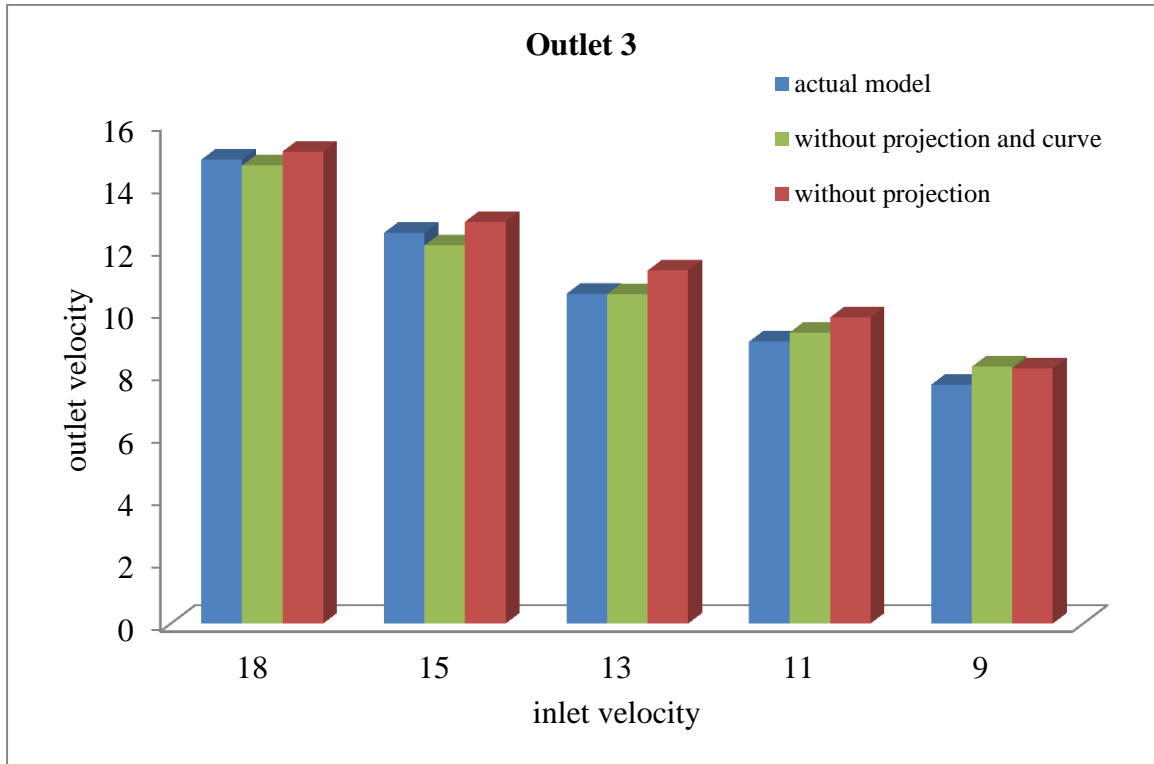


Fig: 5.8 Outlet vs inlet velocities at outlet-3 of all 3 Models

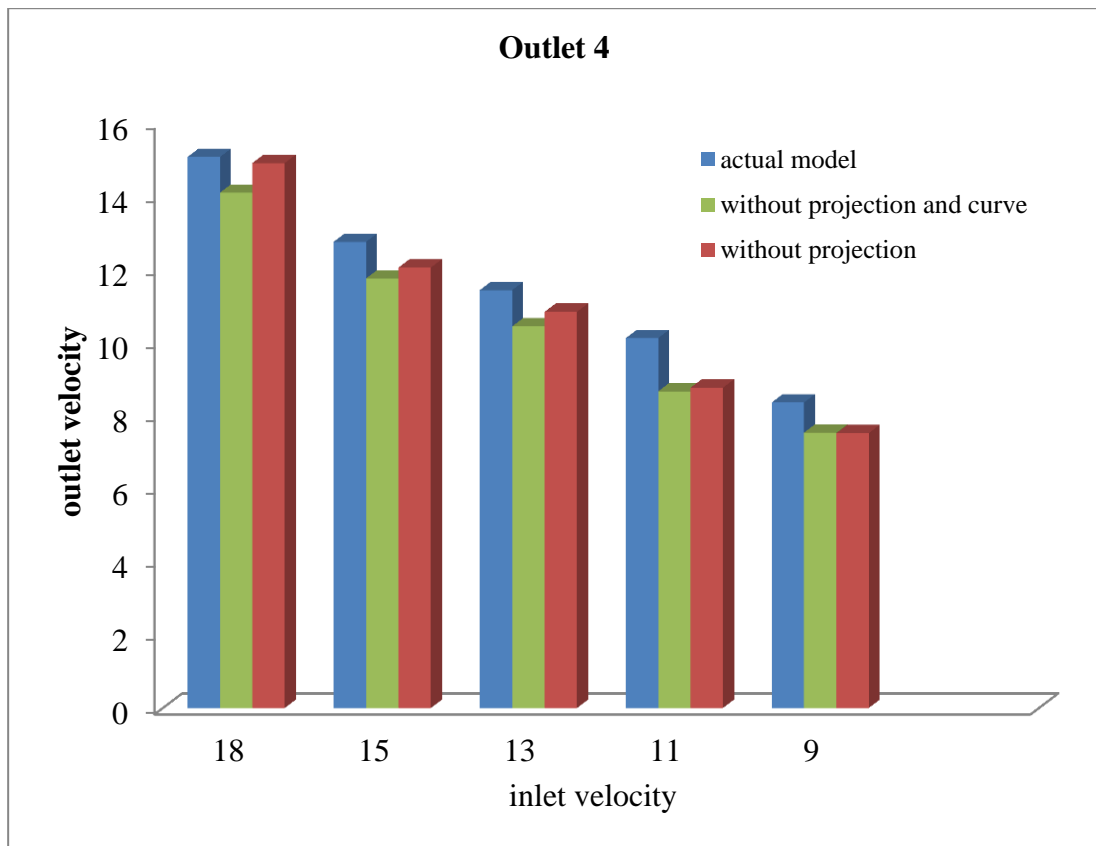


Fig: 5.9 Outlet vs inlet velocities at outlet-4 of all 3 Models

Outlet 1:

At outlet 1(Fig5.6) the actual model show lowest velocity among three models and lowest velocity among four runner also, it show that projection at runner 1 side has actual bad design configuration.

Outlet 2 and Outlet 3:

Outlet 2 (Fig 5.7) and outlet 3 (Fig 5.8) show nearly equal velocity in Model-1 (actual model) and Model-3(model without curve and projections) while the Model-2(model only without projection) show slight high value because of no projection losses at plenum and good design of curves at end of runners.

The other second reason of showing equal velocity is they lying just below the inlet of intake manifold. This show that place of inlet also play important factor in design of intake manifold.

Outlet 4:

At outlet 4 (Fig 5.9) actual model show highest velocity among two models, the results at outlet 4 shows that may be the inside projection of depth cut at extreme side of plenum above runner 4 play significant role and help in improving results of intake manifold

From the above charts we noticed that the model is good at the curving parts of runners and it help in simulate the velocity equally at the four outlets and runner 1 have some bad design projection.

5.6 Examine the three models at different inlet velocities:

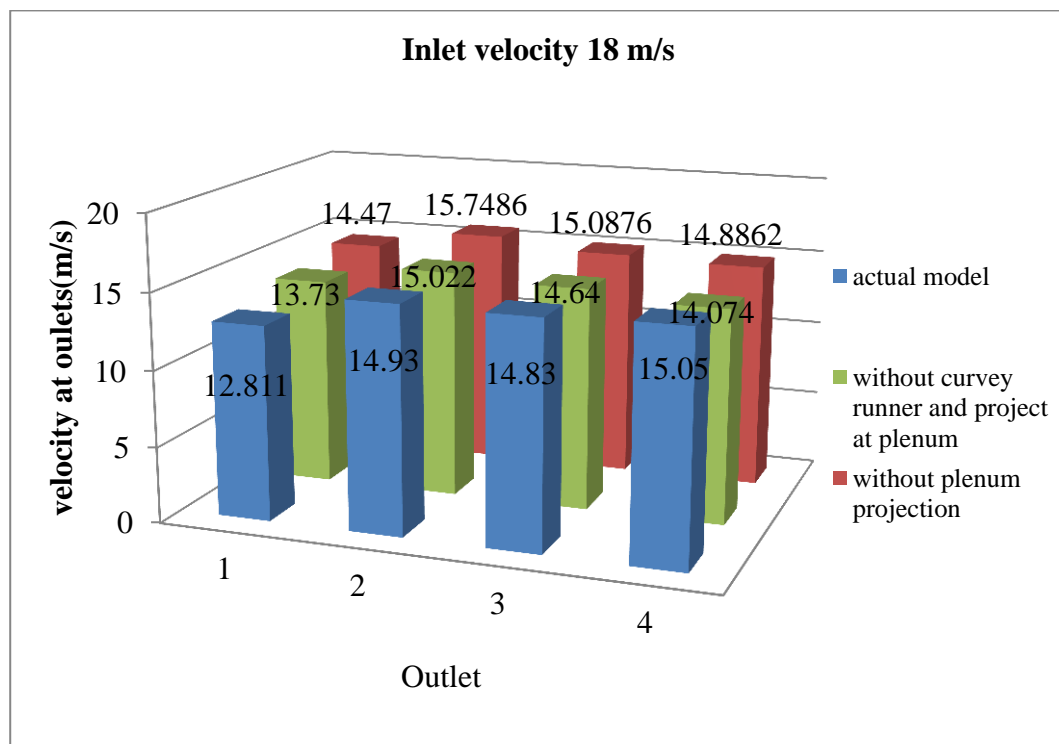


Fig: 5.10 Velocity at outlets vs. outlets of 3 model at Inlet velocity 18m/s

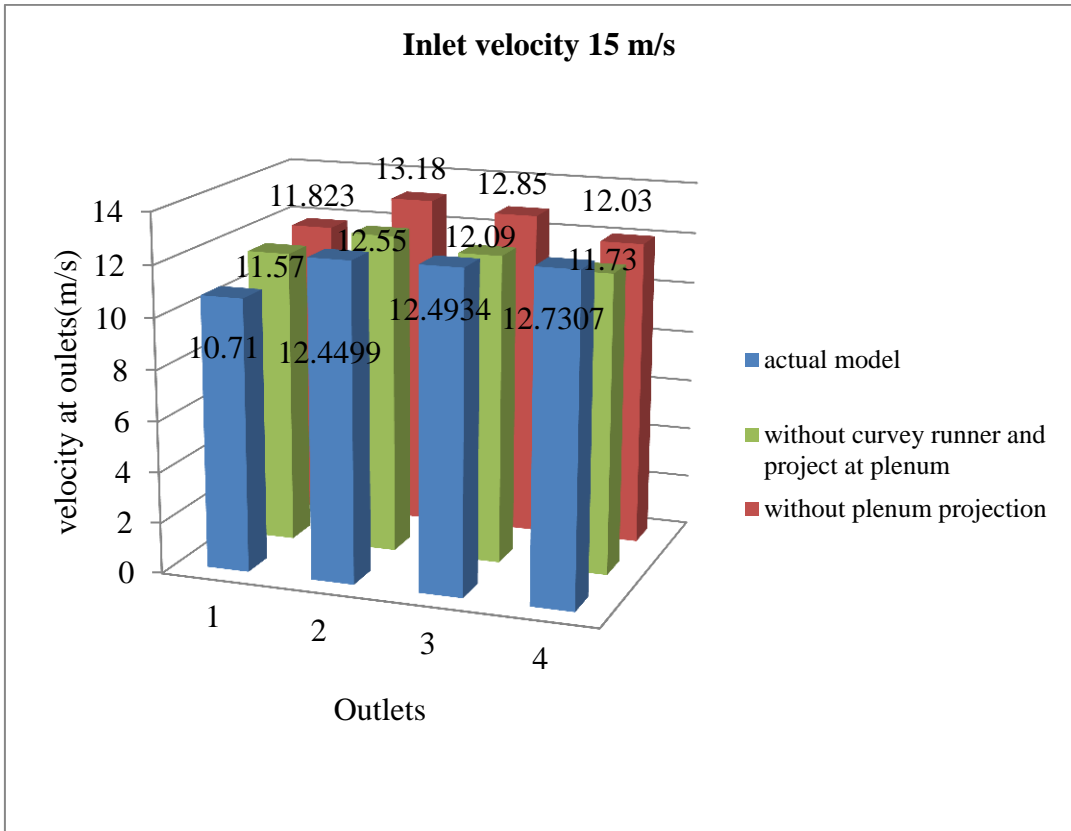


Fig: 5.11 Velocity at outlets vs. outlets of 3 model at Inlet velocity 15m/s

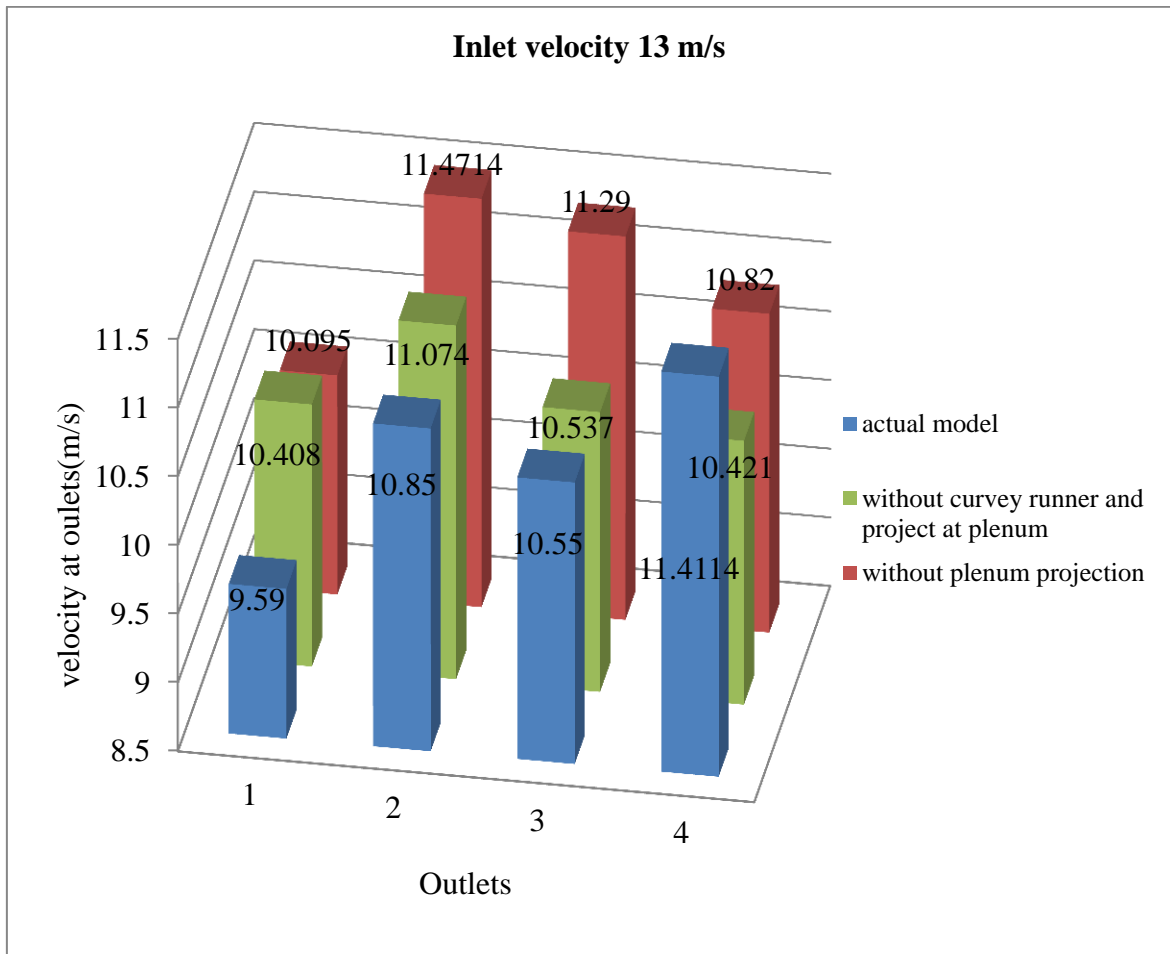


Fig: 5.12 Velocity at outlets vs. outlets of 3 model at Inlet velocity 13m/s

The Fig 5.10, 5.11, 5.12 show velocity at outlets for a particular inlet velocity for three models. The velocity at outlet-2 and outlet-3 almost same and variation show in velocities at outlet-1 and outlet 4. There is slight different in result at inlet velocity 13 m/s because as we lower down the velocity rate of mass of air insertion also diminishing in manifold and it effect on outlet velocities.

5.7 Purposed Geometry :

. The purposed geometry has following design considerations for good results.

- 1) Unwanted projection inside plenum is avoided, Stiffeners of runners and nut projection inside plenum is avoided.
- 2) Depth cuts at extreme sides of plenum is carefully designed, depth cut at runner -1 side is of 10mm depth and runner 4 side it will same as original one of intake manifold.
- 3) Curves design is good to obtain equal flow so not much alteration is required.
- 4) After all alteration geometry of good configuration obtain (Fig 5.13) which giving not only nearly equal velocity in all runners but also discharge air at high velocity compare to previous design.

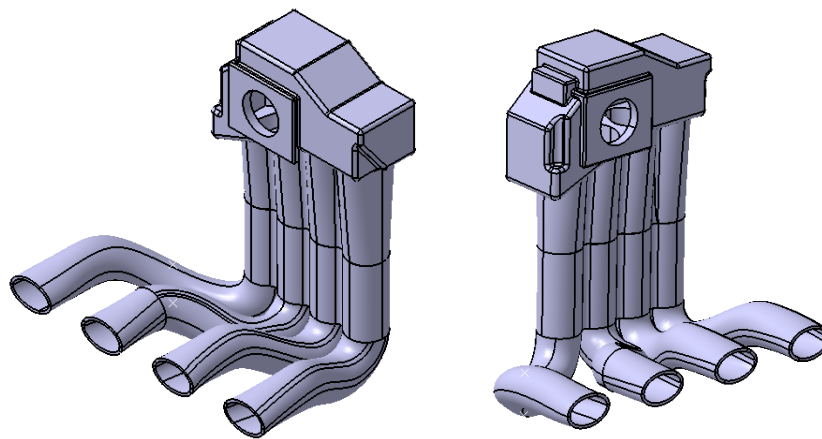


Fig: 5.13 (3-D model of Purposed Geometry)

5.8 Comparison of result of purposed and actual intake manifold:

At inlet velocity 18 m/s:

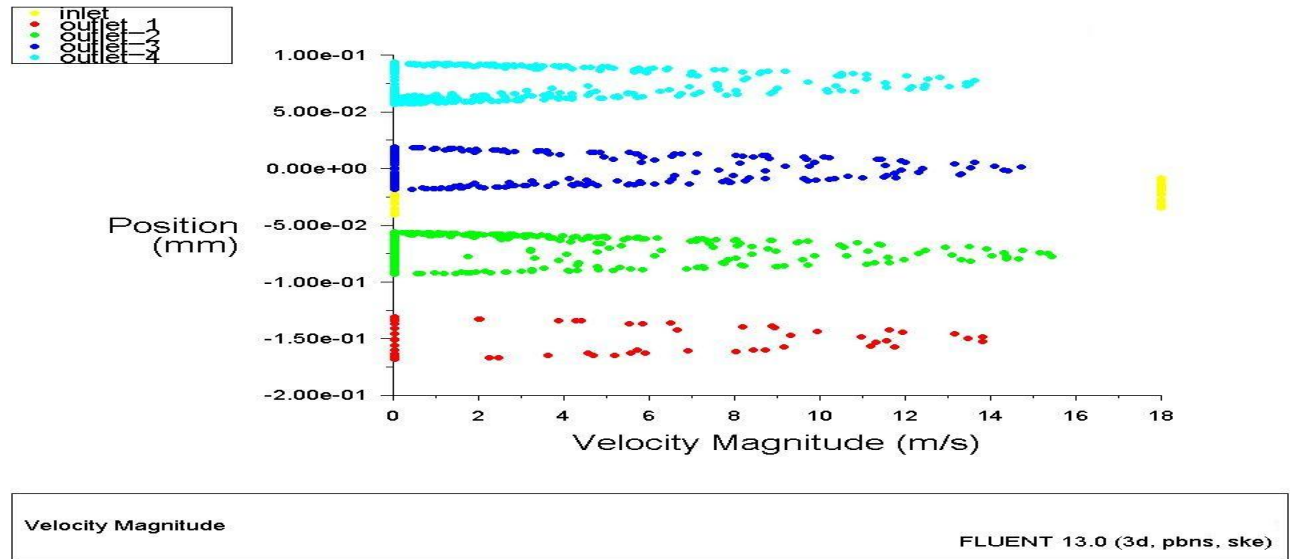


Fig 5.14: Velocity at outlets (Purposed Geometry, 18 m/s)

Table: 5.9

	Outlet 1	Outlet 2	Outlet 3	Outlet 4
Actual	12.811	14.93	14.83	15.05
Purposed	14.69	15.6402	15.188	14.9859

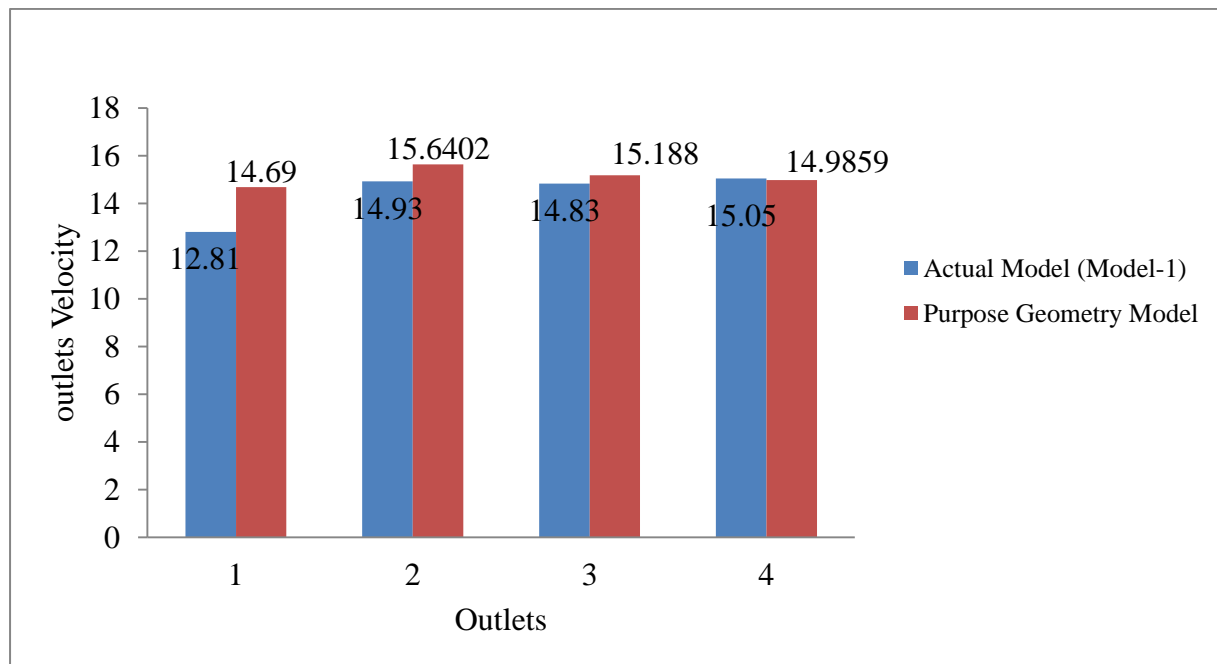


Fig 5.15 Comparison of velocity of Actual and Purposed model

Fig 5.14 and Fig: 5.15 show the velocity is increases and nearly equal in all four outlets of purposed geometry in comparison with original one.

Chapter-6

Conclusions

The purpose of this reported work is to perform an experimental and analysis of an intake manifold for CNG engine by CFD technique. After analysis, the concluded point are as follows:

- 1) The curve at the end of runners is permissible and runners design is upto the mark for given intake manifold.
- 2) The variation in velocity is due to faulty design of plenum chamber.
- 3) Plenum has casting and design defects.
- 4) Outlet-1 has lowest velocity, so pressure losses are more in plenum chamber at runner-1 side.
- 5) The inside projection of nuts as well as depth cut at runner-1 side block the passage of air stream
- 6) Geometry free from unwanted projections of nuts, stiffeners and depth cuts at extreme of plenum show good results. Air flow velocity not only increases in runner-1 by 16%, but improvement of velocity by 5% to 7% approx. in other runners outlets also take place. Nearly equal distribution of velocity in all runners' outlets achieved as compared to original intake manifold.

Future Scope of work

During the present investigation, it is thought that the following areas may be considered for further studies:

- 1) Gasoline engine using GDI(Gas direct injection) technology required high swirl at the end of intake manifold for lean fuel burning, so by properly design of intake manifold high swirl with high mass of air can be achieved.
- 2) Exhaust manifold may also have design defects, so same work can be extended for study of exhaust manifold of an engine.
- 3) CNG engine had less volumetric efficiency than gasoline, so by properly designing the intake manifold considerable improvement in volumetric efficiency can be achieved.